uOttawa

L'Université canadienne
Canada's university

FACULTÉ DES ÉTUDES SUPÉRIEURES ET POSTOCTORALES

uOttawa

L'Université canadienne
Canada's university

FACULTY OF GRADUATE AND POSDOCTORAL STUDIES

Isabelle Louisette Thibodeau
AUTEUR DE LA THÈSE / AUTHOR OF THESIS

M.Sc. (Cellular and Molecular Medicine)
GRADE / DEGREE

Department of Cellular and Molecular Medicine
FACULTÉ, ÉCOLE, DÉPARTEMENT / FACULTY, SCHOOL, DEPARTMENT

Mutations in Connexin43 and Connexin40 Associated with Human Atrial Fibrillation; Physiology and Mechanism

TITRE DE LA THÈSE / TITLE OF THESIS

Michael Gollob
DIRECTEUR (DIRECTRICE) DE LA THÈSE / THESIS SUPERVISOR

Patrick Burgon
CO-DIRECTEUR (CO-DIRECTRICE) DE LA THÈSE / THESIS CO-SUPERVISOR

Balwant Tuana

James Van Huysse

Gary W. Slater
Le Doyen de la Faculte des etudes superieures et postdoctorales / Dean of the Faculty of Graduate and Postdoctoral Studies

Mutations in Connexin43 and Connexin40 Associated with Human Atrial Fibrillation; Physiology and Mechanism

Isabelle Thibodeau

This thesis is submitted as a partial fulfillment of the
Masters of Science program in Cellular and Molecular Medicine

November 25th, 2010

Department of Cellular and Molecular Medicine
Faculty of Medicine
University of Ottawa

Your file Votre référence
ISBN: 978-0-494-74167-2
Our file Notre référence
ISBN: 978-0-494-74167-2

I dedicate this thesis to my spouse and to my family.

Authorization for use of published materials

1. Authorized permission obtained from Nature Publishing Group for the use of Figure 1 published by Goodenough DA and Paul DL in Nature Review Molecular Cell Biology, volume 4, 2003.
   License number: 2454520671055

2. Authorized permission obtained from Nature Publishing Group for the use of Figure 3 published by Mese G et al. in Journal of Investigative Dermatology, volume 127, 2007.
   License number: 2454571373717

Abstract

Atrial Fibrillation (AF), the most common sustained cardiac arrhythmia, is a disease that affects the electrical conductance in the atria. Gap junction channels, composed of connexin (Cx) proteins, allow the electrical signal to propagate between cardiac myocytes. Mutations in two highly expressed cardiac connexin genes, *GJA1* (Cx43) and *GJA5* (Cx40), have been identified by our group in a cohort of patients with lone AF. To characterize trafficking of a novel somatic frameshift Cx43 mutant and three novel Cx40 mutants, fluorescently tagged connexins were visualized in HeLa cells using confocal microscopy. Electrophysiological studies were performed by a member of our lab to test the function of mutant gap junction channels. The Cx43 frameshift mutant (Cx43-932delC) caused intracellular retention of Cx43, resulting in impaired electrical coupling between paired cells. All three Cx40 mutants (F30L, G311S and R113S) demonstrated normal trafficking and electrical coupling between paired N2A cells. Enhanced hemichannel function was observed for the Cx40-F30L mutant, leading to cell death in *Xenopus* oocytes. Increased sensitivity to intracellular pH caused closure of gap junction channels composed of Cx40-G311S or Cx40-R113S. Intracellular localization of a previously published Cx40 mutation (P88S) was determined to be retained within the ER and Golgi compartments. Trafficking rescue was observed when P88S was co-expressed with wild-type Cx40 or Cx43. My results and those of our collaborators demonstrate a novel finding that a Cx43 mutation is associated with AF and also further support reported findings on the association of Cx40 mutations with AF.

Table of contents

Authorization for use of published materials.....iii
Abstract.....iv
Table of contents.....v
List of figures.....vii
List of abbreviations.....x
Acknowledgements.....xiii

1. Introduction.....1
1.1. Electrical conductance in the heart.....1
1.2. Atrial fibrillation.....1
1.3. Gap junction channels.....3
1.4. Isoform distribution in the heart.....4
1.5. Structure and function of connexins.....5
1.6. Connexin biosynthesis.....10
1.7. Oligomerization and channel formation.....12
1.8. Connexin hemichannels.....15
1.9. Protein interactions and post-translation modifications.....17
1.10. Phenotypes of mouse models with connexin deletion.....19
1.11. Connexin mutations associated with AF.....21
1.12. Research rationale.....28
1.13. Hypotheses & Objectives.....28
2. Materials and Methods.....30
2.1. Expression vectors and subcellular markers.....31
2.2. Cloning.....32
2.3. Site-directed mutagenesis.....33
2.4. Cell culture.....34
2.5. cDNA transient expression.....34
2.6. Immunofluorescence.....35
2.7. Confocal microscopy.....36
2.8. Electrophysiology.....36
2.9. Mouse model.....40
2.10. Harvesting of mouse heart tissue.....40
2.11. Total RNA isolation from mouse heart tissue.....41
2.12. Reverse-transcription.....41
2.13. Relative mRNA quantification by real-time PCR.....41
2.14. Statistical analysis.....44
3. Results.....44
3.1. Somatic Cx43 mutation (Cx43-932delC).....44
3.1.1. Cx43-932delC trafficking in mammalian cells and atrial tissue.....44
3.1.2. Cx43-932delC effect on Cx43-WT and Cx40-WT localization.....48
3.1.3. Cx43-932delC subcellular localization.....51

3.1.4. Gap junction conductance of Cx43-932delC in a homozygote and heterozygote state.....53
3.2. Three novel Cx40 mutants (Cx40-G311S, Cx40-F30L and Cx40-R113S).....55
3.2.1. Trafficking of Cx40 mutants.....55
3.2.2. Electrical conductance of Cx40 mutants.....56
3.3. Further characterization of the previously reported Cx40-P88S mutations.....61
3.3.1. Cx40-P88S subcellular co-localization.....61
3.3.2. Cx40-P88S effect on Cx40-WT and Cx43-WT localization.63
3.3.3. The P88S mutation in Cx32 and Cx50.....65
3.4. Relative mRNA expression in transgenic mouse model.....69
3.4.1. Standard Curves.....69
3.4.2. Relative mRNA quantification in our Cx40-P88S mouse model.....75
4. Discussion.....78
4.1. First report of a novel Cx43 somatic mutation (Cx43-932delC) in AF.....78
4.2. Cx40-F30L; first report on leaky hemichannel mechanism in AF.....83
4.3. Cx40-G311S and –R113S mutants; enhanced pH sensitivity.....86
4.4. P88S mutation in connexins.....87
4.5. Real-time mRNA relative quantification in Cx40-P88S transgenic mice.....90
4.6. Summary.....91
References.....94
Contribution of Collaborators.....105
Appendix A, Supplementary figures.....106
Appendix B, Publication.....109

List of figures

Figure 1.....4
Connexin assembly process for gap junction channel formation.

Figure 2.....6
Connexin topology within the cell membrane.

Figure 3.....14
Formation of homomeric/heteromeric hemichannels
and homotypic/heterotypic gap junction channels.

Figure 4.....25
Effect of frameshift mutation in Cx43 (Cx43-932delC).

Figure 5.....27
Schematic structure of Connexin40 with the location
of the four mutations referred to in this report.

Figure 6.....46
Cellular localization of YFP-labeled wild-type and
mutant Cx43 in HeLa cells.

Figure 7.....47
Immunofluorescence of HeLa cells transiently expressing
untagged Cx43-WT and Cx43-932delC constructs.

Figure 8.....50
Effect of Cx43-932delC on Cx43-WT and Cx40-WT
trafficking in HeLa cells.

Figure 9.....52
Subcellular co-localization of Cx43-932delC with
ER and Golgi proteins in HeLa cells.

Figure 10.....54
Effect of Cx43-932delC on Cx43 and Cx40 gap junction
conductance in N2A cells and *Xenopus* oocytes.

Figure 11.....57
Localization of fluorescently labeled Cx40-WT and
three Cx40 mutants in HeLa cells.

Figure 12.....58
Gap junction conductance of paired N2A cells expressing
fluorescently tagged connexin40 constructs.

Figure 13.....59
Effect of intracellular acidification on gap junction conductance in paired N2A cells expressing Cx40-WT, Cx40-G311S or Cx40-R113S constructs.

Figure 14.....62
Cx40-P88S localization in transiently transfected HeLa cells.

Figure 15.....63
Cx40-P88S subcellular localization in HeLa cells.

Figure 16.....64
Effect of Cx40-WT and Cx43-WT on P88S trafficking in HeLa cells.

Figure 17.....65
Frequency gap junction plaques observed in HeLa cells formed by Cx40-WT or Cx40-P88S.

Figure 18.....66
Effect of Cx32-WT on Cx32-P87S trafficking in HeLa cells.

Figure 19.....67
Frequency of gap junction plaques in HeLa cells formed by Cx32-WT or Cx32-P88S.

Figure 20.....68
Trafficking of YFP-labeled Cx50-WT in HeLa cells.

Figure 21.....71
Standard curve analysis for transgene hCx40/hGH.

Figure 22.....72
Standard curve analysis for mCx40.

Figure 23.....73
Standard curve analysis for mGAPDH.

Figure 24.....74
Standard curve analysis for mActB.

Figure 25.....76
Relative expression of mouse endogenous Cx40 expression in WT and P88S transgenic mice.

Figure 26.....77
Relative expression of endogenous mCx40 compared to transgene expression in WT and P88S transgenic mice.

Figure 27.....78
Relative transgene expression between WT and P88S mice.

Figure S1.....106
Cellular localization of Cx40 and Cx43 in atrial tissue of control and affected patients.

Figure S2.....107
Hemichannel current measurements of wild-type and mutant Cx40 in *Xenopus* oocytes.

Figure S3.....108
Effects of F30L mutant on cell viability and effect of calcium on hemichannel opening.

List of abbreviations

ActB	β-actin
AF	Atrial Fibrillation
ANF	Atrial natriuretic factor
ATP	Adenosine triphosphate
$BaCl_2$	Barium chloride
bp	base pair
BSA	Bovine serum albumin
Ca^{+2}	Calcium
$CaCl_2$	Calcium chloride
cDNA	Complementary deoxyribonucleic acid
Cp	Crossing point
cRNA	Complementary ribonucleic acid
CsCl	Cesium chloride
CsOH	Cesium hydroxide
C-terminal	Carboxyl-terminal
Cx	Connexin
DNA	Deoxyribonucleic acid
dsDNA	Double stranded deoxyribonucleic acid
ECFP	Enhanced Cyan Fluorescent Protein
EGTA	Ethylene glycol tetraacetic acid
ER	Endoplasmic Reticulum
EYFP	Enhanced Yellow Fluorescent Protein

GAPDH	Glyceraldehyde 3-phosphate dehydrogenase
g_j	Macroscopic transjunctional conductance
GJA1	Gap junction alpha 1 (gene encoding Cx43)
GJA5	Gap junction alpha 5 (gene encoding Cx40)
hGH	Human growth hormone
I_j	Junctional current
IP_3	Inositol 1,4,5,-triphosphate
KCl	Potassium chloride
kHz	Kilohertz
MgATP	Magnesium adenosine triphosphate
$MgCl_2$	*Magnesium chloride*
mM	Millimolar
msec	Millisecond
mV	Millivolts
MΩ	Megaohms
N2A	Mouse neuro-2-blastoma
Na_2ATP	Sodium adenosine triphosphate
NaCl	Sodium chloride
NAD+	Nicotinamide adenine dinucleotide
nm	Nanometer
nS	NanoSiemens
NTC	No template control
N-terminus	Amino-terminus

ODDD	Oculodentodigital dysplasia
PBS	Phosphate buffered saline
PCR	Polymerase Chain Reaction
pH_i	Intracellular pH
PKC	Protein kinase C
RNA	Ribonucleic acid
RT	Reverse transcription
S.E.M.	Standard error of the mean
TM	Transmembrane domain
uS	MicroSiemens
UTR	Untranslated region
V_j	Transjunctional voltage
WT	Wild-type
ZO-1	Zonula occludens-1

Acknowledgments

I would like to thank my thesis supervisor, Dr. Gollob, for giving me the opportunity to do a master's degree in his lab. During the past few years, I have learned tremendously from my experience as a graduate student. Your guidance and continuous support are greatly appreciated. I am also grateful for my co-supervisor who has provided valuable advice and helpful suggestions on my experiments and thesis. To my advisory committee members, Dr. Tuana and Dr. Tesson, thank you for your time and input. I would also like to thank our collaborators for the functional work conducted on our mutants. Their work has allowed this thesis to have a complete story. Special thanks to two members of the Gollob lab, Qiuju Li who did all the measurements of gap junction conductance and Gele Liu for creating the some of the clones used in experiments included in this thesis. Also, thanks to Shelly Xu who was a great help on the trafficking rescue experiments. To everyone in our lab, especially Jen and Matt, who have helped to keep a perfect level of (in)sanity in the lab. Lastly, thanks to my spouse and family for giving my continuous encouragement and support throughout my studies.

1. Introduction

1.1. Electrical conductance in the heart

Normal atrial and ventricular contractions within the heart are dependent upon the synchronous contraction of individual cardiomyocytes. Every heart beat is initiated by an electrical signal originating in the sinoatrial node. The signal propagates throughout the atrial myocardium resulting in atrial contraction which facilitates the movement of blood to the ventricles. Then, the signal passes through the atrioventricular node and propagates through the ventricles resulting in the ventricular contraction allowing the blood to be pumped out of the heart. It is crucial that the electrical signal propagates rapidly between cardiac myocytes in order to generate coordinated and effective excitation-contraction coupling. Gap junction channels are critical for this rapid communication between cells. These channels connect the cytoplasm of adjacent cells and allow the passage of ions from one cell to the next. A disruption in electrical conductance can result in an irregular heart rhythm known as an arrhythmia.

1.2. Atrial fibrillation

Atrial Fibrillation (AF) is the most common sustained cardiac arrhythmia. AF is characterized by unsynchronized and erratic electrical activity within the atria. Atria are unable to contract effectively resulting in impaired blood flow and a corresponding increased risk of blood clot formation accounting for the close association between AF and stroke. AF was shown to correlate with a 5-fold increase risk of stroke (Wolf PA et al., 1991; Kannel WB et al., 1998). Symptoms

associated with AF range from palpitations, shortness of breath and decreased exercise activity. The risk of developing AF increases with age (Kannel WB et al., 1998) and according to the Framingham Heart Study, there is a 25% lifetime risk of developing AF in individuals 40 years of age (Lloyd-Jones DM et al., 2004). Individuals with cardiovascular conditions such as hypertension, heart failure and valvular heart disease have an increased risk of developing AF (Benjamin EJ et al., 1994; Kannel WB et al., 1998). AF may be defined as 'lone' when it arises spontaneously in the absence of traditional risk factors. Genetic studies investigating familial cases of lone AF have led to the identification of a few causative genes. Thus far, the genes associated with AF, coding mostly for ion channels, are KCNQ1, KCNE2, KCNJ2, KCNE5, KCNA5, GJA5, NPPA and SCNA5 (Roberts JD et al., 2010). Mutations in these genes likely account for a minority of AF cases, leading scientists to believe that other causative genes have yet been discovered (Darbar D et al., 2008). In patients with lone AF, where structural defects and other causative diseases are ruled out, genetic defects presumably play a prominent role for the development of AF given the lack of other identifiable risk factors.

The role of genetics in the development of AF was previously demonstrated by our group where four mutations in the GJA5 (connexin40) gene were identified in patients with lone AF (Gollob MH et al., 2006). Functional studies showed that these mutations impaired electrical conductance between paired cells. This was the first report to associate connexin40 mutations with

lone AF in humans. In addition, three of the four mutations reported were found in cardiac tissue but not in lymphocyte DNA suggesting somatic mutations which may account for the lack of family history. We therefore further explored this concept of genetic defects in two cardiac connexins by studying novel mutations recently identified (unpublished) in connexin40 as well as connexin43.

1.3. Gap junction channels

Rapid and homogenous propagation of action potentials, initiated in the sinoatrial node, is crucial for generating synchronized contractions. These electrical impulses are transmitted between cardiac myocytes through gap junction channels which allow rapid depolarization of adjacent cells. The cytoplasm of adjacent cells are connected together through these aqueous channels which allow electrical and metabolic coupling. Gap junction channels are rather large and nonselective pores allowing the bi-directional flow of ions, small molecules and second messengers smaller than 1 kilodalton (Evans WH et al., 2002). These channels are composed of connexin (Cx) proteins (Figure 1). Six connexins oligomerize to form a hemichannel (or connexon). Adjacent cells will each contribute a hemichannel to form a functional gap junction channel. Gap junction channels localize in high density at the intercalated discs of cardiac myocytes. Aggregation of gap junction channels form clusters referred to as gap junction plaques. Gap junction channels are sensitive to transjunctional voltage, which refers to the voltage difference between two paired cells, and to membrane potential, which is the voltage difference between the interior and exterior of a cell (Gonzalez D et al., 2007). At rest, when there is no transjunctional voltage

difference between paired cells, the majority of the channels are opened. During action potential propagation, a cell becomes depolarized thus resulting in a transjunctional voltage difference with its adjacent cell, inducing channels to close in a time and voltage dependant manner.

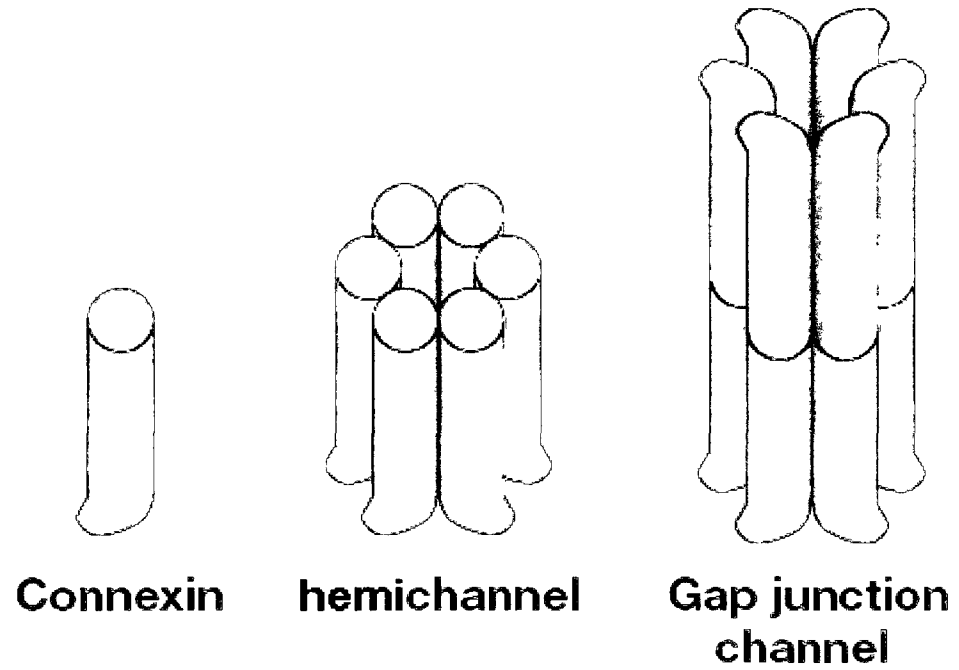

Figure 1. Connexin assembly process for gap junction channel formation. Six connexin proteins oligomerize to form hemichannels. Two opposing hemichannels expressed by adjacent cells assemble into gap junction channels. Adapted with permission from Macmillan Publishers Ltd: [Nat Rev Mol Cell Biol] Goodenough DA et al., copyright 2003.

1.4. Isoform distribution in the heart

Connexins form a large family of proteins composed of 21 known isoforms in the human genome (Sohl G et al., 2004). Connexin isoforms are named according to their predicted molecular weight which varies mostly due to the carboxyl-terminal (C-terminal) length. There are multiple connexin isoforms

expressed in the human heart and within the conduction system of the heart. Only three isoforms are prominent in adult human cardiac myocytes. Cx40 is highly expressed in atrial myocytes but is absent in ventricular tissue. Cx43 is abundantly expressed in both atrial and ventricular tissue. Cx45 expression is very low in both the atria and ventricles. Cx31.9 is mostly expressed in the conduction system such as the sinoatrial node and atrioventricular node. Cx37 expression is specific to the vascular endothelial cells. Therefore the main isoforms found in the working atrial myocardium are Cx40 and Cx43 and their expression levels compared to each other are relatively similar (Vozzi C et al., 1999).

1.5. Structure and function of connexins

Every connexin isoform has a similar topology and oligomerize to form hemichannels composed of six connexin proteins. They have four transmembrane domains, where both amino and carboxyl terminal domains face the cytoplasm, generating two extracellular loops and an intracellular loop (Figure 2). All four transmembrane domains are mostly α-helical, the two extracellular loops are mostly β-sheets and the cytoplasmic domains are largely unstructured with some regions being α-helical (Duffy HS et al., 2006; Bouvier D et al., 2009; Purnick PEM et al., 2000). All four transmembrane domains, the amino terminal and both extracellular loops are highly conserved amongst species and between connexin isoforms. The amino acid sequences of the intracellular loop and C-terminal domain vary the most between species and isoforms.

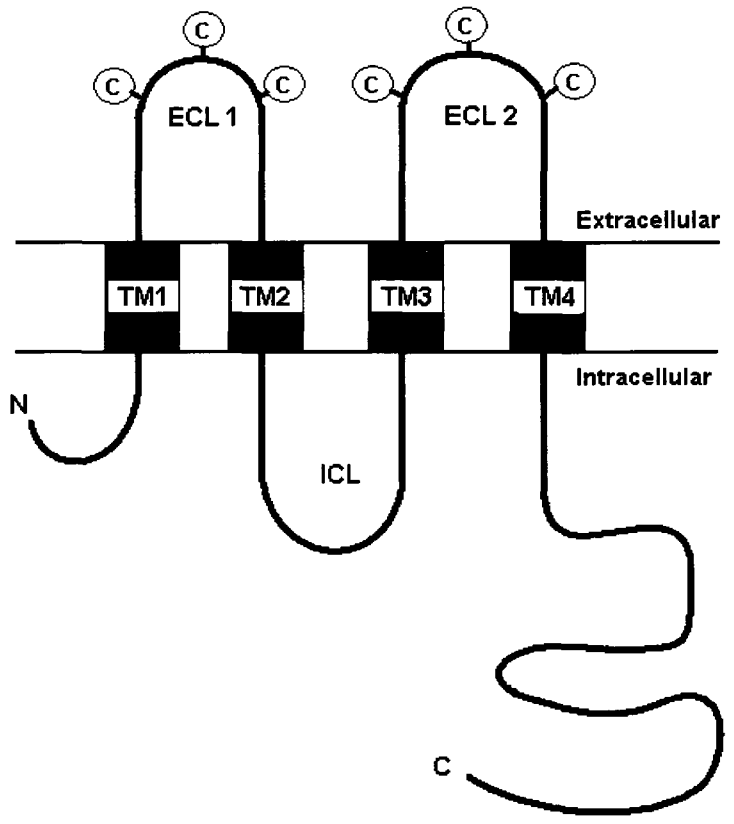

Figure 2. Connexin topology within the cell membrane. Connexins have four transmembrane domains (TM1, TM2, TM3 and TM4). The N- and C- terminus face the cytoplasm as well as the intracellular loop (ICL). Each extracellular loop (ECL1 and ECL2) contains three cysteine residues that form 3 intramolecular disulfide bonds.

The conserved domains most likely have very important roles for channel formation and function. The amino-terminus (N-terminus) is a very short sequence of approximately 20 amino acids. It is known to play a role in voltage gating of hemichannels and gap junction channels (Srinivas M et al., 2005; Dong L et al., 2006; White TW et al., 1995; Purnick PEM et al., 2000). The N-terminus, along with a portion of the first transmembrane domain and first extracellular loop junction, play a role in voltage sensing of connexins (Verselis VK et al., 1994). The N-terminus also influences molecular permeability and single channel conductance (Dong L et al., 2006). This domain plays a minor role in gap junction plaque formation since deleting certain residues can either result in intracellular distribution or normal localization although it plays a crucial role in generating functional channels (Kyle JW et al., 2008; Shibayama J et al., 2005).

All four transmembrane domains (TM1, TM2, TM3 and TM4) are α-helical and therefore are important for insertion and anchoring in the membrane. There is no clear consensus in the literature about which transmembrane domain lines the channel pore. Conflicting results on pore-lining segments arise from studying hemichannel pore and gap junction channel pore. The TM1, TM2 and TM3 have been hypothesized to be involved in the channel pore with TM3 being the major segment lining the pore of Cx32 in *Xenopus* oocytes (Skerrett IM et al., 2002). TM1 as well as a portion of the first extracellular loop are thought to line the intracellular portion of the hemichannel pore (Kronengold J et al., 2003; Zhou X-

W et al., 1997). The first transmembrane segment, more specifically the second half of TM1 determines hemichannel conductance (Hu X et al., 2006). Cysteine substitutions in each TM may result in channel block supporting the notion that a mutation in any of the four TM can disturb the channel pore (Skerrett IM et al., 2002).

The two extracellular loops are critical for the docking of hemichannels and for channel function (Dahl G et al., 1991; Haubrich S et al., 1996). It is hypothesized that the extracellular loops determine the compatibility between hemichannels composed of different connexin isoforms to form functional channels (White TW et al., 1995). There are three cysteine residues in each extracellular loop, all highly conserved, that are covalently bound by three intra-connexin disulfide bonds. The first extracellular loop has also been attributed the function of determinant of charge selectivity in hemichannels (Trexler EB et al., 2000).

There is significant sequence homology between connexin isoforms but the intracellular loop and the carboxyl terminal, the largest domain, contain sequence variation between connexins and species. These two domains are not conserved and allow for varying properties in voltage and ion gating between connexin isoforms. The intracellular loop is crucial for channel function but not necessary for trafficking and gap junction formation (Seki A et al., 2004a). A portion of the intracellular loop, amino acid residues 100 to 102, has been

hypothesized to be involved in trafficking of Cx43 in HeLa cells (Nambara C et al., 2007). Nambara C et al. also show that deletion of any region of the intracellular loop results in complete loss of intercellular dye coupling.

Connexin trafficking to the cell membrane and formation of functional gap junction channels does not seem to be affected by the C-terminus domain. This observation comes from several studies. First, haplodeficient mice expressing a truncated Cx43 protein where amino acids beyond 258 are deleted, show proper localization of Cx43 to intercalated disks and no difference in macroscopic junctional conductance, although single channel conductance was altered (Maass K et al., 2007). Similarly, Cx43 truncated at amino acids 245 and 303 have normal transjunctional conductances similar to wild-type (WT) Cx43 but have different unitary conductances (Fishman GI et al., 1991). Similarly to Cx43, truncation of Cx40 at amino acid 248 does not significantly impair macroscopic junctional conductance in *Xenopus* oocytes (Anumonwo JMB et al., 2001). Truncation of Cx43 at amino acid 251 resulted in intracellular accumulation and reduced biochemical coupling although HeLa cells expressing this truncated form of Cx43 were still electrically coupled (Martinez AD et al., 2003). This effect on trafficking could be explained by a loss of interaction between the missing amino acids of the C-terminal and tubulin through which hemichannels usually traffic to the cell membrane. When co-expressed with Cx43-WT, the truncated protein trafficked to the cell membrane and restored biochemical coupling (Martinez AD et al., 2003). The function of the C-terminal domain points towards channel

gating regulation rather than basic channel functions such as trafficking and ionic or metabolic intercellular coupling.

Gap junction channels are regulated by voltage, intracellular pH and phosphorylation (Morley et al., 1996; Lampe PD et al., 2000a). The gating mechanism is thought to follow a 'ball-and-chain' model where the C-terminal domain binds to a region of the intracellular loop (Stergiopoulos K et al., 1999; Seki A et al., 2004b). Gap junction channels are voltage-dependant; they close when a transjunctional voltage difference is generated between paired cells. These channels are also pH sensitive as they normally close upon intracellular acidification. Deletion of the C-terminus domain of Cx43 abolishes pH sensitivity and allows channels to remain open under intracellular acidification (Morley GE et al., 1996). Normal pH sensitivity is important and advantageous in the heart as it protects adjacent cardiomyocytes from being exposed to intracellular acidification.

1.6. Connexin biosynthesis

Connexin synthesis and trafficking has been widely studied for Cx43 which is the most widely expressed isoform. Protein synthesis follows the classical secretory pathway. Although little is known about Cx40 biosynthesis we can hypothesize that it follows the same pathway. Connexin mRNAs are translated by ribosomes of the rough endoplasmic reticulum (ER) where folding and integration in the ER membrane occurs co-translationally (Falk MM et al., 1994). Vesicles bud off from the ER membrane and move through the Golgi

apparatus. Oligomerization of six connexin proteins occurs between protein insertion in the ER membrane and hemichannel delivery from the *trans*-Golgi network to the cell membrane. The precise intracellular location of oligomerization is unknown and may differ between connexin isoforms. For Cx43, it has been shown that oligomerization occurs after exit from the ER and oligomerized hemichannels are detected once in the *trans*-Golgi (Musil LS et al., 1993). Moving along microtubules, the vesicles containing hemichannels will fuse with non-junctional areas of the cell membrane thereby releasing the hemichannels in the membrane (Lauf U et al., 2002). Microtubules facilitate but are not essential to the delivery of hemichannels to the cell membrane (Thomas T et al., 2001). Hemichannels targeted to non-junctional areas of the cell membrane diffuse laterally to sites of cell-to-cell junctions or they may also be directly integrated at gap junction plaques (Simek J et al., 2008; Shaw RM et al., 2007). There, they will bind to the extracellular loops of hemichannels from adjacent cells to form functional intercellular gap junction channels. In mammalian cells, expression of tagged connexins allowed visualization of gap junction channel degradation occurring from the centre of the plaque (Jordan K et al., 1999). One cell of a cell pair will internalize entire gap junction channels and form vesicles named annular junctions (Naus CC et al., 1993; Jordan K et al., 1999). These annular junctions are then targeted for lysosomal or proteasomal degradation. Proteasomal degradation of Cx43 was shown to be the primary pathway for proteolysis of gap junction channels as opposed to lysosomal degradation (Laing JG et al., 1995). Connexins have very short half-lives, more

specifically the half-life of cardiac connexins is estimated at 1-2 hours, allowing for rapid regulation in response to stress stimulus (Beardslee MA et al., 1998). A C-terminal fluorescent tag has been widely used in the literature for the study of connexin trafficking and function in mammalian cells. Addition of such a tag at the C-terminal does not affect protein trafficking or channel function as compared to untagged connexins (Laird DW et al., 2001; Gong X-Q et al., 2007). Fluorescently tagged connexins at the N-terminus result in normal trafficking and formation of gap junction plaques but do not form functional hemichannels or gap junction channels in mammalian cells (Contreras JE et al., 2003a; Contreras JE et al., 2003b; Gong X-Q et al., 2007; Retamal MA et al., 2007).

1.7. Oligomerization and channel formation

Different connexin isoforms have distinct tissue distributions and a particular tissue may express more than one isoform. Co-expression of different connexins could potentially generate interactions between different isoforms resulting in hetero-oligomerization (Figure 3). Hemichannels are either homomeric or heteromeric. Homomeric hemichannels are composed of identical connexin isoforms and heteromeric hemichannels are formed by at least two different connexins. Upon association of two hemichannels, gap junction channels can be homotypic or heterotypic. A homotypic channel describes the association of identical hemichannels and a heterotypic channel refers to the association of two different hemichannels. Various combinations in hemichannel assembly or channel assembly can generate variability in channel properties different from those of the isoforms composing the channels. The isoform

composition and stoichiometry likely determine the properties of heteromeric hemichannels and heterotypic gap junctions (Bevans CG et al., 1998). Channel properties may vary in terms of electrical conductance, pore size, permeability, selectivity and gating (Bevans CG et al., 1998).

Certain combinations of isoforms were shown to be incompatible for the formation of heteromeric/heterotypic channels (White TW et al., 1996; Gemel J et al., 2004). Whether Cx40 and Cx43 are able to form functional homomeric/heterotypic channels is controversial in the literature. The formation of homomeric/heterotypic channels, composed of Cx43 and Cx40, has been supported by studies on metabolic coupling and electrophysiological studies although the channels were sensitive to the direction of the current (Valiunas V et al., 2000). Gap junctional and single channel conductances were measured in mammalian cells and support the concept of functional homomeric/heterotypic channels composed of Cx43 and Cx40 (Cottrell GT et al., 2001b). Contrarily, other groups have published electrophysiological data on homomeric/heterotypic channels between Cx43 and Cx40 as being non functional in *Xenopus* oocytes and in mammalian cells (Bruzzone R et al., 1993; Elfgang C et al., 1995; Haubrich S et al., 1996; Gu H et al., 2000; Rackauskas M et al., 2007).

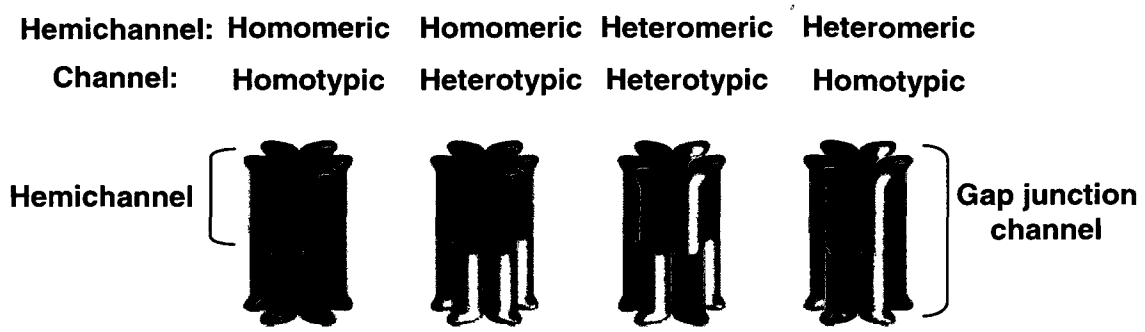

Figure 3. Formation of homomeric/heteromeric hemichannels and homotypic/heterotypic gap junction channels. Different possibilities exist for oligomerization of connexins when more than one isoform is expressed within a cell. Homomeric hemichannels are composed of identical connexins while heteromeric hemichannels contain more than one isoform. Association of identical hemichannels generates homotypic channels whereas binding of different hemichannels results in heterotypic channels. Adapted by permission from Macmillan Publishers Ltd: [J Invest Dermatol] Mese G et al., copyright 2007.

Several studies have looked at the ability of different connexin isoforms to interact together within one cell. It is still unclear which domain is involved in the interactions between connexins during oligomerization. Atrial cells could potentially generate hemichannels composed of Cx40 and Cx43 isoforms as they express high levels of these two isoforms. Formation of functional heteromeric hemichannels between these two isoforms is debated in the literature. Although it is difficult to prove formation of heteromeric channels, researchers have studied these interactions by performing biochemical analyses such as co-immunoprecipitations and have demonstrated that Cx40 and Cx43 co-precipiate together (He DS et al., 1999; Valiunas V et al., 2001). Fluorescent microscopy has demonstrated that Cx43 does not co-localize in the same region of gap junction plaques as Cx32 or Cx26 in HeLa cells co-expressing these isoforms

(Falk MM, 2000). In contrast, fluorescent microscopy shows overlapping fluorescence of Cx43 with Cx40 at gap junction plaques in different cell lines co-expressing both Cx43 and Cx40 (Cottrell GT et al., 2002). Biochemical, biophysical and electrophysiological data support the formation of heteromeric channels formed by Cx40 and Cx43 (He DS et al., 1999; Cottrel GT et al., 2001a; Cottrel GT et al., 2001b; Cottrell GT et al., 2002; Gu H et al., 2000; Bouvier D et al., 2009; Heyman NS et al., 2009). In support for evidence of heteromeric hemichannel formation, the C-terminal domain of Cx40 can restore channel regulation of Cx43, indicating that these two isoforms can interact together (Anumonwo JMB et al., 2001). Whether these heteromeric or heterotypic channels are formed in vivo remains to be elucidated.

1.8. Connexin hemichannels

Hemichannels are found in the non-junctional areas of the cell membrane and will diffuse laterally to sites of intercellular contact. Studies on hemichannel function in the literature are now emerging as it was first thought that hemichannels remained closed until paired with another hemichannel. These "half channels" are considered active or functional if they open in non-junctional areas of the cell membrane and therefore allowing communication with the extracellular environment. Hemichannel conductance is twice the conductance of gap junction channels, as there is half the resistance, and could potentially compromise cell viability by depletion of intracellular metabolites and disruption of the ionic gradient (Hu X et al., 2006). Therefore hemichannel openings must be brief and highly regulated for cell viability to be maintained. Communication

with the extracellular environment through hemichannels represents a recently discovered pathway for exchange of molecules and ions with the environment. The first evidence for hemichannel activity was from a study in *Xenopus* oocytes expressing Cx46 cRNA. After 12h-24h in culture, the oocytes displayed impaired viability and cell death (Paul DL, et al., 1991). The ability of Cx43 hemichannels to communicate with the extracellular space was observed when low molecular weight dyes from the extracellular environment was taken up by cells or when a dye is microinjected into one cell and spreads to surrounding cells (Li H et al., 1996; Contreras JE et al., 2003b).

Several molecules have now been identified as being permeable through hemichannels. Hemichannels communicate with their extracellular environment by releasing various molecules such as ATP, IP_3, glutamate, NAD+ into the extracellular space (Evans WH et al., 2006; Kang J et al., 2008; Bahima L et al., 2006; Gossman DG et al., 2008; Bruzzone S et al., 2001; Ye ZC et al., 2003). IP_3 is a second messenger that induces calcium release (Ca^{+2}) from the sarcoplasmic reticulum. By injecting IP_3 into one cell, Ca^{+2} waves were measured in surrounding cells. This indicates that IP_3 can be released into the extracellular space from the injected cell and activate receptors on the membrane of surrounding cells. In addition to exchange of molecules, hemichannels also conduct current in response to cellular depolarization (Trexler EB et al., 1996).

Studies on different connexin isoforms revealed that hemichannel currents are sensitive to extracellular calcium concentrations (Ebihara L et al., 2003). Connexins have calcium binding sites on their extracellular loops and in response to increased extracellular calcium, hemichannels close. Cell death of *Xenopus* oocytes was observed after injection of Cx46 cRNA, which produced functional hemichannels, and was inhibited by the addition of calcium to the extracellular environment (Ebihara L et al., 1993). In the absence of extracellular divalent cations, hemichannels open and a corresponding increase in dye uptake can be observed (Schalper KA et al., 2008). The sensitivity to extracellular calcium varies between different isoforms. Not every member of the connexin family can form functional hemichannels. For example, Cx43 hemichannels do not open under resting conditions but they generate current upon cellular depolarization or decreased extracellular calcium concentrations (Contreras JE et al., 2003a; Contreras JE et al., 2003b; Kang et al., 2008; Quist AP et al., 2000). Cx43 hemichannels expressed in mammalian cells also permeate fluorescent dyes in reduced extracellular calcium concentrations (Li H et al., 1996). Hemichannels are closed by elevated intracellular pH, elevated intracellular Ca^{+2} and phosphorylation. To this day, the physiological significance of hemichannel openings in the heart remains unclear.

1.9. Protein interactions and post-translational modifications

Gap junctions interact with many cytoplasmic proteins. Most of the binding sites for interacting proteins are found in the C-terminal domain of connexins. Cx43 has been studied the most due to the fact that it was the first

isoform discovered and is widely expressed in different tissues. Cx43 interacts with many different cytoplasmic proteins such as phosphatases and kinases involved in the regulation of gap junction channels (Giepmans BNG, 2004). Cx43 also interacts with certain proteins associated with adherens junctions and tight junctions such as zona occludens-1 (ZO-1) (Giepmans BNG et al., 1998; Giepmans BNG, 2004). As previously mentioned, hemichannel delivery to the cell membrane is facilitated by microtubules. A tubulin binding site in Cx43 was identified in the 35 amino acids following TM4 of the C-terminal domain (Giepmans BNG et al., 2001).

Amongst other proteins associated with adherens junctions and tight junctions, Cx43 is known to directly interact with the second PDZ domain of ZO-1 (Giepmans BNG et al., 1998; Toyofuku T et al., 1998). Zona occludens-1 is a peripheral membrane protein that localizes at gap junctions, tight junctions and adherens junctions. The role of this binding partner is still unclear. The binding site of ZO-1 in Cx43 is located at the very end of the C-terminal domain. Extending the C-terminal tail of Cx43 with a tag or deleting the last amino acid of Cx43, an isoleucine at amino acid position 382, abolishes the binding of ZO-1 to Cx43 (Giepmans BNG et al., 1998; Lau AF et al., 2004). Tagged Cx43, mutated or truncated Cx43 that lose the ZO-1 binding site display normal trafficking to the cell membrane and form functional gap junctions (Maass K et al., 2007; Jin C et al., 2004; Hunter AW et al., 2008). Jin C et al. report a reduction in Cx43 phosphorylation when the interaction with ZO-1 is abolished. Cx40 has also

been shown to interact with ZO-1 although the interaction site remains unknown (Jin C et al., 2004; Nagasawa K et al., 2006).

The C-terminal domain of Cx43 is the only domain to contain phosphorylation sites. Connexins are known to be regulated by phosphatases and kinases. Studies on Cx43 demonstrated that phosphorylation may affect several properties such as connexin transport to the cell membrane, assembly into hemichannels, gap junction internalization, degradation and channel gating. Both Cx43 and Cx40 are phosphorylated although studies on Cx40 are scarce. Cx43 has as many as 14 reported phosphorylation sites (Lampe PD et al., 2004). The three best studied kinases that phosphorylate Cx43 are protein kinase C (PKC), mitogen-activated protein kinase and c-Src. Phosphorylation of Cx43 on residues ser255, tyr265, ser279, ser368, serine 372 and ser282 results in a decrease of intercellular communication (Lampe PD et al., 2000b; Giepmans BNG et al., 2001). Inhibition of PKC, thereby preventing connexin phosphorylation, results in hemichannel and gap junction channel opening (Bao X et al., 2004). Phosphorylation regulates channel opening and closure but may not be crucial for channel function as not all connexin isoforms are phosphorylated.

1.10. Phenotypes of mouse models with connexin deletion

Since Cx43 is widely expressed in different tissues, Cx43 deficient mice have major problems and die before birth (Reaume AG et al., 1995). Inducible Cx43 deletion in adult mice results in premature death due to cardiac

abnormalities (Eckardt D et al., 2003). However, deletion of only one allele of the Cx43 gene to generate heterozygous Cx43 knockout mice ($Cx43^{+/-}$) results in mice with normal lifespan. These $Cx43^{+/-}$ mice have a reduction in Cx43 protein expression that is translated into a reduction in conduction velocity in the ventricles (Thomas SA et al., 1998; Guerrero PA et al., 1997). These mice do not develop spontaneous ventricular arrhythmias but are more prone to develop these arrhythmias when exposed to stress such as ischemia (Lerner DL et al., 2000). To assess the effect of Cx43 deficiency in the heart only, mice with cardiac-specific knock-outs of Cx43 have been developed. These mice have normal cardiac structure and contractile function but show conduction defect and die from sudden cardiac death due to spontaneous ventricular arrhythmias (Gutstein DE et al., 2001a). Similarly, inducible deletion of Cx43 in adult mice hearts reduced ventricular conduction velocity, triggered ventricular tachyarrhythmias and sudden death. Chimeric mice expressing a mosaic pattern of Cx43 in the heart have conduction abnormalities and contraction defects (Gutstein DE et al., 2001b). Oculodentodigital dysplasia (ODDD) is a disease that affects the face, eyes, teeth and digits that is reported to be caused by an autosomal dominant germline mutation in Cx43 (Manias JL et al., 2008). Mouse models carrying an ODDD mutation in Cx43 display ODDD phenotypes with increased susceptibility to cardiac arrhythmias (Kalcheva N et al., 2007; Manias JL et al., 2008). A portion of families affected by ODDD also present with cardiac arrhythmias caused by mutations in Cx43 (Paznekas WA et al., 2003)

Cx40 knockout mouse models have a reduced conduction velocity in the atria and ventricular conduction system, and an enhanced susceptibility to develop atrial arrhythmias (Kirchhoff S et al., 1998; Verheule S et al., 1999; Hagendorff A et al., 1999). However, Cx40 heterozygous knockout mice ($Cx40^{+/-}$) have atrial conduction velocity and arrhythmia susceptibility similar to WT mice (Kirchhoff S et al., 1998; Verheule S et al., 1999; Hagendorff A et al., 1999). Knockout models confirm that gap junction channels are crucial for normal heart development and for normal electrical conduction. Knockout mice have detrimental effects that cannot be rescued by the presence of other connexin isoforms co-expressed it the same cells. Therefore deleting or suppressing expression of one isoform may not result in compensation by a co-expressed isoform.

1.11. Connexin mutations associated with AF

In a previous study, our group has reported four mutations in the GJA5 gene, encoding the gap junction protein Cx40, by genetic screening of a cohort of unrelated lone AF patients (Gollob MH et al., 2006). Three of four mutations were detected in atrial tissue only and were absent from the lymphocyte DNA of the same patient, defining some cases of lone AF to be a somatic genetic disease. Since adult myocytes do not undergo mitosis, it is hypothesized that the existence of somatic mutations in the proportion of heart cells occurs due to a spontaneous mutation in a progenitor cell during early embryologic development. Functional studies on these mutants revealed impaired electrical conductance through gap junctions. One of the mutations, Cx40-Ala96Ser, showed normal

cellular localization although these mutant channels were unable to conduct current. Another mutation, Cx40-P88S, was found in the atrial tissue of two AF patients. The cellular distribution of the fluorescently tagged Cx40-P88S protein showed extensive intracellular retention with no formation of gap junction plaques in transfected mouse neuroblastoma cells (N2A). The same distribution pattern of intracellular retention was also observed in the immunohistochemical staining of Cx40 in the atrial tissue of the patients carrying the P88S mutation. Electrophysiological studies of N2A cells transfected with Cx40-P88S demonstrated no gap junction conductance. This mutant showed a dominant negative effect on Cx40-WT and Cx43-WT conductance when co-expressed in *Xenopus* oocytes. Interestingly, the P88S mutation mentioned above has also been associated with other diseases when found in two other connexin isoforms. A P87S mutation in Cx32, which corresponds to the proline 88 residue in Cx40 according to protein sequence homology, gives rise to Charcot-Marie-Tooth X-linked syndrome. This disease is characterized by a loss of muscle tissue and loss of touch sensation as Cx32 in expressed in neurons. Additionally, a P88S mutation in Cx50, expressed in lens epithelial cells, was reported to cause cataract disease by thickening the lens (Shiels A et al., 1998). This proline to serine change at position 88 of connexins seems to be an important substitution since it has been found in different connexin isoforms and has been shown to cause different human diseases.

In order to study the effect of the mutation *in vivo,* transgenic mice were generated to carry the human Cx40-WT sequence with or without the Cx40-P88S mutation. These mice were generated by our group to study whether the phenotype of atrial fibrillation could be observed in mice carrying the human Cx40 mutation. Recent work has shown that these mice have a low copy number of the transgene inserted in their genome (unpublished). Using telemetry to monitor heart rhythm of transgenic mice, it was determined that mice carrying the human mutation develop spontaneous AF, while mice carrying the WT copy of Cx40 are not susceptible to arrhythmias (unpublished). Immunohistochemical staining of heart tissue from these mice show intracellular retention of Cx40, similar to the staining of atrial tissue reported in the two individuals carrying this mutation (unpublished). It remains to be determined whether the similar number of transgene insertions in the mouse genome translates into similar transgene expression levels between these two groups of mice.

Recent work from our group has identified a mutation in the coding region of Cx43 (Circulation, In Press). The atrial tissue and lymphocyte DNA was isolated from 10 individuals with an early onset of AF at an age less than 50 years old that underwent surgery for persistent AF. One patient carried a Cx43 frameshift mutation which was identified from atrial tissue DNA while lymphocyte DNA showed a normal sequence for Cx43, thereby indicating a somatic mutation. Using TA cloning of atrial tissue polymerase chain reaction (PCR)

products and subsequent sequencing, the frameshift was determined to be caused by a cytosine nucleotide deletion on one of the alleles at nucleotide position 932. Only 33% of the cloned left atrial tissue PCR products that were sequenced had a cytosine deletion, suggesting that only a subpopulation of atrial myocytes carried the mutant allele, consistent with a non-germline inheritance. The deletion occurs in the C-terminal domain and changes the reading frame (Figure 4). The frameshift causes the translation of 36 aberrant amino acids followed by a premature stop codon, deleting the last 35 amino acids of the native protein. This mutation was absent from 100 alleles sequenced from DNA isolated from the heart tissue of individuals unaffected by AF. An additional 200 alleles, isolated from lymphocyte DNA of healthy controls, were sequenced and found to lack Cx43 mutations.

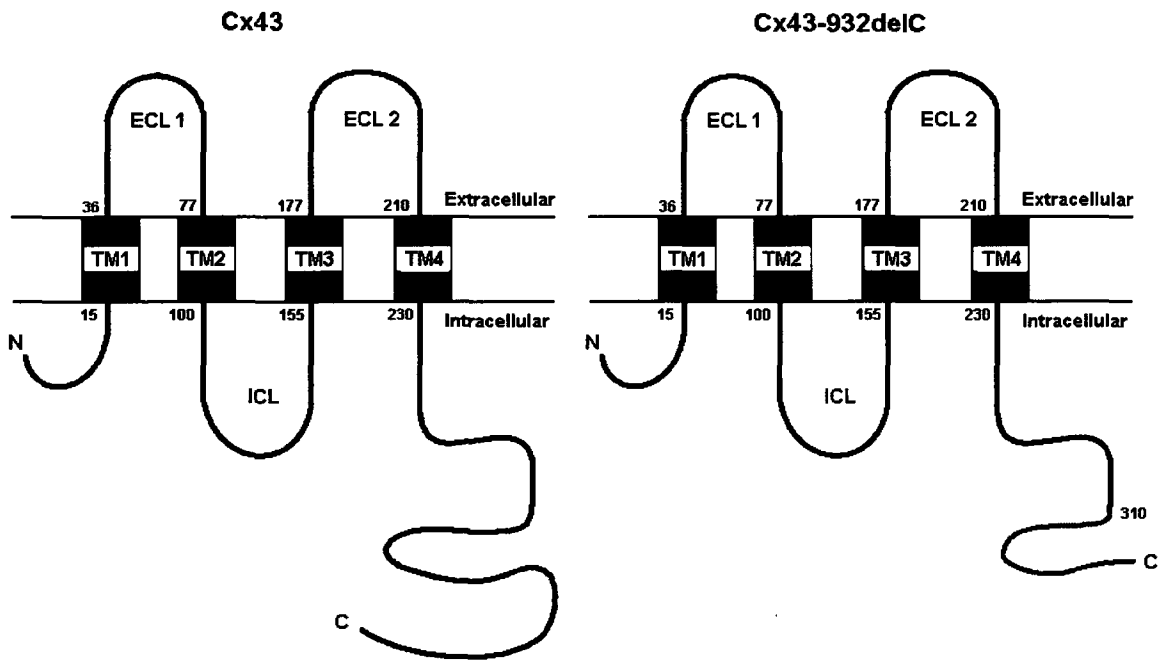

Figure 4. Effect of frameshift mutation in Cx43 (Cx43-932delC). A cytosine deletion in the C-terminus of Cx43 causes a frameshift, encoding for 36 aberrant amino acids followed by a premature stop codon, deleting the last 35 amino acids normally encoded by WT Cx43. The 36 aberrant amino acids of the mutant protein are represented in red while the deleted amino acids are not shown.

Three mutations in Cx40 were recently identified in a cohort of AF patients (unpublished). Lymphocyte DNA was analyzed by heteroduplex analysis using a technique called denaturing gradient gel electrophoresis. Double-stranded DNA (dsDNA) with a mismatch, or mutation, migrates differently on a gel than non mutated dsDNA. Abnormal conformers were directly sequenced. The Cx40-G311S and Cx40-F30L mutations were found in two different patients. Both of these patients had an onset of AF at less than 40 years of age. The Cx40-R113S mutation was found by our collaborators in Cleveland by screening a different cohort of patients with lone AF and coronary artery disease. The Cx40-

F30L mutation (phenylalanine to leucine) is caused by a nucleotide change from a T to A at nucleotide position 88. This mutation is located in the first transmembrane domain (Figure 5) of the connexin40 protein and is a highly conserved residue between the human, wolf, rat, mouse and hamster species. The G311S mutation (glycine to serine) is caused by a nucleotide change from a G to A at nucleotide position 931. This mutation is located in the C-terminal domain of the protein (Figure 5) and is also conserved amongst the species specified above. The R113S mutation (arginine to serine) is caused by a nucleotide change from a G to C at nucleotide position 339 and is located in the intracellular loop (Figure 5). This arginine residue is only conserved in human and wolf, whereas rat, mouse and hamster have a lysine at residue 311.

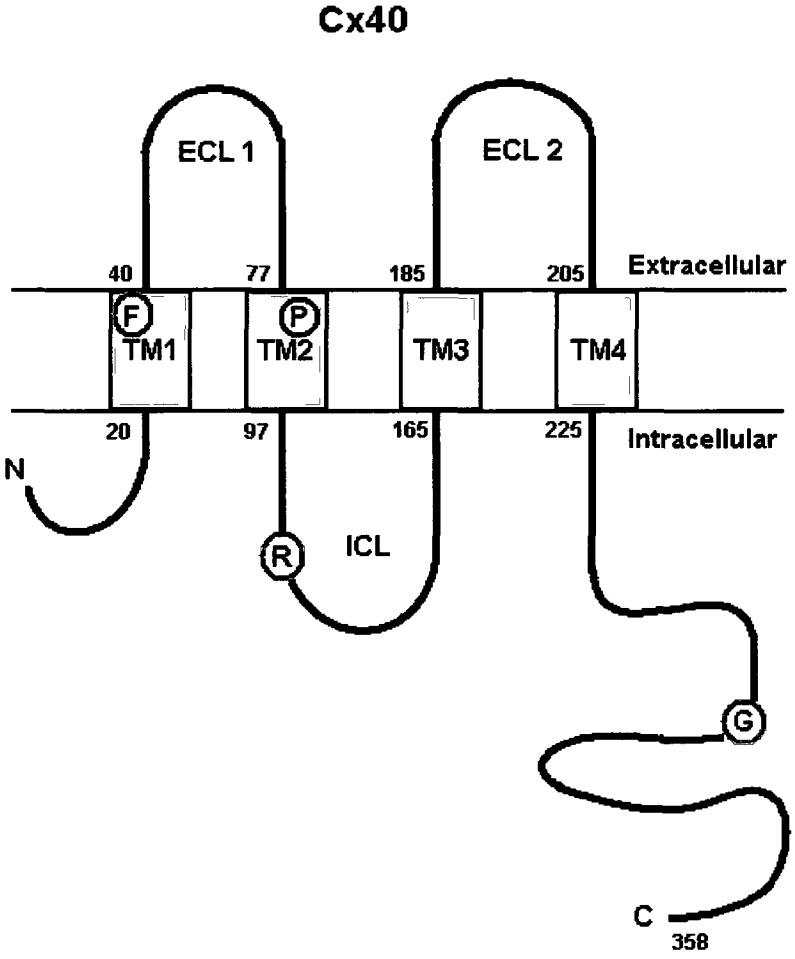

Figure 5. Schematic structure of Connexin40 with the location of the four mutations referred to in this report. The phenylalanine (F) to leucine mutation at amino acid 30 is located in the first transmembrane domain. The proline (P) to serine mutation at position 88 is in the second transmembrane domain. The arginine (R) to serine mutation at residue 113 is in the intracellular loop. The glycine (G) to serine mutation at position 311 is in the cytoplasmic C-terminal domain.

1.12. Research rationale

Previous reports on Cx40 mutations associated with AF have shown an impairment in electrical conductance between paired cells by either affecting protein trafficking or channel function. Recently, our group has identified four new mutations in the GJA1 (Cx43) and GJA5 (Cx40) genes. To date, no Cx43 mutations have been associated with AF. To investigate this novel finding and to further support the concept of Cx40 mutations in AF, all four Cx43 and Cx40 mutants will be characterized by trafficking and electrophysiological studies for functional assessment of the channels. To characterize the effect of the mutants on protein trafficking, an enhanced cyan fluorescent protein (ECFP) or an enhanced yellow fluorescent protein (EYFP) is expressed at the C-terminus of each connexin construct for visualization in mammalian cells. To assess the ability of connexins to conduct current, the macroscopic gap junctional conductance can be measured in paired cells exhibiting fluorescence. N2A cells are communication-deficient and are widely used for electrophysiological studies in the literature.

1.13. Hypotheses & Objectives

Hypotheses

i) A novel Cx43 mutation (Cx43-932delC) identified in a patient with lone AF impairs Cx43 and Cx40 gap junction formation and/or function thereby demonstrating a functional abnormality of Cx43 in association with AF.

ii) Three novel mutations in Cx40 (G311S, F30L, and R113S) identified in patients with lone AF impair Cx40 hemichannel or gap junction formation and function thereby supporting previous reports of a Cx40 association with AF.

iii) Human WT (hCx40) and mutant (hCx40-P88S) transgenic mice, determined to have similar genomic transgene insertions, do not have similar transgene mRNA levels.

Objectives

1. *Characterize the cellular localization of four Cx43 and Cx40 mutants and their ability to form gap junction channels in mammalian cells.*

Previously reported Cx40 mutations have shown impaired protein trafficking and thereby impaired electrical conductance. To assess cellular localization of four new connexin mutants, WT and mutant Cx43 and Cx40 constructs were tagged at the C-terminus with a fluorescent protein. The tagged connexins were visualized in a homozygous state in HeLa cells using confocal microscopy.

2. *Examine cellular localization of connexin mutants in a heterozygous state.*

Adult atrial myocytes co-express Cx43 and Cx40 which may interact together to form heteromeric channels. Therefore, characterizing the mutants in a heterozygous state with their respective wild-type isoforms, or with a naturally co-expressed isoform, better reflects what may occur *in vivo*. HeLa cells were co-

transfected with equal amounts of WT and mutant constructs and subsequently visualized using confocal microscopy.

3. Analyze gap junction conductance of connexin mutants in a homozygous and heterozygous state.

The basic function of cardiac gap junctions is to conduct current between adjacent cells. In order to determine if our mutants affect the function of gap junction channels, the macroscopic junctional conductance is measured in paired N2A cells and paired *Xenopus* oocytes expressing the mutant alone or a combination of the mutants with wild-type Cx43 and/or Cx40.

4. Compare the relative mRNA expression levels between WT and P88S Cx40 transgenes and compare to mouse endogenous Cx40 mRNA levels.

Recently, the number of transgene copies inserted in the mouse genome of WT and P88S Cx40 transgenic mice was estimated to be relatively similar. To determine whether a similar transgene copy number reflects a similar transgene expression level in each group, the mRNA levels were relatively quantified using real-time PCR. In addition, the transgene expression level compared to endogenous mouse Cx40 can be determined.

2. Materials and Methods

Clones were constructed by either G. Liu or myself, as described below (2.1). I was in charge of culturing the HeLa cell line while the mouse neuroblastoma

(N2A) cells were cultured by Q. Li (2.4). Transfections for trafficking studies were performed by me whereas transfections for electrophysiological experiments were performed by Q. Li (2.5). Immunofluorescence of cells were conducted entirely be me (2.6). Imaging of cells using confocal microscopy was performed by either S. Xu or myself (2.7). I have performed and analyzed the data of the experiments for, and leading up to, real-time PCR (2.10, 2.11, 2.12, 2.13). Electrophysiological data on N2A cells was measured by our lab technician, Q. Li (2.8). All electrophysiological experiments in *Xenopus* oocytes were performed by our collaborators, B.J. Nicholson or L. Ebihara.

2.1. Expression vectors and subcellular markers

Cx43-WT-EYFP, Cx43-932delC-EYFP, Cx40-WT-EYFP, Cx40-P88S-EYFP, Cx40-F30L-EYFP, Cx40-G311S-EYFP, Cx43-WT-pcDNA3.1 and Cx43-932delC-pcDNA3.1 clones were made by Gele Liu using the pEYFP vector (Clontech) and pcDNA3.1 vector (Invitrogen). I generated the mutant Cx40-R113S-EYFP by site-directed-mutagenesis from Cx40-WT-EYFP. For co-transfection studies, I had to subclone Cx43-WT, Cx43-932delC, Cx40-WT and Cx40-P88S sequences from the pEYFP vector into a pECFP (Clontech) vector using the Kpn1 and AgeI restriction sites. ER-ECFP was a gift from Dr. Regis Grailhe (Institut Pasteur) and the Golgi-EYFP, pEYFP, pECFP were gifts from Dr. Heidi McBride (University of Ottawa). The ER marker codes for calreticulin, an endoplasmic reticulum resident protein which binds Ca^{+2} ions. The Golgi marker codes for 1,4-galactosyltransferase, a *trans*-Golgi resident protein which catalyses the

glycosylation of proteins. All clones are under the control of the CMV promoter and suitable for expression in mammalian cells.

2.2. Cloning

Shelly Xu, a summer student under my direct supervision, helped me on the Cx32 and Cx50 rescue experiments. Wild-type Cx50 and Cx32 sequence were amplified from genomic DNA since the coding sequence is a single exon. The primers designed for the amplification of the gene by PCR contained the EcoRI and KpnI sites (underlined). The restriction site of the reverse primers was designed to inactivate the stop codon in order to allow translation of the fluorescent protein. The primer sequences are the following (5'→ 3'):

hCx50:	F: cctcatttcttcaggtgaattcgaaatgggcgactggagtttcc	(EcoRI site)
	R: ctttgggtaccctacatacggttagatcgtctgacctggctcggc	(KpnI site)
hCx32:	F: gttttgcaggtgtgaattcggcaggatgaactggacagg	(EcoRI site)
	R: ggaggttgcctggtacctggcaacagcaggccg	(KpnI site)

The PCR protocol used was 1x(98°C for 3min), 5x(98°C for 10s, 72°C for 30s, 72°C for 1 min), 5x(98°C for 10s, 70°C for 30s, 72°C for 1 min), 5x(98°C for 10s, 68°C for 30s, 72°C for 1 min), 20x(98°C for 10s, 66°C for 30s, 72°C for 1 min), 1x(72°C for 10 min). Amplified products were separated on agarose gel stained with ethidium bromide to confirm specific amplification of the band of interest and purified using the QIAquick PCR Purification kit (Qiagen). Purified PCR products and empty vectors (pEYFP and pECFP) were digested using EcoRI and KpnI. The digested products were purified as mentioned above. Ligation was performed at 6°C overnight with the DNA Ligation Kit (Stratagene) using a ratio of

insert:product of 3:1. Ligated products were transformed into Subcloning Efficiency DH5a Competent Cells (Invitrogen) following the supplier's protocol. Transformed bacteria were plated on agar plates with kanamycin antibiotic. Colonies were picked and grown overnight in LB broth with kanamycin and a miniprep was performed the following day. DNA isolated from minipreps was sequenced with BigDye Terminator (Applied Biosystems) to confirm an errorless coding sequence and to assure that the connexin gene was in frame with the start codon of the fluorescent protein. Bacteria containing the sequence-confirmed clones were grown in large scale overnight in LB broth with kanamycin and purified the next day using a maxiprep kit (Qiagen). Maxiprep clones were sequenced again.

2.3. Site-directed mutagenesis

Site-directed-mutagenesis was performed with the QuikChange II XL Site Directed Mutagenesis kit (Stratagene) according to the manufacturer's instructions. The primers used containing the mutation (underlined) were as follows (5'→ 3'):

hCx40-R113S (G339C): F: ggaggccgagagcgccaaagaggtcc

R: ggacctctttggcgctctcggcctcc

hCx50-P88S (C262T): F: cttcgtctccacctcgtccctgatgtacg

R: cgtacatcagggacgaggtggagacgaag

hCx32-P87S (C259T): F: gctcatcctagtttccacctcagctctcctcgtggccatgc

R: gcatggccacgaggagagctgaggtggaaactaggatgagc

The Cx40-R113S, Cx50-P88S and Cx32-P87S mutants were generated from their corresponding wild-type vector generated beforehand. The mutant vectors were maxipreped and the sequence was confirmed by sequencing.

2.4. Cell culture

HeLa cells and N2A cells were cultured in high glucose Dulbecco's modified Eagle's Medium (Gibco) supplemented with 10% fetal bovine serum and 2mM L-Glutamine. Cells are cultured in humidified incubators at 37°C containing 5% CO_2. Cells were grown on glass coverslips for transfection up to 75-90% confluency for HeLa cells or 50-60% confluency for N2A cells.

2.5. cDNA transient expression

A glass coverslip was placed at the bottom of each well of a 24-well plate before plating cells. HeLa and N2A cells were transfected in OPTI-MEM medium using Lipofectamine 2000 (Invitrogen). A total amount of 1ug per well of a 24-well plate was used for transfections in HeLa cells. For co-transfection studies in HeLa cells, 0.5ug of each construct was used per well. The cDNA and lipofectamine were each mixed with 50ul of OPTI-MEM and incubated for 15min at room temperature and then mixed together followed by 15min incubation at room temperature. Lipofectamine/cDNA complexes were added to the cells with 500ul of media. Every transfection was performed a minimum of three times for each scenario.

2.6. Immunofluorescence

Immunofluorescence was performed on HeLa cells transiently transfected for 48 hours with untagged connexin constructs. Cells were rinsed with phosphate buffered saline (PBS) followed by fixation and permeabilization in ice-cold methanol and acetone at -20°C. Cells were washed with PBS and then blocked with PBS/0.5% bovine serum albumin (BSA) for 45 min. The monoclonal mouse anti-Cx43 antibody (Chemicon), recognizing amino acids 131-142 in the intracellular loop, was diluted to 1:50 in blocking solution and incubated for 45 min at room temperature. Cells were rinsed with blocking solution followed by incubation for 45 min with the DyLight488-conjugated goat anti-mouse IgG secondary antibody (Jackson ImmunoResearch laboratories) diluted at 1:1000 in blocking solution. Immunolabeled cells were visualized using confocal microscopy and were assigned the color green. All transfections were repeated a minimum of three times. A transfection is considered successful only if a minimum of 10 cell pairs can be visualized per transfection.

Immunohistochemistry experiments were performed by Louise Pelletier from the Department of Pathology at the University of Ottawa. Tissue staining was performed on 7 µm thick sections of formalin fixed and paraffin-embedded left atrial appendage tissue. Tissue sections were deparaffinized and antigen retrieval was performed by microwave in a citrate buffer (pH 5.6). Specimens were blocked in normal horse serum, and incubated with an anti-Cx43 antibody (Chemicon) specific to amino acid residues 131-142 within the cytoplasmic loop

common to both wild-type and mutant Cx43. Similarly, immunostaining was performed for Cx40 using an anti-Cx40 antibody (Santa Cruz) recognizing specific residues within the C-terminus. Primary antibody was detected using the DAB (diaminobenzidene) chromagen system (DAKO, Carpinteria, CA).

2.7. Confocal microscopy

Live cells were visualized using a laser scanning confocal microscope (Olympus) 24 hours post-transfection for single transfections and 48 hours post-transfection for co-transfection studies. ECFP-tagged proteins were excited at 440nm and the emission wavelength was captured at 475nm. EYFP-tagged proteins were excited at a wavelength of 515nm and the emission wavelength was captured at 527nm. Immunolabeled cells were excited at 488nm and emission wavelength was captured at 510nm. Confocal images were obtained using Olympus Fluoview (FV10-ASW1.7) software. For co-transfection studies images were taken be scanning at each wavelength sequentially in order to minimize non specific fluorescence signals. All images were photographed at 100x magnification. Overlay images were assembled using Adobe Photoshop software.

2.8. Electrophysiology

Electrophysiological recordings were carried out in N2A cells which are gap junction deficient. Gap junctional conductance was measured using the dual whole cell voltage-clamp technique at room temperature. To measure gap junction conductance between two paired cells, the dual whole cell voltage clamp

technique is used. The method consists of sealing a pipette, containing electrodes, on the membrane of each cell of a cell pair. The membrane under the pipette is broken to give access to the intracellular environment. Each pipette controls the membrane potential of the cell it is in contact with. Initially, each cell is maintained at the same membrane potential. A transjunctional voltage is established when stepwise membrane potential depolarizations are induced in one of the cells (cell 1) while the membrane potential of the second cell (cell 2) is kept at its initial holding membrane potential. A current can be recorded in cell 2 upon creation of a transjunctional voltage only if functional gap junction channels are expressed at the cell-to-cell interface.

Macroscopic junctional conductance in N2A cells: These experiments were perfomed by Qiuju Li in Dr. Gollob's laboratory. N2A cells were perfused with a solution containing (in mM): NaCl 140, KCl 5, CsCl 2, $CaCl_2$ 2, $MgCl_2$ 1, Hepes 5, D-glucose 5, pyruvate 2, and $BaCl_2$ 1, at pH=7.4. The recording pipette had a resistance of 3-5 MΩ when filled with an internal solution containing (in mM): CsCl 130, EGTA 10, $CaCl_2$ 0.5, MgATP 3, Na_2ATP 2, and Hepes 10, at pH=7.2 with CsOH. The current signal was digitized at a sampling rate of 1-2 kHz via a Digidata 1322a (Axon Instruments Inc.) and analyzed using pClamp9 software. Each cell of a pair was initially held at a common holding potential of 0 mV. To evaluate transjunctional coupling, 300 msec hyperpolarizing pulses to -30 mV were applied to one cell, from the holding potential of 0 mV, to establish a transjunctional voltage gradient (V_j), while the junctional current was measured in

the second cell. Macroscopic junctional conductance (g_j) was calculated, as: $g_j = I_j/V_j$, where I_j is the measured junctional current and V_j is the transjunctional voltage. For measurements at lowered intracellular pH (pH_i), the internal solution of the recording pipette was adjusted to pH values of 7.2, 7.0, 6.8, 6.6 or 6.4. Following 24 hour transfection, paired N2A cells exhibiting fluorescence were selected for electrical conductance studies. Data were pooled from different transfections.

Macroscopic junctional conductance in *Xenopus* oocytes: These experiments were performed by our collaborators at the University of Health Science Centre in San Antonio, Texas. Electrophysiological recordings in *Xenopus* oocyte cells were injected with specific cRNA quantities of untagged wt and mutant constructs, avoiding the potential issues of variable cellular uptake of clones that may occur during co-transfection of mammalian cells. Cx40-WT, Cx43-WT, and mutant Cx43 were first subcloned into a pGEM-7zf vector. cRNA was prepared by use of the mMessage mMachine kit (Ambion) with Cx40 under T3 promoter and Cx43 under SP6 promoter. Oocytes were treated as previously described and injected with 4 ng antisense phosphorothioated oligonucleotide directed against nucleotides 327 to 353 of endogenous *Xenopus* Cx38 with sequence G*C*C* ACC AGA ATC CTT GAT TCA TTC* T*C*C (asterisks represent phosphorothioate bond). After 3 days, oocytes were injected again with connexin RNA mixed with 4 ng antisense oligonucleotide. After injection, oocytes were incubated at 17°C for 24 hours, stripped off their vitelline membrane, and paired

overnight in agar wells. Oocytes were continuously bathed in half-strength L15 media (Sigma). Junctional currents were assessed by dual oocyte voltage-clamp technique with 2 Geneclamp500 amplifiers (Axon Instruments). Oocytes were clamped at 30 mV, and transjunctional conductances were measured by a 10 mV voltage pulse. In addition, a series of 10-second voltage pulses were used to generate a gating profile of the expressed channels over a transjunctional voltage (Vj) range of 100 to 100 mV to ensure that the properties were consistent with the connexin expressed. Data were acquired and analyzed with Pclamp8 software (Axon Instruments).

Hemichannel current measurements in Xenopus oocytes: These experiments were conducted by our collaborators at the Rosalind Franklin University in Chicago, Illinois. Briefly, oocytes were injected with 4 ng of antisense phosphorothioated oligonucleotide directed against nucleotides 327-353 of endogenous *Xenopus* Cx38. After 3 days, oocytes were injected again with connexin RNA mixed with 4 ng antisense oligonucleotide. Approximately 24 h after injection, oocytes were stripped of their vitelline membrane and paired overnight in agar wells. Oocytes were continuously bathed in half-strength L15 media (Sigma). Junctional currents were assessed using the dual oocyte voltage clamp technique as described previously (Skerrett IM et al., 2001). Oocytes were clamped at approximately -30 mV using two Geneclamp500 Amplifiers (Axon Instruments). Transjunctional conductances were measured by a 10 mV

voltage pulse. Data were acquired and analyzed using Pclamp8 software (Axon Instruments).

Data are expressed as mean ± standard error of the mean (S.E.M.). A Student's *t* test was used to test statistical significance. Differences were deemed significant at a p value <0.05.

2.9. Mouse model

A transgenic mouse model expressing the human Cx40 mutation, P88S, found in a patient with AF (Gollob MH et al. 2006) or human WT Cx40 were used for relative quantification studies. The transgenes were designed to code for the human sequence of Cx40 under expression of the atrial-specific atrial natriuretic factor (ANF) promoter. The 3'UTR of the transgene corresponds to the 3'UTR of human growth hormone (hGH) sequence.

2.10. Harvesting of mouse heart tissue

Heart tissue was taken from hCx40-WT and hCx40-P88S transgenic mice. Mice were injected with an analgesic (buprinex) 1hr prior to tissue harvest and then anesthetized using 2.5-4% isoflurane. Hearts were perfused with 1X PBS to wash out blood from the heart. Left atria and right atria were cut and separated in different tubes. Heart tissues were frozen in liquid nitrogen and then transferred to -80°C. The mice from each group had a mean age of 7-8 months at time of death. Procedure was carried out in accordance with the Animal Care and Veterinary Services Committee of the University of Ottawa.

2.11. Total RNA isolation from heart tissue

Heart tissues were retrieved from -80°C immediately prior to RNA isolation. TRIzol (Invitrogen) was used for the isolation of total RNA according to the manufacturer's protocol. Tissues were homogenized in TRIzol using a glass mortar and pestle. The concentration of isolated RNA and the quality of the RNA were determined using a spectrophotometer. RNA samples were treated with RNase-free DNaseI for 2hrs at 37°C (Promega) prior to reverse transcription.

2.12. Reverse-transcription

Reverse transcription (RT) was performed on total RNA with the Omniscript Reverse Transcription Kit (Qiagen). First-strand cDNA was synthesized at 37°C for 2 hours using an oligo-$dT_{(15)}$ in conjunction with Qiagen Rnase Inhibitors (4u/20ul RT reaction). 100ng of total RNA is used per 20uL for each RT and RT-minus control reactions. cDNA from five transcription reactions were pooled together and cleaned using the QIAquick PCR Purification kit (Qiagen). Cleaned cDNA was eluted from the column in 10ul of Rnase free water.

2.13. Relative mRNA quantification by real-time PCR

Relative mRNA quantification was performed by real-time PCR using the LightCycler480 (Roche) instrument and the LightCycler 480 SYBR Green I Master kit (Roche). Mouse glyceraldehydes-3-phosphate dehydrogenase (mGAPDH) and mouse β-actin (mActB) were chosen as reference genes. A no template control (NTC) reaction was run on each plate. PCR reactions of 10ul contained 5ul of SYBR Green, 2.5ul of cDNA, 0.5mmol of each primer and water.

Cycling protocol was as follows: 1x(95°C for 10min), 45x(95°C for 10s, 63°C for 10s, 72°C for 10s). Fluorescence intensity was acquired after the end of each extension phase at 72°C for every cycle. Primer sequences were as follows (5'→3'):

Mouse GAPDH:	F: actcccactcttccaccttcg
	R: caccctgttgctgtagccgta
Mouse ActB:	F: tgatggtgggaatgggtcagaa
	R: tcgtcccagttggtaacaatgc
Mouse Cx40-3'UTR:	F: atagtggaggcaggatcaggaa
	R: ggtatgttgctggtgttgaacc
Human Cx40/human Growth Hormone:	F: gctatcatagtgacaagcgacg
	R: actggagtggcaacttccagg

The transgenes were amplified with a forward primer annealing to the hCx40 sequence and a reverse primer annealing to the 3'UTR human growth hormone sequence thus allowing for specific amplification of the transgene and not endogenous mCx40.

The amplicon lengths of each gene in base pair (bp) were as follows:

mGAPDH	107bp
mActB	115bp
mCx40	73bp
hCx40/hGH	139bp

SYBR Green is a fluorescent dye which intercalates between any dsDNA and therefore does not distinguish between the specific amplicon and primer dimmers or non specific amplification. To ensure that amplification was specific to the gene of interest, a melting curve analysis was performed at the end of every real-time PCR experiment. The melting curve protocol was 1x(95°C for 5s, 65°C for 1min then denaturing up to 97°C at 0.11°C/s and continuously acquiring fluorescence every 5 seconds). The amplified products were also separated on agarose gels to confirm the amplification of single PCR products. Data was collected and analyzed using the LightCycler480 software. The analysis method used for generating the standard curve is the Second Derivative Maximum Method from the LightCycler software. The analysis method used for relative quantification is the Advanced Relative Quantification Method from the LightCycler software.

The relative expression levels will be determined by normalization to a reference gene. The use of two reference genes corrects for differences in RNA and cDNA quality and quantity. Every sample, calibrator and negative controls were prepared in triplicates. Calibrators allow us to compare samples between different runs without having to run a standard curve each time. The calibrator normalizes the target/reference ratio of each sample in order to correct for differences between different real-time PCR runs. A standard curve needs to be generated for each gene studied in order to obtain a reaction efficiency that represents best the performance of the PCR amplification. The reaction

efficiency obtained from the standard curve of each gene is applied to the analyses of relative quantification allowing for more precise and accurate results. Triplicates with a greater than 0.4 crossing point (Cp) difference were excluded from the quantification analyses.

2.14. Statistical analysis

Statistical analysis was carried out with the Microsoft Excel software. Values are reported as mean ± standard error of the mean (SEM). An unpaired Student's t-test was used to test statistical significance between two samples. Differences were deemed significant at a p value <0.05.

3. Results

3.1. Somatic Cx43 mutation (Cx43-932delC)

3.1.1. Cx43-932delC trafficking in mammalian cells and atrial tissue

HeLa cells, a human cervix carcinoma cell line, which does not express significant levels of connexins, are considered communication deficient. This cell line has been used in numerous papers for studying connexin trafficking (Valiunas V et al., 2000). HeLa cells transiently transfected with Cx43-WT showed normal localization and formation of gap junction plaques at sites of cell-to-cell contact (Figure 6.a). The gap junction plaque observed on the left corresponds to the site of cell-to-cell contact on the right (right panel). In contrast, expression of Cx43-932delC alone consistently showed intracellular

retention and aggregation with no formation of gap junction plaques at the interface of paired cells (Figure 6.b). Gap junction formation was absent at the site of cell-to-cell contact (right panel). Fluorescently tagged connexins at the C-terminus have been widely used in the literature and don't affect trafficking or function of connexins. To confirm that intracellular retention of the mutant was not caused by the fluorescent tag, immunolabeling of cells expressing untagged constructs was performed (Figure 7). Localization of wild-type and mutant protein was similar to what was observed for fluorescently tagged connexins. The Cx43 frameshift mutation causes intracellular retention uncharacteristic of wild-type connexin trafficking.

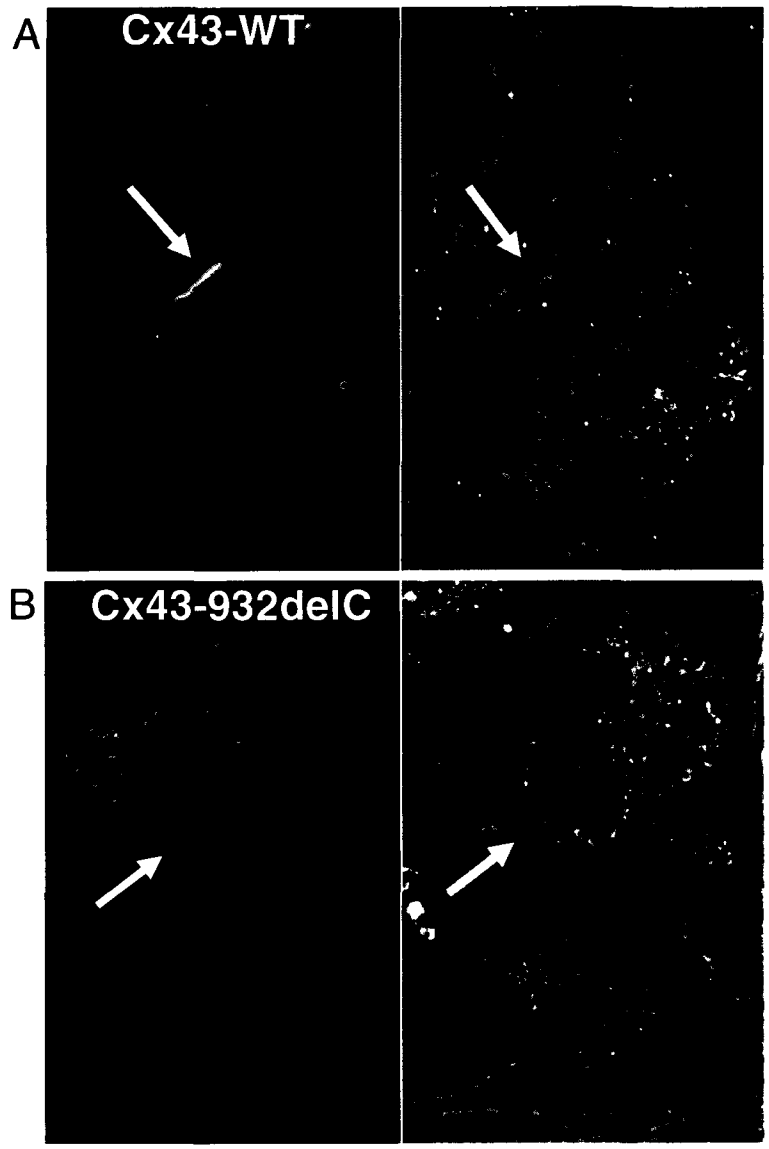

Figure 6. Cellular localization of YFP-labeled wild-type and mutant Cx43 in HeLa cells. HeLa cells transiently transfected with Cx43-WT (A) and Cx43-932delC (B) constructs. Live cells were visualized under a confocal microscope 24 hours post-transfection. Phase contrast images (Right panels) of cells displayed on the left indicate sites of cell-to-cell contact (arrows).

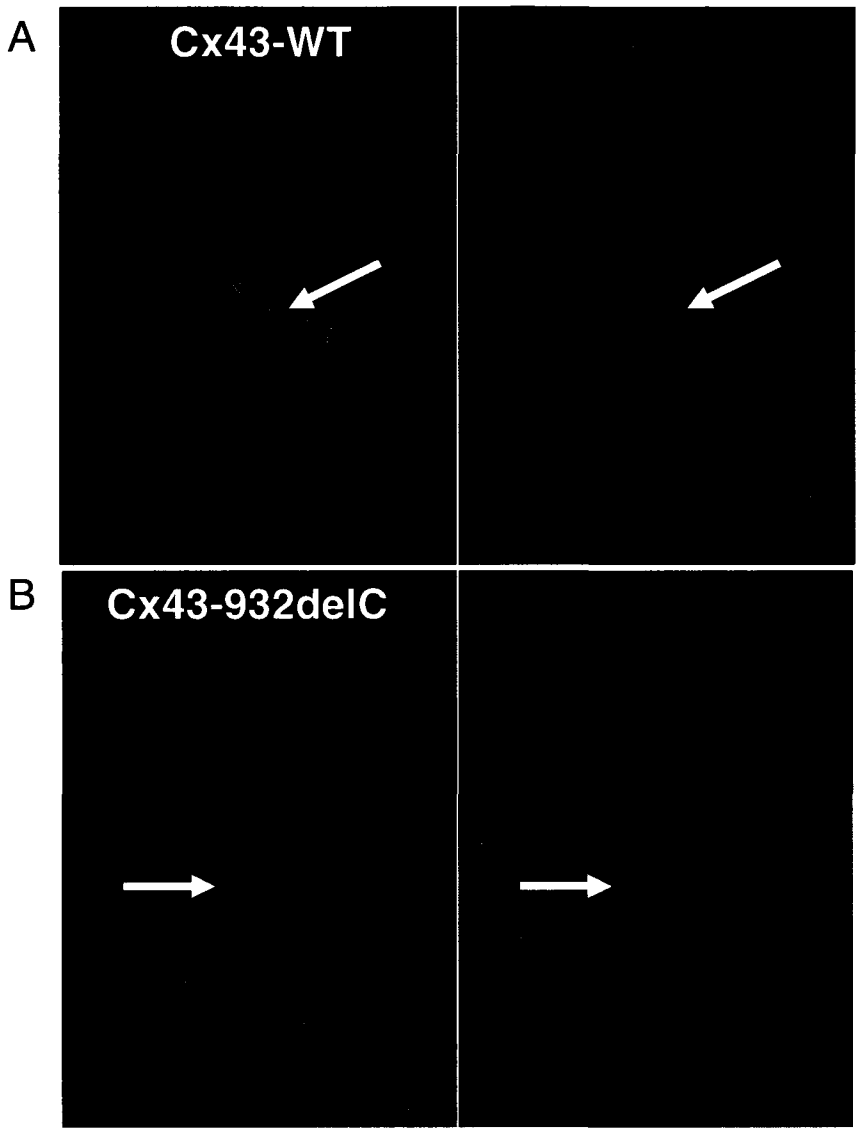

Figure 7. Immunofluorescence of HeLa cells transiently expressing untagged Cx43-WT and Cx43-932delC constructs. Cells expressing WT (A) or mutant Cx43 (B) were immunolabeled with a Cx43 antibody recognizing amino acids 131-142 of the intracellular loop. DyLight488-conjugated secondary antibody enabled visualization under a confocal microscope. Phase contrast images (Right panels) of cells displayed on the left indicate sites of cell-to-cell contact (arrows).

Immunohistochemical stainings of atrial tissue were performed by Louise Pelletier from the Department of Pathology at the University of Ottawa (Appendix A, Figure S1). The Cx43 antibody targets amino acids 131-142 which corresponds to a region in the intracellular loop therefore able to recognize both WT and mutant Cx43 proteins. Atrial tissue from control patients immunolabeled with antibodies against Cx43 (Appendix A, Figure S1, A) or Cx40 (Appendix A, Figure S1, C) demonstrate typical localization of gap junction plaques at the intercalated disks between adjacent cells. Staining of the atrial tissue from the affected patient, in which the Cx43-932delC mutation was identified, demonstrated a mosaic pattern of intracellular retention as well as normal trafficking of Cx43 (Appendix A, Figure S1, B). Thin arrows indicate intercalated disks that look normal while thick arrows indicate intracellular staining. Immunodetection of Cx40 (Appendix A, Figure S1, D) in the atrial tissue of the affected patient resulted in a similar mosaic pattern of intracellular retention, suggesting that Cx40 is retained inside the cell due to co-expression of mutant Cx43 in myocytes. This observation is consistent with the intracellular aggregation of Cx43-932delC and Cx43 observed in HeLa cells, indicating that HeLa cells are a good cell model for the study of connexin trafficking.

3.1.2. Cx43-932delC effect on Cx43-WT and Cx40-WT localization

To assess the ability of Cx43-932delC to form gap junction plaques in a heterozygous state, Hela cells were co-transfected with Cx43-932delC and wild-type Cx43 or Cx40. Cx43-932delC caused the intracellular retention of Cx43-WT

(Figure 8.a) suggesting that the mutant Cx43 has a dominant negative effect on Cx43-WT trafficking. To assess for a *trans*-dominant effect of Cx43-932delC on Cx40 WT, HeLa cells were first co-transfected with Cx43-WT and Cx40-WT. Both WT isoforms seemed to co-localize and trafficked properly to the cell membrane where they formed gap junction plaques at the interface of paired cells (Figure 8.b). Co-transfection of Cx43-932delC with Cx40-WT caused intracellular retention of Cx40-WT suggesting that mutant Cx43 has a *trans*-dominant negative effect on Cx40-WT trafficking (Figure 8.c). These results support the concept that Cx43 and Cx40 may interact to form heteromeric channels.

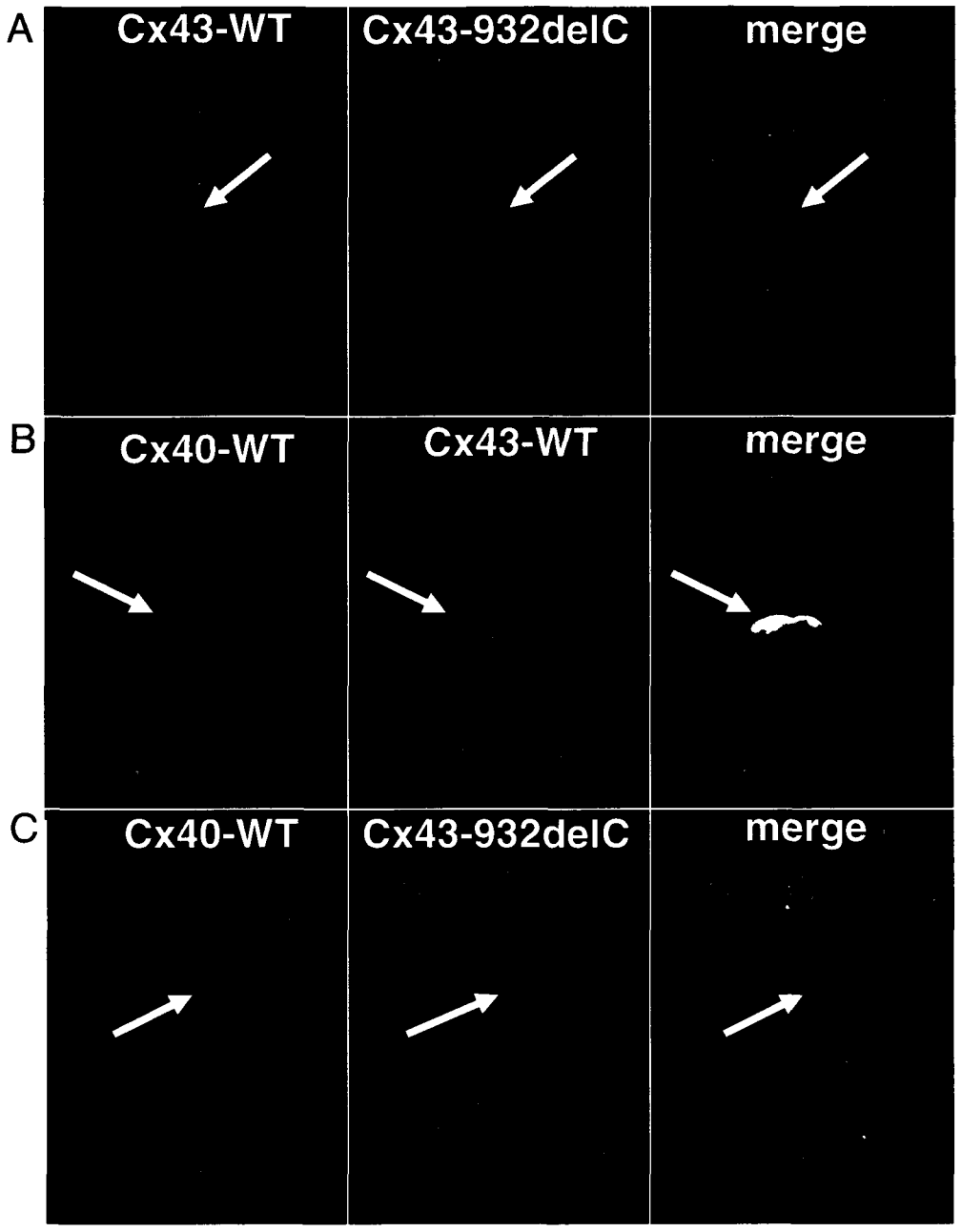

Figure 8. Effect of Cx43-932delC on Cx43-WT and Cx40-WT trafficking in HeLa cells. (A) Co-transfection of fluorescently tagged Cx43-932delC and Cx43-WT in HeLa cells simulates the effect of a heterozygous state. Cx43-WT and Cx40-WT were first co-expressed (B) to insure proper trafficking of both wild-type isoforms. To test for a *trans*-dominant effect, Cx43-932delC and Cx40-WT were co-transfected in HeLa cells (C). Arrows indicate sites of cell-to-cell contact.

3.1.3. Cx43-932delC subcellular co-localization

Figures 6b and 7b demonstrated that Cx43-932delC is retained inside the cell. To determine in which subcellular compartment the mutant protein is retained, HeLa cells were co-transfected with Cx43-932delC and a fluorescently tagged ER or Golgi resident protein. These two organelles were chosen since connexins follow the classical secretory pathway. By assigning a color of red and green to the fluorescent signal of each protein, co-localization can be seen as yellow in merged images. The ER marker codes for calreticulin and the Golgi marker codes for 1,4-galactosyltransferase. Cx43-WT traffics normally in cells co-expressing the calreticulin protein (Figure 9.a). Cells co-expressing Cx43-932delC with calreticulin do not show co-localization of the mutant with the resident ER protein (Figure 9.b). Cx43-WT traffics normally when cells are co-expressing the 1,4-galactosyltransferase protein (Figure 9.c). Co-localization of Cx43-932delC with 1,4-galactosyltransferase was evident, indicating that the mutant connexin is mostly retained within the Golgi apparatus (Figure 9.d).

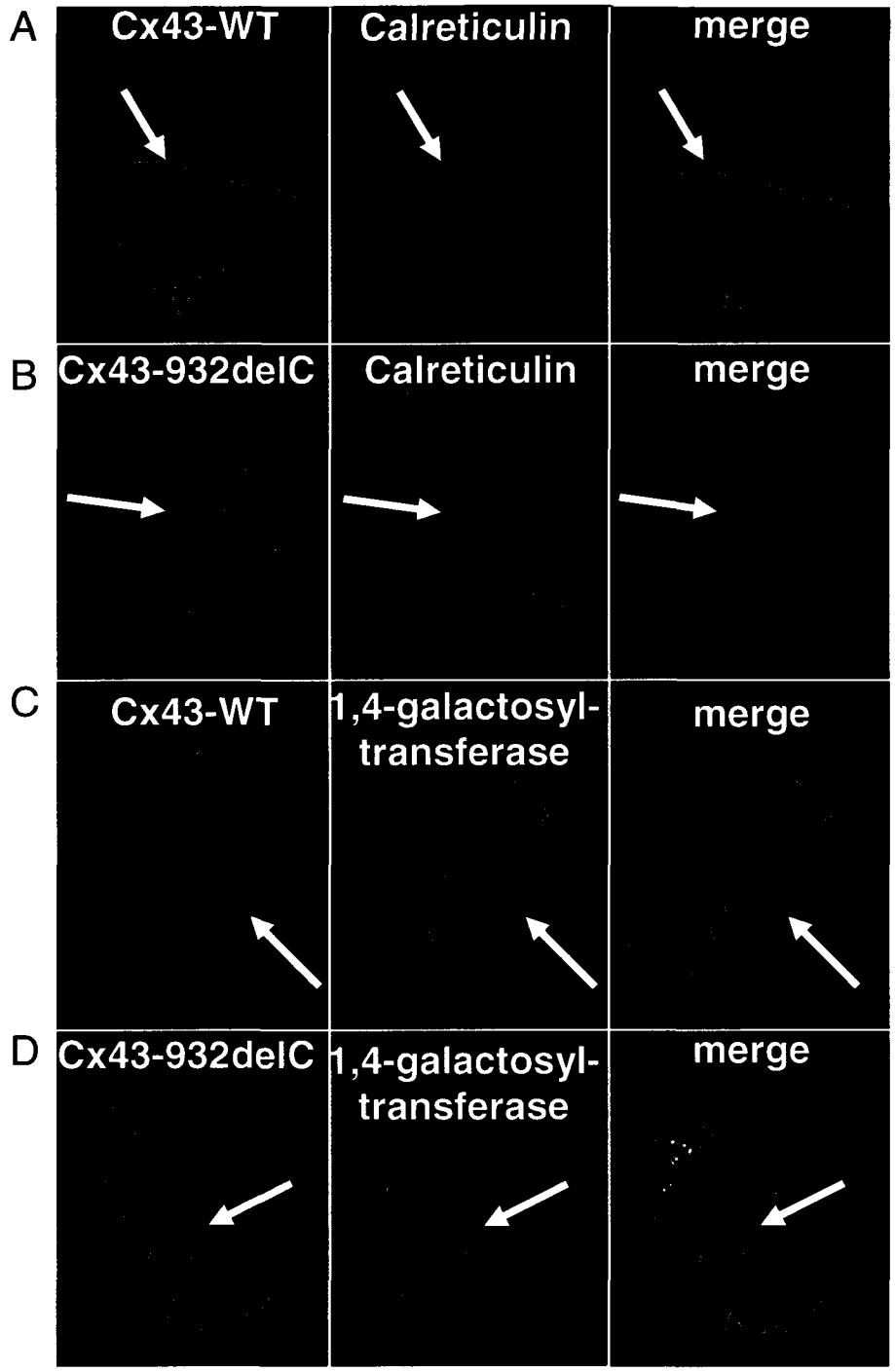

Figure 9. Subcellular co-localization of Cx43-932delC with ER and Golgi proteins in HeLa cells. An ER marker, coding for calreticulin, was co-transfected with Cx43-WT (A) and Cx43-932delC (B). A Golgi marker, coding for 1,4-galactosyltransferase was co-transfected with Cx43-WT (C) and Cx43-932delC (D). Co-localization, in yellow, seen in (D, merge) corresponds to overlapping red and green fluorescence. Arrows indicate sites of cell-to-cell contact.

3.1.4. Gap junction conductance of Cx43-932delC in a homozygote or heterozygote state

Gap junction conductance is measured by the dual whole cell voltage clamp technique which was performed by Qiuju Li. Gap junction deficient N2A cells are often used in patch clamp recordings of gap junctions because they do not express detectable levels of endogenous connexins. By applying a voltage protocol to one cell of a cell pair of untransfected N2A cells, Fang W et al. recorded no current response in the second cell (Fang W et al., 2000). A representative current tracing demonstrates a large reduction in current measured in paired N2A cells expressing mutant Cx43, as compared to cells expressing Cx43-WT, in response to the voltage protocol applied to cell 1 (Figure 10.a). Pooled data from numerous N2A cell pairs obtained from several transfections show a significantly reduced gap junction conductance in cells expressing mutant Cx43 alone in comparison to cells expressing Cx43-WT alone ($p<0.01$) (Figure 10.b). Paired N2A cells co-transfected with Cx43-932delC and Cx43-WT in equal ratios had a significant reduction in conductance compared to cells expressing Cx43-WT alone ($p<0.04$) (Figure 10.b). Co-expression of Cx43-932delC and Cx40-WT also produced a significant decrease in conductance when compared to cells expressing Cx40-WT alone ($p<0.04$) (Figure 10.b). These results support the observations made in trafficking studies that Cx43-932delC has a dominant negative and *trans*-dominant negative effect on Cx43-WT and Cx40-WT, respectively.

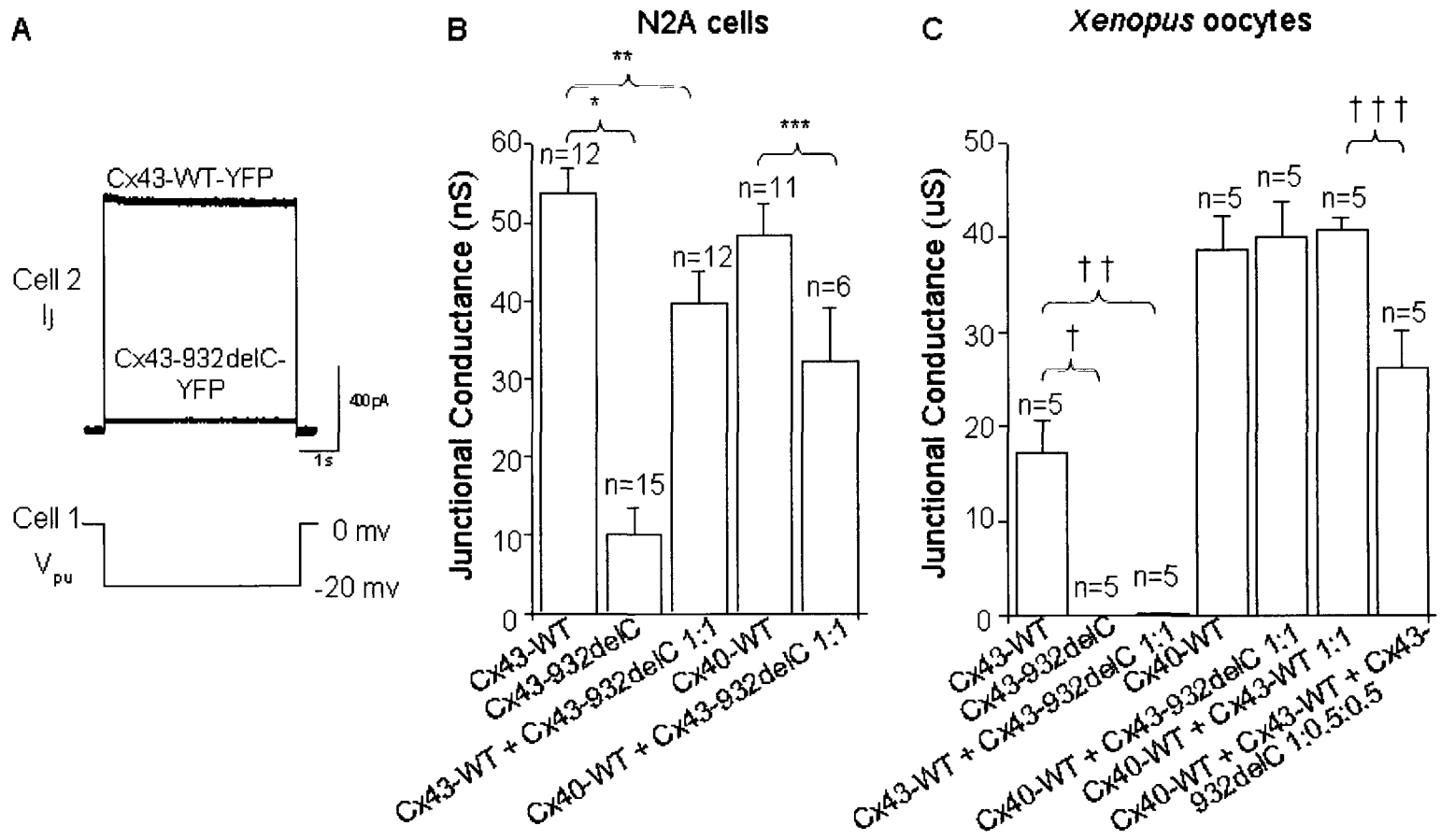

Figure 10 Effect of Cx43-932delC on Cx43 and Cx40 gap junction conductance in N2A cells and *Xenopus* oocytes (A) Representative current tracing of N2A cells expressing tagged Cx43-932delC and tagged Cx43-WT (B) Mean junctional conductance of paired N2A cells transfected with YFP- or CFP-labeled connexins (*p<0 01, **p<0 04 as compared to Cx43-WT, ***p<0 04 as compared to Cx40-WT) (C) Mean junctional conductances of *Xenopus* oocyte pairs injected with various combinations of untagged Cx43, Cx43-932delC and Cx40 cRNAs in the ratios indicated (†<0 00003, ††<0 00004 as compared to Cx43-WT, †††<0 007 as compared to Cx40-WT+Cx43-WT 1 1) The number of cell pairs tested for each condition is indicated above each bar which were pooled from various transfections Data shown in (A) and (B) were acquired by Qiuju Li and data in (C) by our collaborators at the University of Texas Health Science Centre in San Antonio

Since co-transfection protocols cannot assure an equal ratio of cDNA uptake into cells and therefore cannot assure a 1:1 stoichiometry of mutant and WT clones, the studies were repeated in a *Xenopus* oocyte cell model by our collaborators in Texas. In oocyte studies, a precise cRNA quantity for each clone is directly injected into cells. The same conclusion was reached although some differences were observed between the results obtained from the oocyte and mammalian cell studies. Expression of the mutant Cx43 alone or with Cx43-WT completely abolished conductance between paired oocytes ($p<0.00003$ and $p<0.00004$, respectively) (Figure 10.c). Contrarily to studies in N2A cells, co-expression of the mutant with Cx40-WT did not alter the conductance suggesting that in the oocyte expression system, these two isoforms could not interact together to form heteromeric channels (Figure 10.c). Co-expression of Cx43-932delC with Cx43-WT and Cx40-WT, in ratios that reflect more physiological conditions, resulted in significant reduction in gap junction conductance in paired *Xenopus* oocytes ($p<0.007$) (Figure 10.c). Results obtained from both expression models indicate that mutant Cx43-932delC has a dominant and *trans*-dominant effect on the gap junction conductance of both Cx43-WT and Cx40-WT.

3.2. Three novel Cx40 mutants (Cx40-G311S, Cx40-F30L and Cx40-R113S)

3.2.1. Trafficking of Cx40 mutants

HeLa cells transfected with YFP-tagged Cx40-WT showed proper localization to the cell membrane and formation of gap junction plaques at sites

of cell-to-cell contact (Figure 11.a). The Cx40-G311S mutant showed a similar localization pattern to Cx40-WT (Figure 11.b). Cx40-R113S also trafficked normally and was able to form gap junction plaques (Figure 11.c). Cells transfected with the Cx40-F30L mutant also showed formation of gap junction plaques with a slight increase in intracellular retention (Figure 11.d). The discontinuity of the plaque in D does not reflect abnormal trafficking. Thus, these mutants appeared to exhibit normal cellular localization.

3.2.2. Electrical conductance of Cx40 mutants

Pairs of N2A cells expressing Cx40-G311S, Cx40-F30L or Cx40-R113S demonstrated junctional conductances with mean values similar to those in cells transfected with Cx40-WT (Figure 12). Although we observed a trend of lower conductance in cells transfected with Cx40-G311S and Cx40-F30L, no significant differences in conductance were measured compared to Cx40-WT. These experiments were repeated by our collaborators in *Xenopus* oocytes where the same conclusion was reached (data not shown).

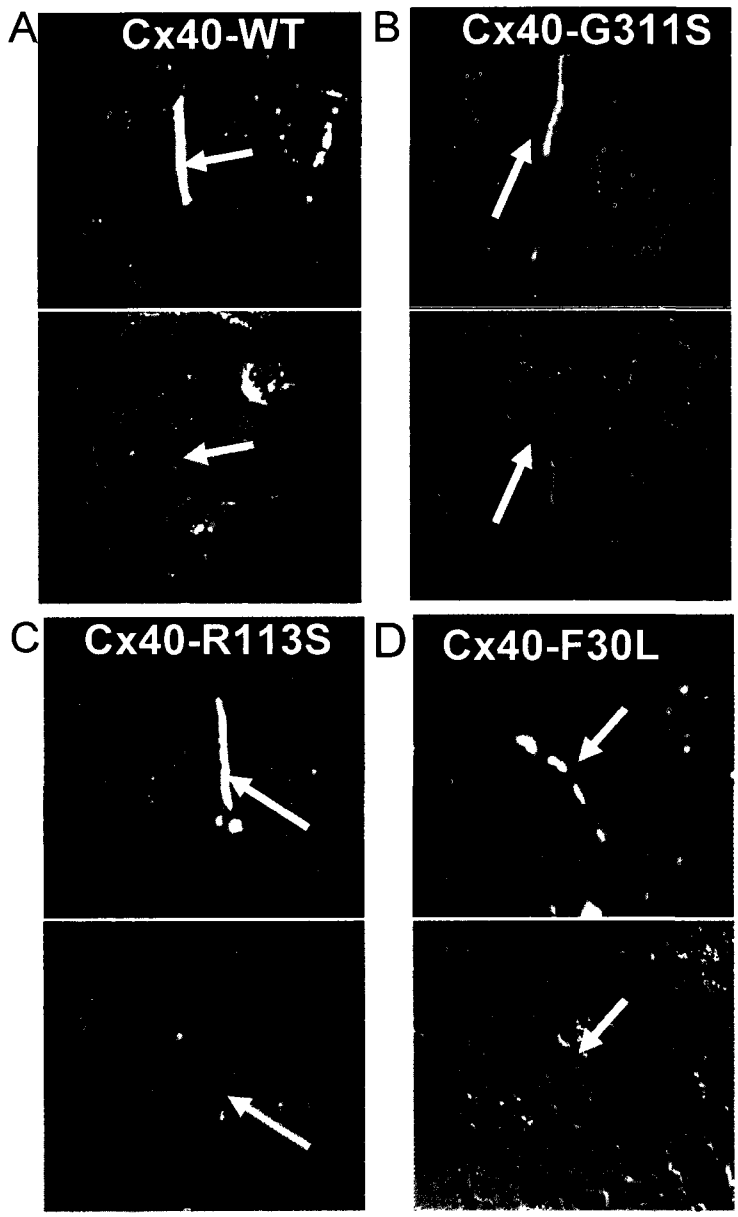

Figure 11. Localization of fluorescently labeled Cx40-WT and three Cx40 mutants in HeLa cells. HeLa cells were transiently transfected with 1 ug of YFP-labeled Cx40-WT (A), Cx40-G311S (B), Cx40-R113S (C) or Cx40-F30L (D) as shown in top images. The discontinuity of the plaque in D does not reflect abnormal trafficking. Bottom images correspond to phase contrast images of the cells shown on top. Arrows indicate sites of intercellular contact.

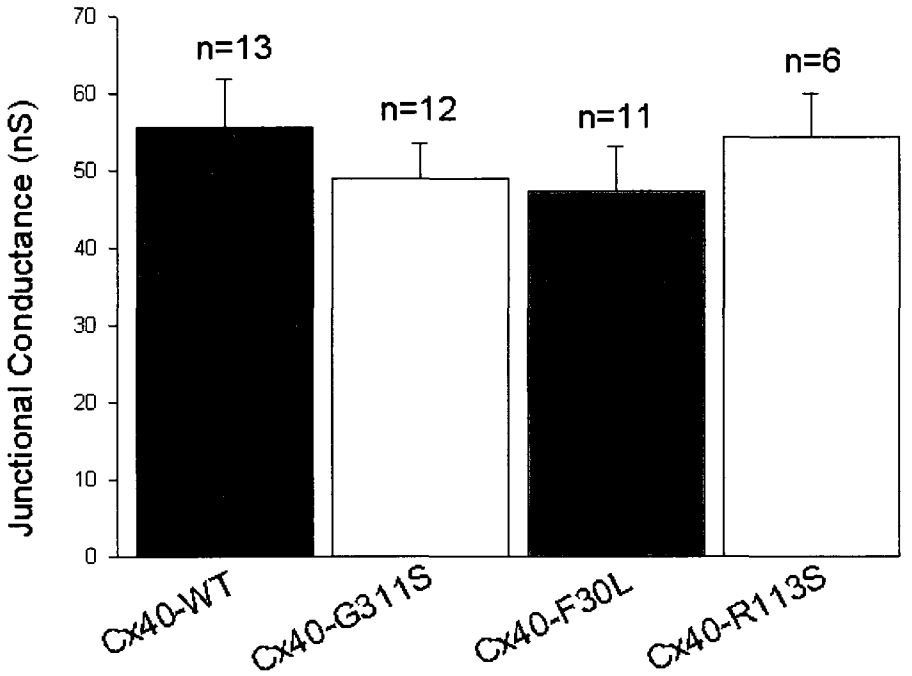

Figure 12. Gap junction conductance of paired N2A cells expressing fluorescently tagged connexin40 constructs. Data pooled from numerous paired N2A cells transiently transfected with Cx40-WT, Cx40-G311S, Cx40-F30L or Cx40-R113S. The number of cell pairs tested is indicated above each bar which was pooled from various transfections. Variation in mean junctional conductances between mutants and WT were not statistically significant. Experiments performed by Qiuju Li.

Cx40-G311S and -R113S are found in the C-terminal and intracellular loop, respectively, which are the two domains involved in the "ball and chain" gating mechanism for pH sensitivity. Under intracellular acidification, gap junction channels close to prevent acidification of surrounding cells. These experiments were performed by Qiuju Li. The junctional conductance was measured in response to various intracellular pH values. Both mutants showed a significant increase in sensitivity to intracellular acidification (Figure 13). G311S channels started to show a significant reduction in conduction at pH 7.0

(p=0.046) and R113S started to show a reduction in conductance at pH 6.8 (p=0.044). At pH 6.4, the conductance was very poor for all three constructs, suggesting that at this level of acidification the gap junction channels were non functional.

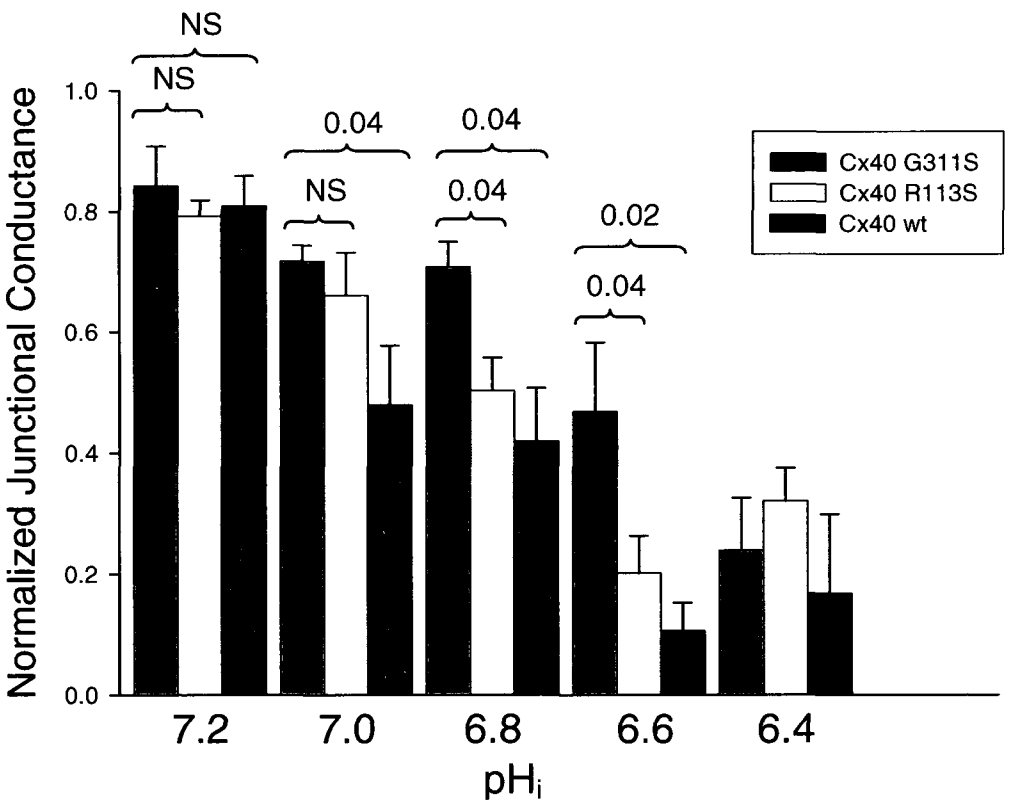

Figure 13. Effect of intracellular acidification on gap junction conductance in paired N2A cells expressing Cx40-WT, Cx40-G311S or Cx40-R113S constructs. Paired cells expressing tagged connexin constructs were exposed to different measures of intracellular pH. Data pooled from numerous transfections and averaged with an *n* between 4 and 11 cell pairs. P values are indicated above bar graph. NS denotes no statistical difference between samples. Experiments performed by Qiuju Li.

The ability of hemichannels to open in non-junctional areas of the cell membrane is an emerging concept in the literature. Several mutant connexins associated with various human diseases have demonstrated abnormal hemichannel activity. To test this concept in the case of Cx40 mutations associated with AF, our collaborators at the Rosalind Franklin University measured hemichannel currents in *Xenopus* oocytes injected with Cx40-WT, Cx40-G311S or Cx40-F30L mutants. Cx40-WT and Cx40-G311S did not produce functional hemichannels as the current response was similar in control oocytes injected with water (Appendix A, Figure S2.a). Interestingly, Cx40-F30L hemichannel currents were significantly greater than currents measured in oocytes injected with Cx40-WT suggesting a gain-of-function mutation (Appendix A, Figure S2.a).

Our collaborators also observed cell death of oocytes injected with Cx40-F30L cRNA after an incubation period of 12-18 hours shown by blebbing of ooplasm (white arrow) and pigment disorganization (black arrow) of oocytes (Appendix A, Figure S3.c). Cell death was not observed in control oocytes injected with water or Cx40-WT (Appendix A, Figure S3.a, b). Numerous studies have shown that increasing extracellular Ca^{+2} concentrations suppresses gap junction hemichannel activity. The addition of 2mM calcium in the media prevented cell death supporting the concept that calcium inhibits hemichannel activity (Appendix A, Figure S3.d). The addition of 1mM Ca^{+2} in the media

resulted in hemichannel closure of the mutant F30L (Appendix A, Figure S2.b). This cell death phenomenon was not examined in mammalian cells.

3.3. Further characterization of the previously reported Cx40-P88S mutation

A P88S mutation has been reported in Cx40, Cx32 and Cx50 in association with AF, Charcot-Marie-Tooth and cataracts, respectively. Expression of the Cx40-P88S alone in mammalian cells demonstrated diffused intracellular retention inside the cell (Gollob MH et al., 2006). The Cx40-P88S mutation arises from a C to T mutation at nucleotide position 262 (where 'A' of ATG is position 1) and results in a proline change to a serine. The mutation is located in the highly conserved second transmembrane domain (Figure 5). To determine the site of intracellular retention and to demonstrate the effect of the mutant on wild-type connexin trafficking, all three connexin P88S mutant constructs were fluorescently tagged and expressed alone or with their respective wild-type isoform in HeLa cells.

3.3.1. Cx40-P88S subcelluar co-localization

Intracellular trafficking of fluorescently tagged Cx40-P88S was observed in transiently transfected HeLa cells. The cellular distribution of P88S was very diffuse inside the cell and it is rarely observed at the cell membrane or at sites of cell-to-cell contact (Figure 14). The P88S localization observed was the same as the previously published result in N2A cells (Gollob MH et al., 2006). To determine in which subcellular compartment the mutant P88S protein is retained,

HeLa cells were co-transfected with a fluorescently tagged ER or Golgi marker. Cells co-transfected with Cx40-P88S and the ER marker show co-localization which is shown in orange in the overlay (Figure 15.a). Cx40-P88S also co-localizes to a similar extent with the Golgi marker which is shown in yellow in the overlay (Figure 15.b). Co-localization with both ER and Golgi markers indicates that the retention is not confined to a specific intracellular compartment. This observation suggests that the mutation may affect protein insertion or folding into the membrane which normally occurs in the ER, or it may interfere with the oligomerization process which is known to occur in the Golgi.

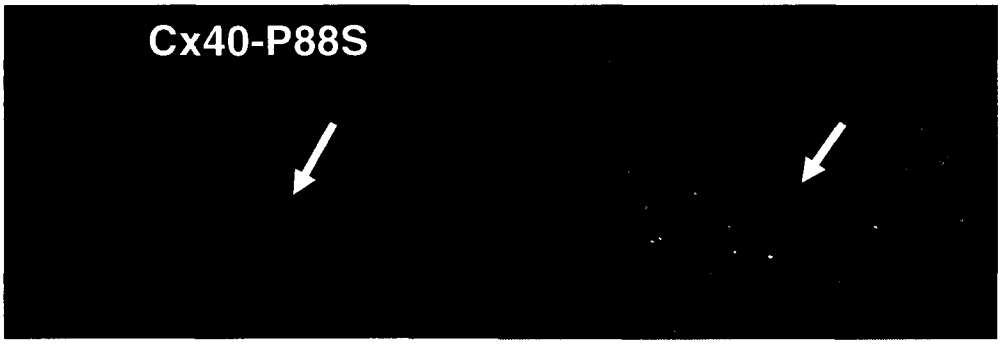

Figure 14. Cx40-P88S localization in transiently transfected HeLa cells. *Left*, Fluorescently labeled Cx40-P88S expression in HeLa cells confirm previously reported findings of intracellular retention. *Right,* phase contrast images of cells shown on the left. Arrows indicate sites of intercellular contact.

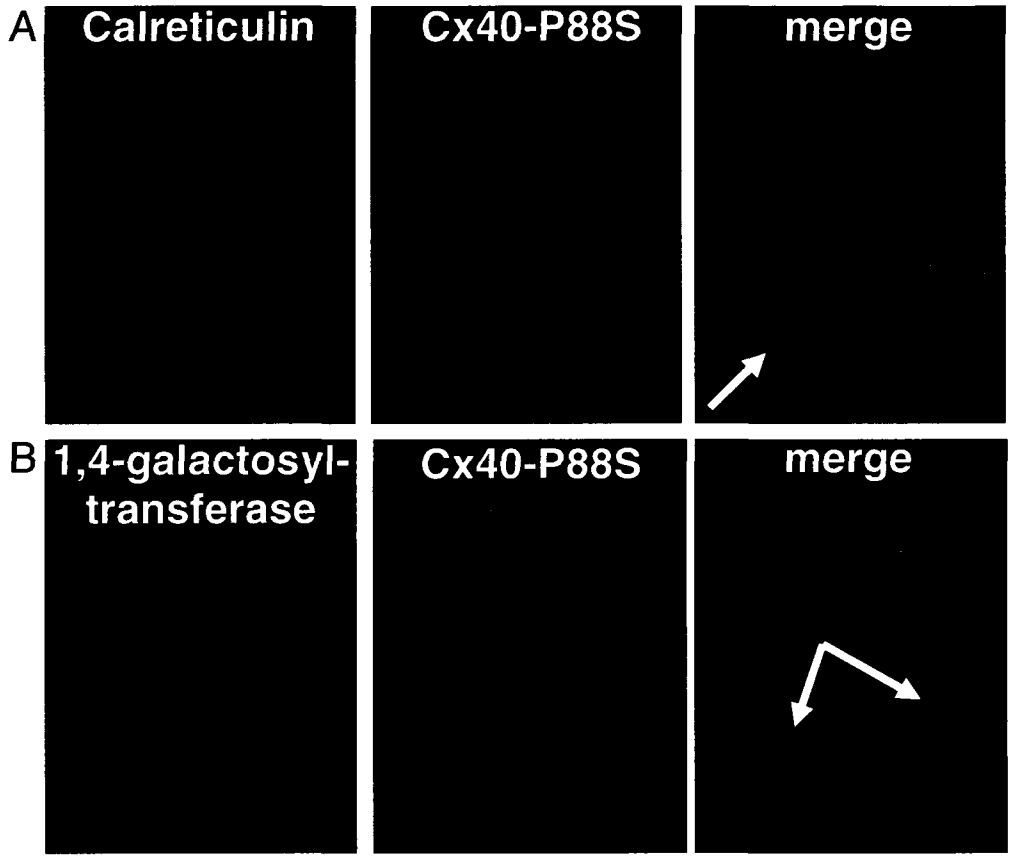

Figure 15. Cx40-P88S subcellular localization in HeLa cells. Cx40-P88S co-transfected with calreticulin (A) or 1,4-galactosyltransferase (B) which are ER and Golgi protein markers, respectively. Co-localization corresponds to overlapping red and green fluorescence. Arrows indicate areas of co-localization.

3.3.2. Cx40-P88S effect on Cx40-WT and Cx43-WT localization

HeLa cells co-expressing Cx40-P88S and Cx40-WT demonstrated rescue of P88S to gap junction plaques (Figure 16.a). A phenotype of rescue was also observed when Cx40-P88S and Cx43-WT were co-transfected together (Figure 16.b). These results were surprising given the data previously published which showed a loss of electrical coupling between oocytes co-injected with mutant

P88S and Cx40-WT or Cx43-WT. However, rescue of trafficking of the mutant P88S to the membrane may not predict rescue of conductance and remains a focus for ongoing evaluation in our lab.

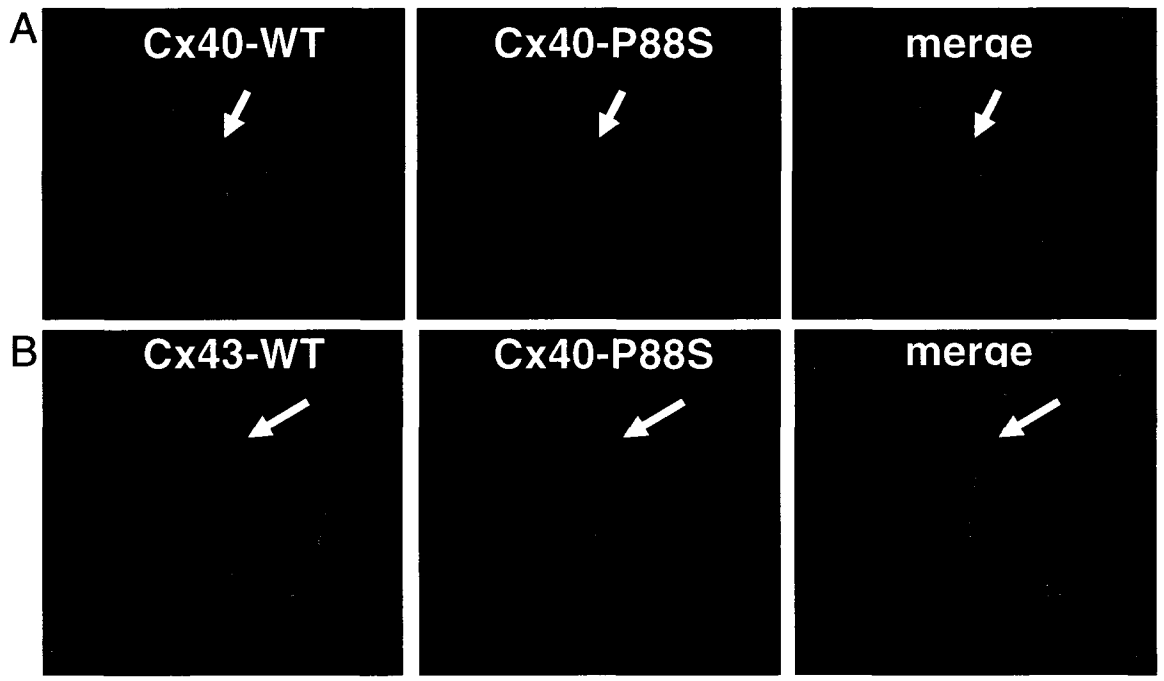

Figure 16. Effect of Cx40-WT and Cx43-WT on P88S trafficking in HeLa cells. Cellular localization of Cx40-P88S when co-expressed with Cx40-WT (A) or Cx43-WT (B). Co-localization, shown in yellow, corresponds to overlapping red and green fluorescence. Arrows indicate sites of cell-to-cell contact.

In order to assess the frequency of observed rescue in HeLa cells co-transfected with Cx40-P88S and Cx40-WT, the number of paired cells showing localization of Cx40-P88S at gap junction plaques was divided by the number of paired cells showing expression of both construct. The frequency of Cx40-P88S observed at gap junction plaques was significantly greater in the presence of Cx40-WT (38%) compared to the frequency of observed gap junction plaques in

cells transfected with P88S alone (10%) (*p=0.0004) (Figure 17). Cx40-WT forms gap junction plaques on its own in approximately 61% of paired HeLa cells observed.

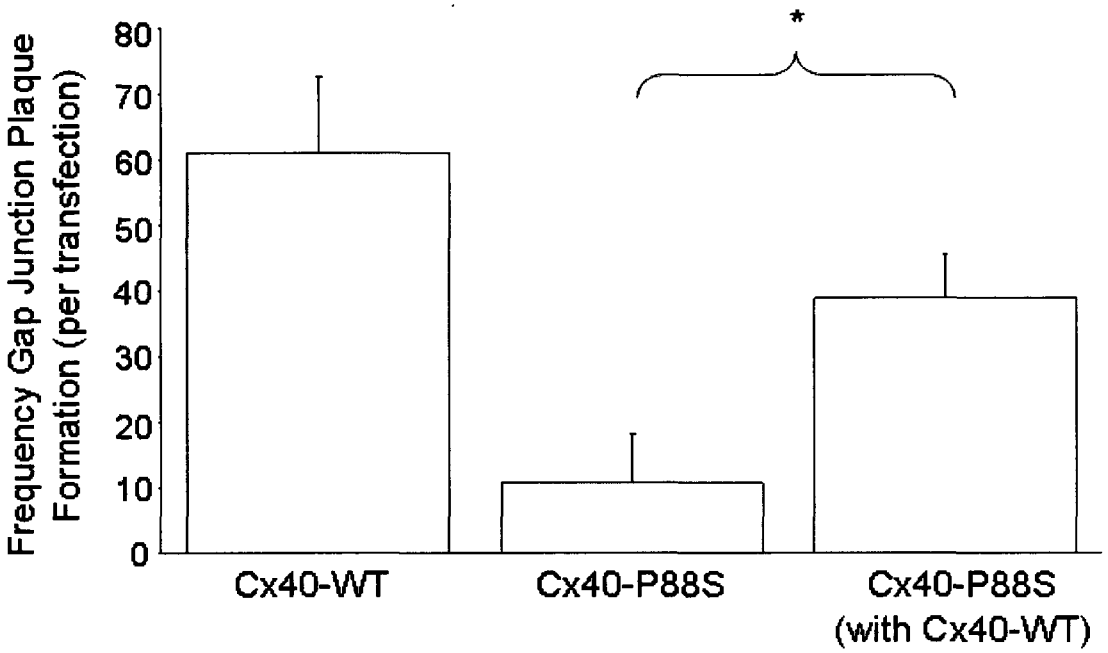

Figure 17. Frequency gap junction plaques observed in HeLa cells formed by Cx40-WT or Cx40-P88S. Pairs of HeLa cells showing gap junction plaques formed by either Cx40-WT alone, Cx40-P88S alone or by Cx40-P88S when co-expressed with Cx40-WT. Each column represents a mean percentage of gap junction plaques observed per transfection. Data was pooled from 5 to 6 transfections with a total number of 54 (Cx40-WT), 46 (Cx40-P88S) and 82 (Cx40-WT + Cx40-P88S) paired cells observed. The error bar corresponds to the standard deviation of the mean. A student t-test was performed between the averages calculated for Cx40-P88S and Cx40-WT+Cx40-P88S (*p=0.0004).

3.3.3. The P88S mutation in Cx32 and Cx50

Transfection of Cx32-WT in HeLa cells demonstrates normal gap junction formation (Figure 18.a). In contrast to wild-type, transfection of Cx32-P87S

revealed an inability to form gap junctions at the interface of paired cells (Figure 18.b). Co-transfection of Cx32-WT and Cx32-P87S demonstrated a rescue pattern of P87S to gap junction plaques as seen with the P88S mutation in Cx40 (Figure 18.c). Co-localization is shown in yellow by overlapping red and green fluorescence signals.

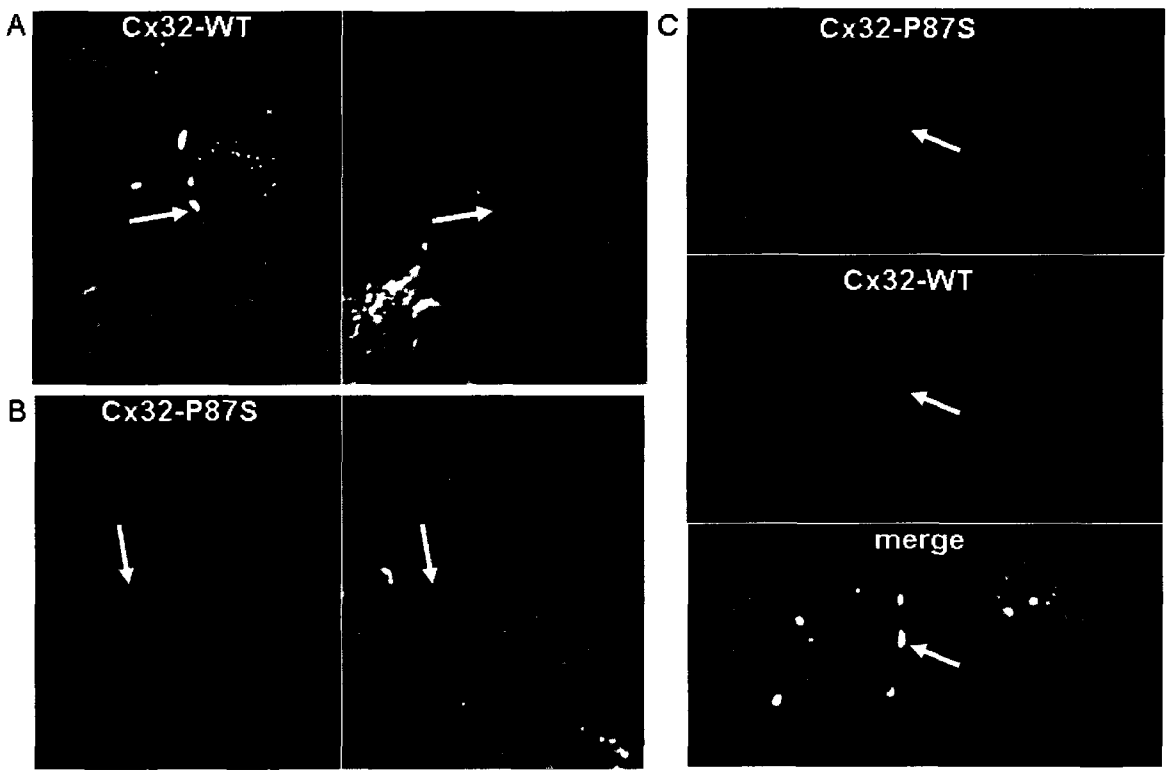

Figure 18. Effect of Cx32-WT on Cx32-P87S trafficking in HeLa cells. (A) *Left*, Transfection of HeLa cells with Cx32-WT (A, left), Cx32-P87S (B, left) or co-transfection of both WT and P87S mutant (C). Co-localization, shown in yellow, corresponds to overlapping red and green fluorescence. Phase contrast images (A and B, right) represent cells shown on the left. Arrows indicate sites of intercellular contact.

In order to assess the frequency of observed rescue in HeLa cells co-transfected with Cx32-P87S and Cx32-WT, the number of paired cells showing rescue of Cx32-P87S by Cx32-WT was divided by the number of paired cells showing expression of each construct. The frequency of Cx32-P87S observed at gap junction plaques was significantly greater in the presence of Cx32-WT (36%) compared to the frequency of observed gap junction plaques in cells transfected with P87S alone (9%) (*p=0.0014) (Figure 19). Cx32-WT forms gap junction plaques on its own in approximately 43% of paired HeLa cells observed.

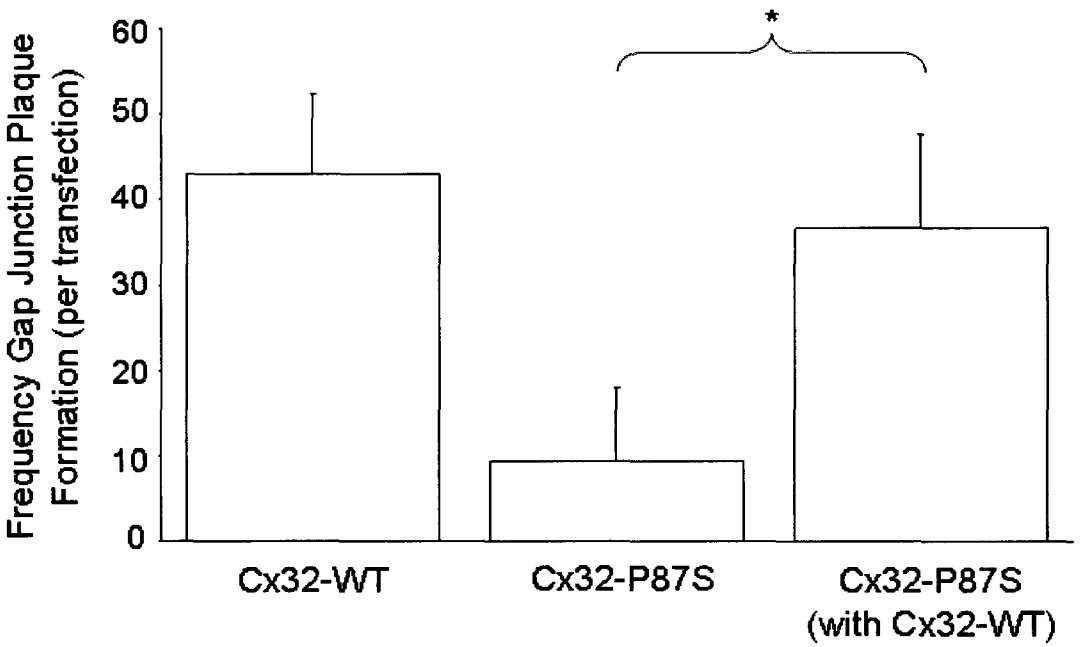

Figure 19. Frequency of gap junction plaques in HeLa cells formed by Cx32-WT or Cx32-P88S. Pairs of HeLa cells showing gap junction plaques formed by either Cx32-WT alone, Cx32-P87S alone or by Cx32-P87S when co-expressed with Cx32-WT. Each column represents a mean percentage of gap junction plaques observed per transfection. Data was pooled from 5 to 6 transfections with a total number of 67 (Cx32-WT), 48 (Cx32-P87S) and 86 (Cx32-WT + Cx32-P87S) paired cells observed. The error bar corresponds to the standard deviation. A student t-test was performed between the averages calculated for Cx32-P87S and Cx32-WT+Cx32-P87S (*p=0.0014).

The Cx50-WT protein fluorescently tagged at the C-terminus is unable to traffic normally. It forms aggregates inside the cell that are uncharacteristic of Cx50 trafficking (Figure 20). Different amounts of the vector used for transfection were tested (1ug, 0.5ug, 0.25ug and 0.1ug). Cells transfected with a lower amount of vector showed the same localization pattern as cells transfected with 1ug of vector. Immunofluorescence of transfected Cx50-WT in HeLa cells has been published and showed normal localization of Cx50-WT to gap junction plaques (Beyer EC et al. 2003). Since we are unable to study trafficking of Cx50 tagged with a C-terminal fluorescent protein in HeLa cells, we cannot analyze the Cx50-P88S mutant for rescue by its WT isoform.

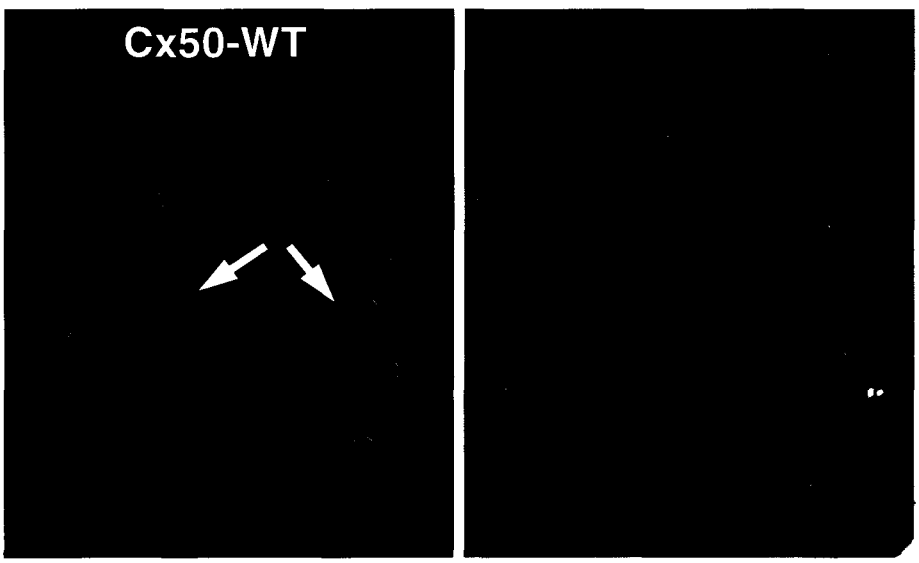

Figure 20. Trafficking of YFP-labeled Cx50-WT in HeLa cells. HeLa cells transiently transfected with Cx50-WT fluorescently tagged at the C-terminus. Right, phase contrast images of cells shown on the left. Arrows indicate intracellular aggregates uncharacteristic of WT trafficking in HeLa cells.

3.4. Relative mRNA expression in transgenic mouse model

To determine the relative expression levels of transgenes in each group, real-time PCR experiments were performed on RNA isolated from the heart of these transgenic mice.

3.4.1. Standard Curves

A standard curve for all four genes (two target genes and two reference genes) was generated and the reaction conditions were optimized to obtain a reaction efficiency as close to 2 as possible. To generate the standard curves, the cDNA from the left atria (LA) of a WT mouse was used and subsequently served as the calibrator for every real-time PCR run that followed. The standard curves consisted of six serial dilutions of cleaned cDNA samples covering 3 logs of concentration (1:10, 1:50, 1:100, 1:500, 1:1000, 1:5000 and 1:10000). The LC480 software calculates the PCR efficiency by determining the slope of the standard curve. The slope is calculated from the linear part of the amplification curve. The formula for PCR efficiency is E=10^(-1/slope). A reaction efficiency of 1.867 was achieved for mCx40/hGH (Figure 21.c), 2.035 for mCx40 (Figure 22. c), 1.955 for mGAPDH (Figure 23.c) and 2.005 for mActB (Figure 24.c).

The mean crossing point (Cp) of every dilution point, ran in triplicate, is indicated in figures 21a, 22a, 23a and 24a. The standard deviation (Std Cp) indicates the reproducibility between samples. As the dilution factor increases, the std Cp increases since it is more difficult to obtain precise results at lower cDNA concentrations. For endogenous mCx40 (Figure 22), none of the 1/10000

dilutions amplified and were therefore excluded from the standard curve analysis. Also, the 1/5000 dilutions have a relatively high Std Cp of 1.34 indicating large variations in Cp values between these triplicates therefore these dilution points were excluded from the standard curve analysis.

The melting curve analyses demonstrate a melting peak for every sample amplified (Figures 21.b, 22.b, 23.b, 24.b). This analysis is crucial to determine if the PCR reaction was specific and to determine the contribution of primer dimmers to the signal detected. Amplification of every sample for all four genes is shown to be specific.

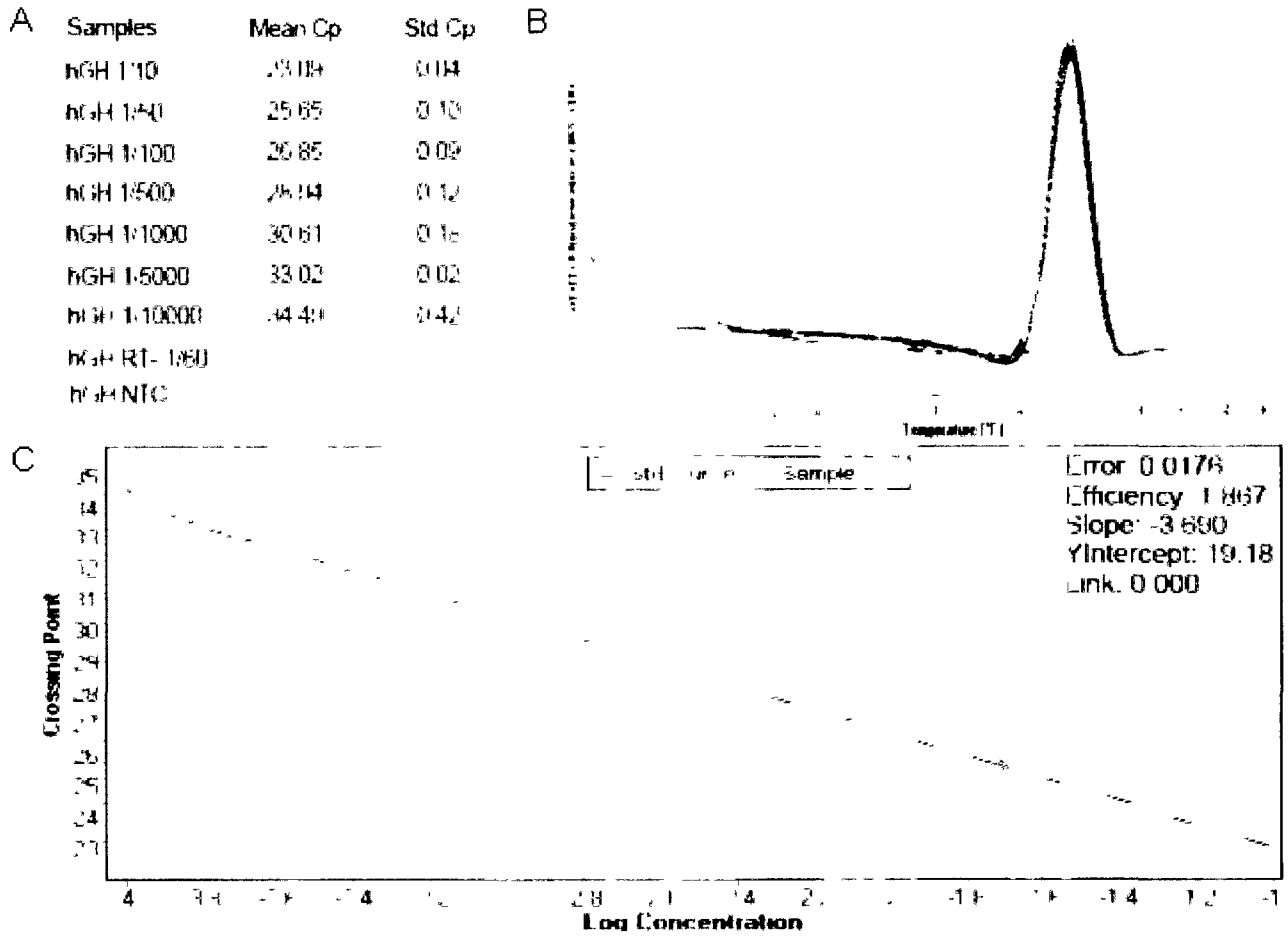

Figure 21. Standard curve analysis for transgene hCx40/hGH. (A) The table indicates the mean Cp of every triplicate and the standard deviation between Cp of triplicate samples. A low Std Cp indicates high reproducibility between triplicates (B) Melting peaks of every sample overlap indicating that the amplification was specific (C) Standard curve created by plotting Cp of every sample against the log concentration. A reaction efficiency of 1.867, indicated on the right, is determined by the software according to the standard curve generated.

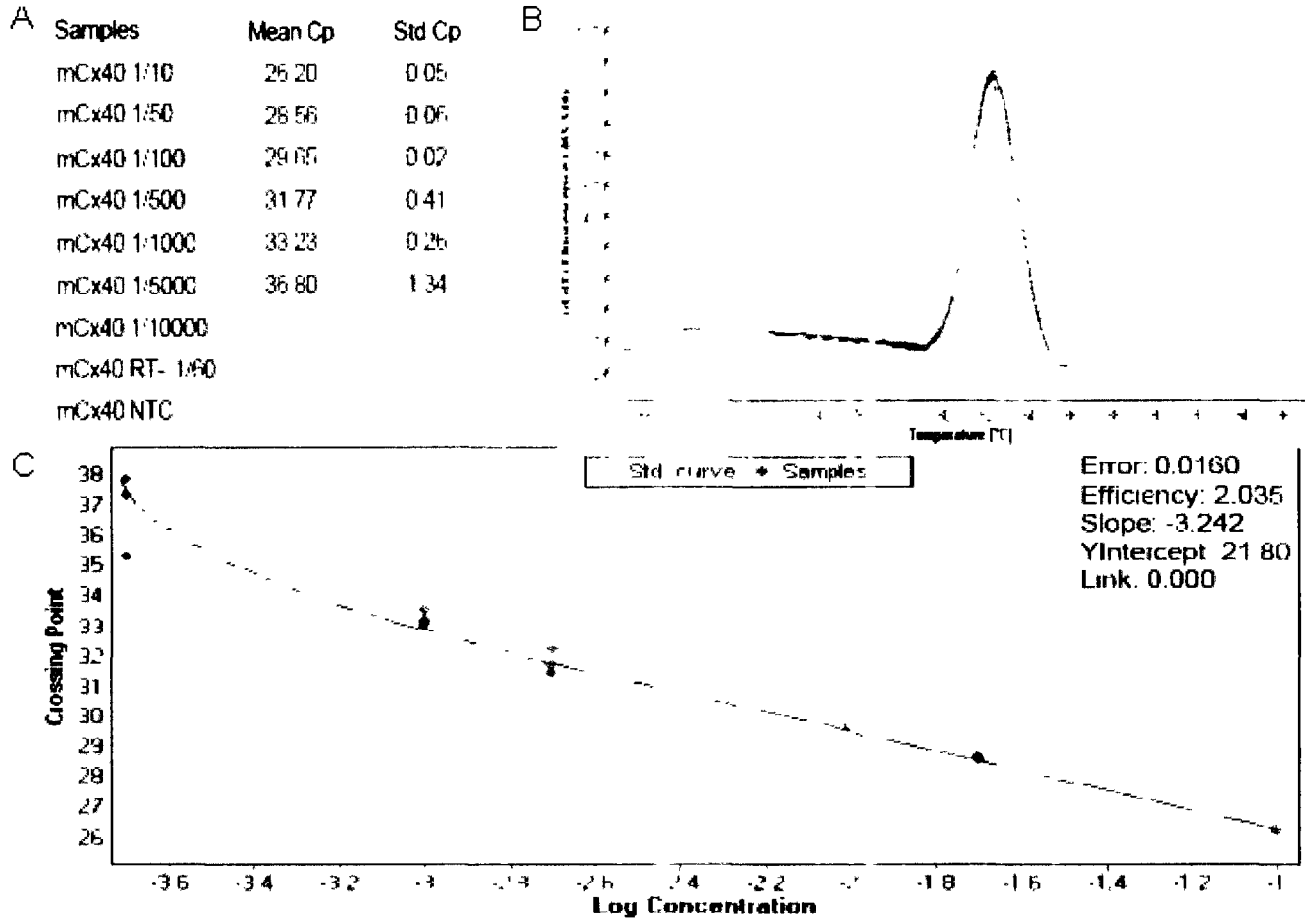

Figure 22. Standard curve analysis for mCx40 (A) The table indicates the mean Cp of every triplicate and the standard deviation between Cp of triplicate samples. A low Std Cp indicates high reproducibility between triplicates. (B) Melting peaks of every sample overlap indicating that the amplification was specific. (C) Standard curve created by plotting Cp of every sample against the log concentration. An reaction efficiency of 2.035, indicated on the right, is determined by the software according to the standard curve generated

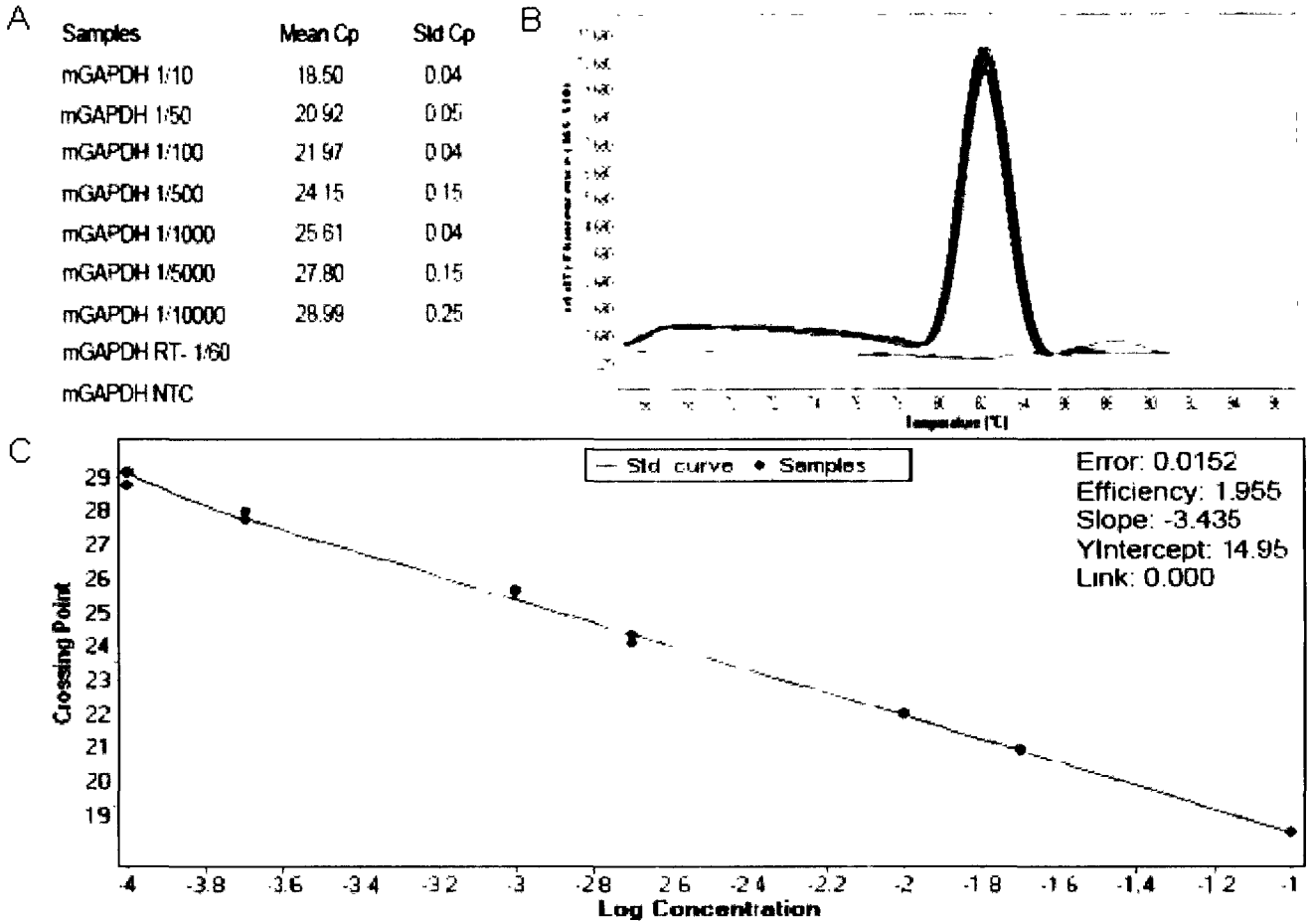

Figure 23. Standard curve analysis for mGAPDH. (A) The table indicates the mean Cp of every triplicate and the standard deviation between Cp of triplicate samples. A low Std Cp indicates high reproducibility between triplicates. (B) Melting peaks of every sample overlap indicating that the amplification was specific. (C) Standard curve created by plotting Cp of every sample against the log concentration. An reaction efficiency of 1.955, indicated on the right, is determined by the software according to the standard curve generated.

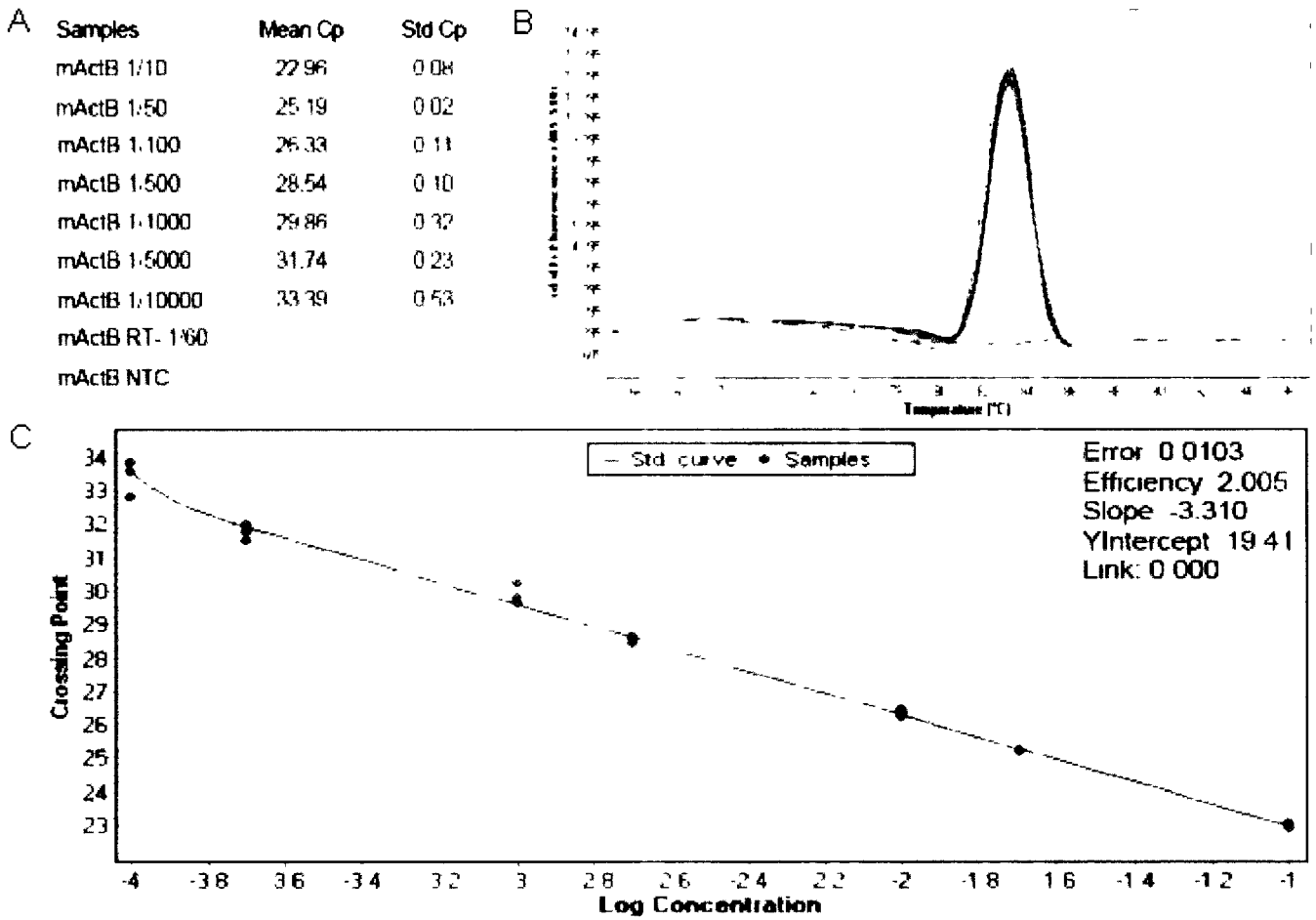

Figure 24. Standard curve analysis for mActB. (A) The table indicates the mean Cp of every triplicate and the standard deviation between Cp of triplicate samples. A low Std Cp indicates high reproducibility between triplicates. (B) Melting peaks of every sample overlap indicating that the amplification was specific (C) Standard curve created by plotting Cp of every sample against the log concentration. An reaction efficiency of 2.005, indicated on the right, is determined by the software according to the standard curve generated.

3.4.2. Relative mRNA quantification in our Cx40-P88S mouse model

Triplicate samples with Cp variations greater than 0.4 were excluded from the analyses. The normalized target to reference ratios from 4 WT and 3 mutant mice was averaged and summarized in bar graphs. To compare the relative difference in expression between two samples, the data was illustrated as a fold. The endogenous mCx40 expression level was determined to be relatively the same in Cx40-WT and Cx40-P88S mutant mice for both left and right atria (Figure 25). The endogenous mCx40 of WT mice in left atria (LA) is approximately 1.5 fold higher than the WT-transgene and approximately 2.2 fold higher in the right atria (RA) (Figure 26.a). In the P88S transgenic mice, the endogenous mCx40 in the left atria is expressed approximately 100 fold higher than the P88S-transgene and 63 fold higher in the right atria (Figure 26.b). The WT-transgene appears to be expressed by over 60 fold compared to the mutant P88S transgene expression levels in the LA of mutant transgenic mice (Figure 27). The WT-transgene seems to have a 30 fold higher expression in the RA of WT transgenic mice compared to the mutant P88S transgene expression levels in the RA of mutant transgenic mice (Figure 27).

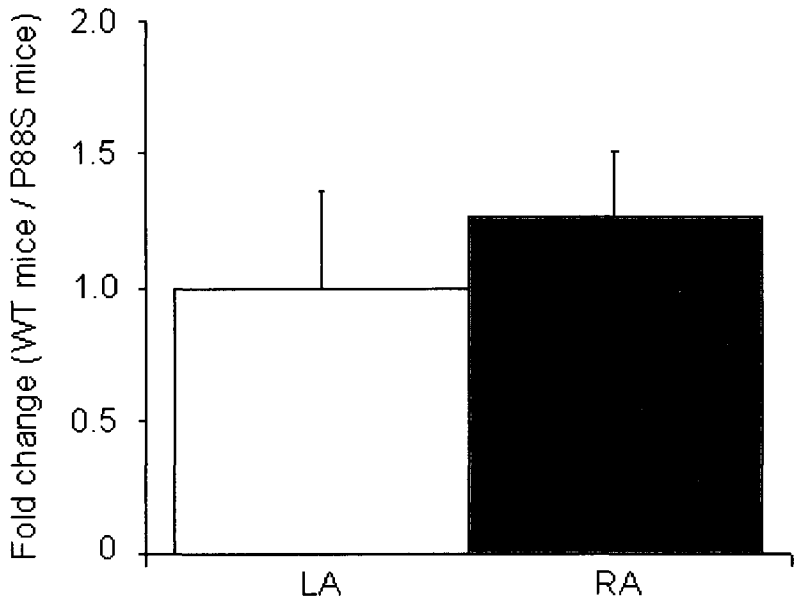

Figure 25. Relative expression of mouse endogenous Cx40 expression in WT and P88S transgenic mice. Mean target/reference ratios for each target gene in both left atria (LA) and right atria (RA). N of 3 mutant mice and 4 WT mice were used for the experiment. Error bars represent standard deviation of the mean.

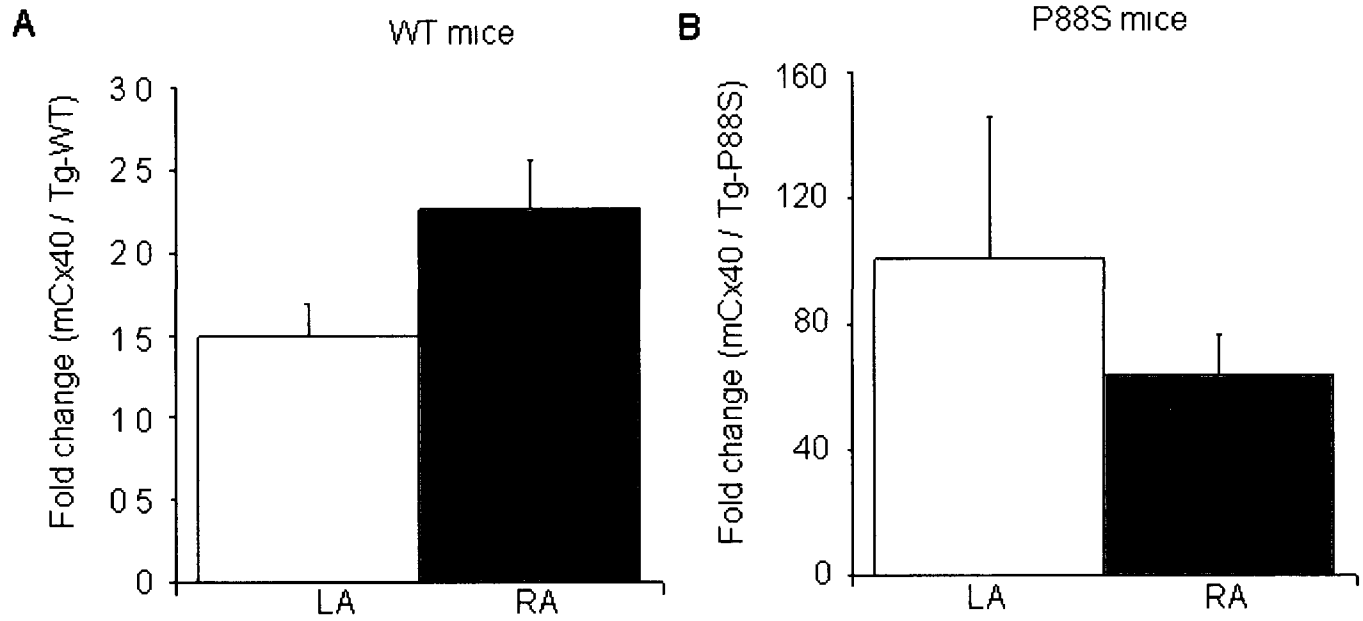

Figure 26 Relative expression of endogenous mCx40 compared to transgene expression in WT and P88S transgenic mice Mean target/reference ratios for the mouse endogenous Cx40 was divided by mean target/reference ratios of WT (A) and P88S (B) transgenes N of 3 mutant mice and 4 WT mice Error bars represent standard deviation of the mean

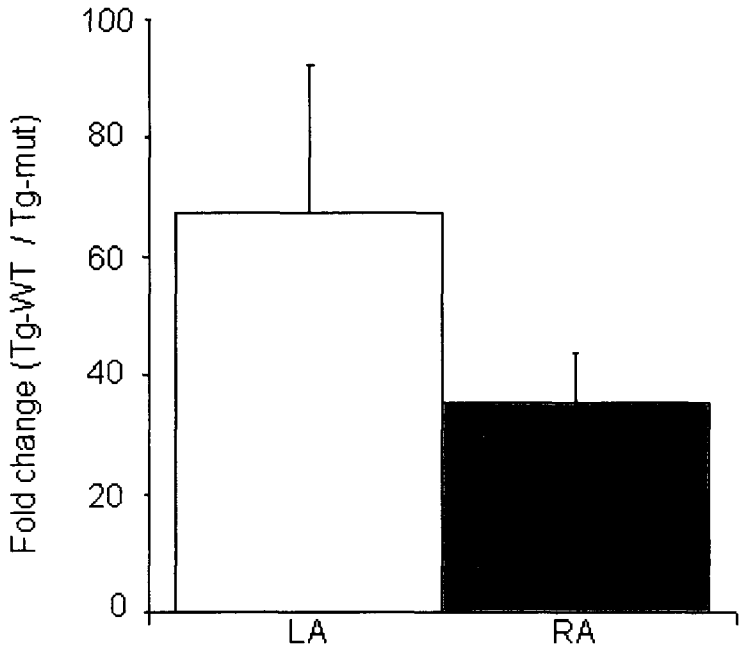

Figure 27. Relative transgene expression between WT and P88S mice. Mean target/reference ratios for WT transgene was divided by target/reference ratios for the P88S mutant transgene in both left atria (LA) and right atria (RA). N of 3 mutant mice and 4 WT mice. Error bars represent standard deviation of the mean.

4. Discussion

4.1. First report of a novel Cx43 somatic mutation (Cx43-932delC) in AF

A somatic Cx43 mutation, Cx43-932delC, found in a patient with lone AF causes a loss-of-function of the protein. This frameshift mutant protein showed extensive intracellular retention within the Golgi apparatus. Cx43 oligomerization is thought to occur in the *trans*-Golgi. Aggregation within this compartment may indicate that the frameshift mutant interferes with the normal oligomerization

process. The small vesicles that do not co-localize with the Golgi marker may be vesicles containing mutant proteins targeted for degradation by lysosomes or proteasomes.

Intracellular retention within the Golgi apparatus, where oligomerization of Cx43 proteins is thought to occur, indicates that the mutation affects hemichannel formation. Several reports on connexin frameshift mutants in the literature suggest that the presence of aberrant amino acids in the C-terminal domain seem to interfere with normal protein trafficking. Intracellular retention in the Golgi was observed for a Cx46 frameshift mutant (Cx46fs380) associated with cataracts. Removal of the aberrant amino acids, by truncation of the protein at amino acid 380, restored normal trafficking and channel function (Minogue PJ et al., 2005). Certain mutations reported in Cx43, in association with oculodentodigital dysplasia (ODDD), have also demonstrated a trafficking defect resulting in co-localization with ER or Golgi-resident proteins (Shibayama J et al., 2005; Gong X-Q et al., 2006). A frameshift mutation of Cx43 occurring at amino acid 260 results in intracellular retention in the ER when expressed in mammalian cells and also exhibits a dominant-negative effect on Cx43-WT (Gong X-Q et al., 2006). Their frameshift mutant occurs in the C-terminus and results in the translation of 46 aberrant amino acids before reaching a premature stop codon. Gong et al. also compared protein trafficking between their mutant with and without the aberrant amino acids and found that without the aberrant amino acids the truncated protein traffics normally. Another Cx43 frameshift

mutant reported in ODDD causes truncation of the C-terminal domain at amino acid 258 without expression of aberrant amino acids and showed the ability to traffic to the cell membrane and to form gap junction plaques (Maass K et al., 2007). Deletion of a large portion of the C-terminal domain does not prevent protein trafficking to the cell membrane or channel function. Our frameshift mutation occurs after amino acid 310 and results in translation of 36 aberrant amino acids followed by a premature stop codon. The intracellular retention of Cx43-932delC is most likely due to the aberrant amino acids rather than the missing amino acids. Retention of the mutant protein within the *trans*-Golgi suggests that the presence of aberrant amino acids interferes with the oligomerization process of Cx43 into hemichannels. The mutant Cx43 could be preventing formation of hemichannels or their trafficking to the cell membrane. These results support the notion that the C-terminal domain is not required for normal trafficking but that expression of aberrant amino acids results in improper localization of connexins.

Formation of heteromeric channels by Cx43 and Cx40, two highly expressed isoforms in atria, is debated in the literature. It is not known which portion of connexin proteins is responsible for oligomerization. Co-expression of Cx43-932delC with Cx43-WT or Cx40-WT demonstrated a dominant and *trans*-dominant negative effect on protein trafficking in a mammalian cell model. In addition, intracellular retention was observed in the atrial myocytes of the patient harboring the Cx43-932delC mutation indicating that our expression systems

replicate what occurs *in vivo*. Our results support the concept that Cx43 and Cx40 can interact together as the trafficking and function of Cx43-WT and Cx40-WT is impaired by co-expression of the mutant.

As expected, N2A cells expressing Cx43-932delC had significantly reduced gap junction conductance due to the observed lack of trafficking of the mutant at the interface of paired cells. Cells co-expressing Cx43-WT or Cx40-WT with Cx43-932delC also had significantly reduced conductance due to the intracellular retention of wild-type Cx43 and Cx40 by the mutant Cx43. The small conductance observed in these paired cells suggests that some gap junction channels are still being formed and are conducting current. This discrepancy may be due to the presence of a relatively small number of functional channels at the intercellular junction that is below the detection threshold for visualization using confocal microscopy. This loss-of-function on electrical coupling highlights the fact that a genetic defect in one allele may not be compensated by the expression of a normal allele or even by co-expression of other isoforms. The effect of our mutant on other cardiac connexins illustrates how much of an impact this mutation can have physiologically.

Results obtained from the *Xenopus* oocyte cell system gave a more robust dominant-negative effect of the mutant on Cx43-WT. However, the *trans*-dominant effect of Cx43-932delC on Cx40-WT was not observed unless Cx43-WT was present. This observed discrepancy between expression systems may

be due to the difference in incubating temperatures during the oligomerization process. N2A cells, incubated at 37°C, represent a more physiological temperature whereas oocytes are incubated at 17°C. Incubation at a lower temperature may affect oligomerization of the mutant with Cx40 although the lower incubation temperature does not seem to affect oligomerization of the mutant with its wild-type isoform. Perhaps certain proteins involved in hetero-oligomerization are less active at 17°C resulting in improper interactions between mutant Cx43 and Cx40-WT. Nonetheless, the most physiologically relevant scenario where mutant Cx43, Cx43-WT and Cx40-WT are all expressed in one cell resulted in a significant reduction of electrical conductance. The data from both expression systems support the concept that heteromeric formation of hemichannels composed of Cx43 and Cx40 contribute to the formation of gap junction channels in the atria.

The electrical and metabolic coupling of cardiac myocytes occurs through gap junctions. Disrupting the function of these channels may alter the electrical conduction and action potential propagation. In the case of the germline ODDD Cx43 frameshift mutation, the affected individuals had multiple organ defects as Cx43 is widely expressed. In our case, the Cx43 mutation was found in tissue DNA and was absent from lymphocyte DNA suggesting a somatic mutation. Cardiac myocytes do not divide therefore the mutation must have occurred in a progenitor cell during cardiac development. Since Cx43 is widely expressed in different tissues, a somatic mutation explains why the patient didn't have clinical

phenotypes other than atrial fibrillation. Somatic mutations, being less common than germline mutations, have been identified as disease causing in a case of ventricular tachycardia where a mutation was found in a G-coupled protein identified in the heart but not in lymphocyte DNA (Lerman BB et al., 1998). Studies on chimeric mice by Gutstein et al., showed conduction defects as a result of heterogeneous Cx43 expression in mice and support our findings that mosaic expression of our loss-of-function Cx43 mutant could lead to heterogeneous conduction throughout the atria and promote vulnerability to AF (Gutstein DE et al., 2001b).

4.2. Cx40-F30L; first report on leaky hemichannel mechanism in AF

The Cx40-F30L mutation did not seem to affect the trafficking and formation of gap junction plaques although slight intracellular retention was observed. Cx40-F30L formed functional gap junction channels although a gain-of-function effect on hemichannel activity was observed which led to cell death in *Xenopus* oocytes. Similar observations have been made on leaky hemichannels from mutations identified in various connexin isoforms associated with human diseases. For example, several Cx26 mutations associated with deafness have demonstrated enhanced openings of hemichannels. Injection of mutant Cx26 cRNA (G12R, N14K, D50N or G45E) in *Xenopus* oocytes led to cellular depolarization and osmotic lysis (Lee JR et al., 2009; Stong BC et al., 2006). The Cx26 hemichannels produced large currents that were enhanced upon depolarization and were inhibited by elevated external calcium ions. Mutations in

Cx30 (G11R and A88V) associated with skin disease, demonstrated leakage of ATP in the extracellular space with slightly impaired cell viability following transfection in HeLa cells (Essenfelder GM et al., 2004). Connexin32 mutations (S85C, F235C) associated with X-linked Charcot-Marie-Tooth disease produce large hemichannel currents in *Xenopus* oocytes resulting in cell death although protein trafficking was normal in HeLa cells (Abrams CK et al., 2002; Lin Liang GS et al., 2005). Mutations in Cx50, primarily expressed in the lens, have been linked to congenital cataracts. A Cx50-G46V mutation showed normal trafficking in HeLa cells and normal intercellular coupling between pairs of *Xenopus* oocytes (Minogue PJ et al., 2009). Injection of Cx50-G46V generated large hemichannel current upon depolarization and induced cell death (Minogue PJ et al., 2009). Cx50-G46V hemichannel current reported by Minogue et al. was reduced and cell death was rescued by increasing the extracellular Ca^{+2} concentrations of the culture media. As described here, there are numerous studies that have correlated enhanced hemichannel function to disease causing mutations. This observation that cell death can be induced by enhanced hemichannel function has never been reported for Cx40 mutants.

The F30L mutant is located within the second half of the first transmembrane segment which has been shown to play a crucial role on hemichannel conductance (Hu X et al., 2006). A common feature of functional hemichannels is that they close when exposed to extracellular divalent cations (Ebihara L et al., 2003). Connexins have calcium binding sites on their

extracellular loops and in response to increased extracellular calcium, hemichannels close. Our Cx40-F30L mutant demonstrated a cell death phenotype that was prevented by increased extracellular calcium concentrations. Cell death was not assessed in either mammalian cell systems that we used. In addition, fluorescently tagged connexins may affect hemichannel function since a slight reduction in hemichannel opening has been reported with tagged Cx43 (Kang J et al., 2008) as well as altered gating compared to untagged Cx43 (Contreras JE et al., 2003a; Contreras JE et al., 2003b). The mechanism linking enhanced hemichannel function to cell death is unknown. Abnormal opening of hemichannels could have serious consequences on cell survival. Hemichannel currents are twice as large as gap junctional currents therefore improper closing could deplete the cell from nutrients, metabolites and the ionic concentration gradient would be abolished. Leaky hemichannels have been shown to release ATP in the extracellular environment (Essenfelder GM et al., 2004; Kang J et al., 2008). Enhanced ATP release in the extracellular space can stimulate purinergic receptors on the membrane of neighboring cells and result in intracellular calcium release from the sarcoplasmic reticulum in the stimulated cells (Gossman DG et al., 2008; Stout CE et al., 2002). Overall, these factors could perhaps play a direct or indirect role in the mechanism leading to cell death.

Leaky hemichannels represent a mechanism by which certain mutation can cause different diseases. Such a mechanism has been reported in Cx30 in association with hidrotic ectodermal dysplasia, a rare disease that affects skin,

hair and nails. Other diseases include deafness (Cx26), X-linked Charcot-Marie-Tooth (Cx32) and cataracts (Cx50). Our data represents the first report of leaky hemichannel mechanism in Cx40 in association with atrial fibrillation. Cell death caused by enhanced hemichannel may cause tissue fibrosis *in vivo* which is a known substrate for development of arrhythmias. Tissue fibrosis can cause conduction delays within the atria and promotes generation of re-entrant electrical circuits.

4.3. Cx40-G311S and -R113S mutants; enhanced pH sensitivity

The G311S mutation, located in the C-terminal domain, the R113S mutation, located in the intracellular loop domain, are two conserved residues although they are located in two domains that are not conserved. The Cx40-G311S and Cx40-R113S mutations did not seem to affect the trafficking and formation of gap junction plaques. Macroscopic junctional conductance for these two mutants was similar to that of Cx40-WT in N2A cells. The C-terminal and intracellular loop domains are involved in pH gating. C-terminal domain binds to the intracellular loop following the "ball-and-chain" model. Upon intracellular acidification, Cx43 gap junction channels close (Morley GE et al., 1996; Stergiopoulos K et al., 1999). The G311S and R113S mutations didn't affect the macroscopic current under physiological pH although increased intracellular pH (pH_i) sensitivity was observed. These results demonstrate that gap junction channels composed of either mutant at a slightly more acidic pH_i result in significant channel closure as compared to WT channels. This difference in pHi

sensitivity is physiologically relevant as the intracellular pH values reported in cardiomyocytes vary from 6.8 to 7.1 depending on the species (Roos A et al., 1981). Gap junction conductance may be impaired under only slight ischemia or acidification therefore resulting in reduced conduction in the heart. Closure of channels would result in a delayed non-uniform electrical conduction promoting site of re-entry within the atrial myocardium.

4.4. P88S mutation in connexins

A P88S mutation in Cx40 was previously reported in a patient with atrial fibrillation (Gollob MH et al., 2006). This mutation was reported to be retained inside the cell and abolished intercellular coupling when expressed alone in N2A cells and when expressed with Cx40-WT or Cx43-WT in *Xenopus* oocytes. In this study, Cx40-P88S was determined to co-localize with both the ER and Golgi markers. Similarly, a P87S mutation reported in Cx47, associated with Pelizaeus-Merzbacher-like disease, resulted in intracellular localization in HeLa cells (Orthmann-Murphey JL et al., 2007). Surprisingly, Cx40-P88S was rescued to gap junction plaques by Cx40-WT and Cx43-WT when co-expressed with these wild-type isoforms in HeLa cells. The presence of WT connexins allows for oligomerization with the mutant P88S whereas mutant proteins by themselves may not be able to interact together. The gap junctions showing rescue in N2A cells may be non functional but future experiments will be conducted to test whether there is a rescue of channel function.

The proline residue at position 88, located in the second transmembrane domain, is conserved among connexin isoforms. In Cx32, a P87S mutation is associated with Charcot-Marie-Tooth disease (Ri Y et al., 1999). To determine if the trafficking rescue observed in Cx40 also applied to Cx32 and Cx50 with a mutated P88 residue, cells were co-transfected with WT and mutant Cx32 and Cx50 constructs. The P87S mutation in Cx32 also demonstrated significant trafficking rescue to gap junction plaques by Cx32-WT in HeLa cells. Paired cells showing rescue will also be tested for rescue of channel function in future experiments.

A P88S mutation in Cx50 was reported in association with cataracts (Shiels A et al., 1998). The Cx50-P88S has been studied in *Xenopus* oocytes and was unable to form functional gap junctions (Pal JD et al., 1999). When co-expressed with WT Cx50, the P88S mutant displayed a dominant-negative effect (Pal JD et al., 1999). Similar results were obtained from HeLa and N2A cells and trafficking studies revealed cytoplasmic accumulations of Cx50-P88S in HeLa cells (Berthoud VM et al., 2003). The above studies have shown similar results to studies conducted on Cx40 and Cx32 P88S mutants. Contrary to Cx32 and Cx40, the Cx50-P88S mutant formed intracellular accumulations that didn't significantly co-localize with ER and Golgi markers (Berthoud VM et al., 2003). A Cx50-P88Q mutation also reveals impaired trafficking, abolished intercellular conductance and exerted a dominant-negative effect on Cx50-WT (Arora A et al., 2006). A mutated P88 residue in Cx50, to a serine or glutamine, results in similar

phenotype suggesting that the loss of the proline88 residue causes abnormal protein function. Here, we have been unable to determine the trafficking rescue with Cx50-P88S since C-terminal tagging of Cx50-WT results in improper localization in mammalian cells. Other studies have used *Xenopus* oocytes or expression in mammalian cells without a fluorescent tag. Immunodetection of Cx50-WT in mammalian cells show normal localization pattern although for our purpose the use of antibodies would not distinguish between Cx50-WT and rescued mutants and would not allow us to assess rescue of channel function.

Studies on Cx26-P87 have shown that when this residue was mutated to a leucine, glycine, isoleucine, alanine or valine, it rarely produced detectable intercellular conductance (Suchyna TM et al., 1993). The mutants also inhibited the function of wild-type Cx26 and the loss of the proline residue led to impaired intercellular conduction regardless of the mutated amino acid. This emphasizes the concept that the loss of the proline residue, rather than the aberrant amino acid, results in a loss-of-function. Proline residues are hydrophobic residues that often introduce kinks in α-helices (Ri Y et al., 1999). Replacement with another amino acid may result in conformation changes, thereby compromising the structure and function of proteins. The fact that a P88S mutation has naturally occurred in four different connexin isoforms which have all been linked to human diseases emphasizes the importance of this amino acid. Understanding the pathology of this mutation is not only relevant to atrial fibrillation but also to other connexin-associated diseases.

4.5. Real-time mRNA relative quantification in Cx40-P88S transgenic mice

The purpose of this study was two fold; the first was to determine the relative expression between WT and mutant transgenes for each group of mice. The second is to determine the relative expression levels between the transgenes and endogenous mouse Cx40 for each group. We are looking at the RNA level because the human and mouse Cx40 proteins (hCx40 and mCx40 respectively) are too similar in sequence to perform western blots using antibodies specific for each species. Therefore relative quantification of mRNA levels was performed by real-time PCR using a SYBR Green. SYBR Green is a fluorescent dye that can emit significantly greater fluorescence when intercalated into double stranded DNA (dsDNA) as compared to freely dissociated dye in solution or in presence of single stranded nucleic acids.

The data obtained showed a significant difference in expression between the WT and mutant transgenes. The WT transgene was expressed at slightly lower levels compared to endogenous mCx40 whereas the mutant P88S transgene approached 1% expression levels of endogenous mCx40 expression levels. The mild phenotype of increased susceptibility to AF observed in mutant mice may be due to the significantly lower expression of the transgene compared to endogenous mCx40. The immunohistochemical staining of atrial tissue from mutant mice did show a heterogeneous pattern of intracellular retention suggesting that even though the mutant is present at low levels, it may still affect

the localization of endogenous mCx40. The sample size for this experiment was small and so we intend on repeating this experiment in the near future. The WT and mutant mice were shown to have a relatively similar copy number of the transgene although here we show that this does not translate into a similar expression of mRNA. To explain the large difference in mRNA expression, we can speculate that the mutant transgene is being suppressed by the mouse genome as this has been suggested to occur in transgenic mouse models over time. A possible explanation for the observed difference in expression levels may be due to the site of transgene insertion in the mouse genome. The transgenes are regulated under the ANP promoter which normally expresses ANP in a small population of adult atrial myocytes (Hamid Q et al., 1987). ANP is also expressed in the ventricles during development but is not detected in adult atrial myocytes. Since the transgenes are not expressed in every adult atrial cell, this may explain a lower expression of the transgenes compared to endogenous Cx40 which is expressed in every atrial cell. However, this explanation does not account for large difference observed between WT and mutant transgene expression.

4.6. Summary

A Cx43 mutation has never been previously reported to be associated with AF. Our functional studies on the somatic Cx43-932delC mutant demonstrated a loss-of-function mutation that impaired connexin trafficking and displayed intracellular retention in the Golgi. Cx43-932delC also significantly reduced

electrical coupling and exerted a dominant and trans-dominant negative effect on Cx43 and Cx40 WT, respectively. These results confirm previous findings that a loss of gap junction cell-to-cell coupling may predispose the atria to fibrillation. It also supports the novel paradigm that non-familial, common diseases may have a genetic basis which is confined to the diseased tissue.

Three novel Cx40 mutations have also been characterized which do not seem to affect connexin trafficking nor macroscopic junctional conductance. Hemichannel studies on Cx40-F30L demonstrated enhanced hemichannel currents leading to cell death. Although cell death caused by enhanced hemichannel activity has been reported for other connexin related diseases, our data is the first to show this observation for Cx40 in association with atrial fibrillation. We also showed that Cx40-G311S and Cx40-R113S mutations, located in domains responsible for the gating of gap junction channels, lead to a reduction in conductance at slightly reduced intracellular pH. Enhanced pH sensitivity is also a mechanism never previously reported in AF.

There are five main mechanisms by which mutations may affect connexin function. First, mutations may impair protein trafficking and therefore gap junction channel formation resulting in a loss of electrical coupling. Second, mutant connexins may have a dominant-negative and *trans*-dominant-negative effect on wild-type connexins expressed within the same cell thereby resulting in impaired gap junction formation. Thirdly, mutant connexins may traffic normally

or be rescued to gap junction plaques but may still form non functional channels and can therefore result in a loss of electrical coupling. Fourth, mutations affecting the binding of the C-terminal and intracellular loop involved in channel gating can affect conductance by inducing channel closure upon intracellular acidification. Lastly, hemichannels composed of mutant connexins may exhibit an enhanced activity leading to cell death. It remains to be elucidated whether cell death also occurs *in vivo*. We can speculate that fibrosis of cardiac tissue, a known proarrhythmic factor, could result from cell death of cardiac myocytes.

In the heart, gap junction channels are responsible for rapid action potential propagation through myocardial tissue allowing for synchronous contractions. Atrial fibrillation is characterized by a rapid erratic activation of atrial myocardium. A well known theory in the literature, called the multiple wavelet hypothesis, attempts to describe the mechanism by which AF is generated and sustained (Moe GK et al., 1964). The theory suggests that the erratic electrical activity in the atria is caused by multiple re-entrant circuits. Electrical re-entries are thought to be generated by heterogeneity in cells available for re-excitation after depolarization. Fibrosis is a known pro-arrhythmic factor leading to conduction heterogeneity in the heart. Conduction delays through defective gap junction channels may also generate sites of re-entry thus rendering the atria susceptible to AF. My data and data from our lab and collaborators demonstrate that cardiac connexin mutations may cause conduction delays and heterogeneity promoting the atria to fibrillation.

References

Abrams CK, Bennett MVL, Verselis VK and Bargiello TA. 2002. Voltage opens unopposed gap junction hemichannels formed by a connexin 32 mutant associated with X-linked Charcot-Marie-Tooth disease. Proc. Natl. Acad. Sci. USA. 99, 3980-3984.

Anumonwo JMB, Taffet SM, Gu H, Chanson M, Moreno AP and Delmar M. 2001. The carboxyl terminal domain regulates the unitary conductance and voltage dependence of connexin40 gap junction channels. Circ. Res. 88, 666-673.

Arora A, Minogue PJ, Liu X, Reddy MA, Ainsworth JR, Bhattacharya SS, Webster AR, Hunt DM, Ebihara L, Moore AT, Beyer EC and Berthoud VM. 2006. A novel GJA8 mutation is associated with autosomal dominant lamellar pulverulent cataract: further evidence for gap junction dysfunction in human cataract. J. Med. Genet. 43, e2.

Bahima L, Aleu J, Elias M, Martin-Satué M, Muhaisen A, Blasi J, Marsal J and Solsona C. 2006. Endogenous hemichannels play a role in the release of ATP from *Xenopus* oocytes. J. Cell. Physiol. 206, 95-102.

Bao X, Altenberg GA and Reuss L. 2004. Mechanism of regulation of the gap junction protein connexin 43 by protein kinase C-mediated phosphorylation. Am. J. Physiol. Cell. Physiol. 286, C647-C654.

Beardslee MA, Laing JG, Beyer EC and Saffitz JE. 1998. Rapid turnover of connexin43 in the adult rat heart. Circ. Res. 83, 629-635.

Benjamin EJ, Levy D, Vaziri SM, D'Agostino RB, Belanger AJ and Wolf PA. 1994. Independent risk factors for atrial fibrillation in a population-based cohort. The Framingham Heart Study. JAMA. 271, 840-844.

Berthoud VM, Minogue PJ, Guo J, Williamson EK, Xu X, Ebihara L, and Beyer EC. 2003. Loss of function and impaired degradation of a cataract-associated mutant connexin50. Eur. J. Cell Biol.. 82, 209-221.

Bevans CG, Kordel M, Rhee SK and Harris AL. 1998. Isoform composition of connexin channels determines selectivity among second messengers and uncharged molecules. J. Biol. Chem. 273, 2808-2816.

Bouvier D, Spagnol G, Chenavas S, Kieken F, Vitrac H, Brownell S, Kellezi A, Forge V and Sorgen PL. 2009. Characterization of the structure and intermolecular interactions between the connexin40 and connexin43 carboxyl terminal and cytoplasmic loop domains. J. Biol. Chem. 284, 34257-34271.

Bruzzone R, Haefliger J-A, Gimlich RL and Paul DL. 1993. Connexin40, a component of gap junctions in vascular endothelium, is restricted in its ability to interact with other connexins. Mol. Biol. Cell. 4, 7-20.

Bruzzone S, Guida L, Zocchi E, Franco L, De Flora A. 2001. Connexin 43 hemichannels mediate Ca^{2+}-regulated transmembrane NAD+ fluxes in intact cells. FASEB J. 15, 10-12.

Contreras JE, Saez JC, Bukauskas FF and Bennett MV. 2003a. Functioning of Cx43 hemichannels demonstrated by single channel properties. Cell Commun. Adhes. 10, 245-249.

Contreras JE, Saez JC, Bukauskas FF and Bennett MV. 2003b. Gating and regulation of connexin 43 (Cx43) hemichannels. Proc. Natl. Acad. Sci. U. S. A. 100, 11388-11393.

Cottrel GT, Wu Y and Burt JM. 2001a. Functional characteristics of heteromeric Cx40-Cx43 gap junction channel formation. Cell Commun. Adhes. 8, 193-197.

Cottrell GT and Burt JM. 2001b. Heterotypic gap junction channel formation between heteromeric and homomeric Cx40 and Cx43 connexons. Am. J. Physiol. Cell Physiol. 281, 1559-1567.

Cottrell GT, Wu Y and Burt JM. 2002. Cx40 and Cx43 expression ratio influences heteromeric/heterotypic gap junction channel properties. Am. J. Physiol. Cell Physiol. 282, C1469-C1482.

Dahl G, Levine E, Rabadan-Diehl C and Werner R. 1991. Cell/cell channel formation involves disulfide exchange. Eur. J. Biochem. 197, 141-144.

Darbar D. 2008. Genetics of atrial fibrillation rare mutations, common polymorphisms, and clinical relevance. Heart Rhythm. 5, 483-486.

Dong L, Liu X, Li H, Vertel BM and Ebihara L. 2006. Role of the N-terminus in permeability of chicken connexin45.6 gap junctional channels. J. Physiol. 576, 787-799.

Duffy HS, Fort AG and Spray DC. 2006. Cardiac connexins: genes to nexus. Adv. Cardiol. 42, 1-17.

Ebihara L and Steiner E. 1993. Properties of a nonjunctional current expressed from rat connexin46 cDNA in *Xenopus* oocytes. J. Gen. Physiol. 102, 59-74.

Ebihara L, Liu X and Pal JD. 2003. Effect of external magnesium and calcium on human connexin46 hemichannels. Biophys. J. 84, 277-286.

Eckardt D, Theis M, Degen J, Ott T, Van Rijen HVM, Kirchhoff S, Kim J-S, De Backker JMT and Willecke K. 2003. Functional role of connexin43 gap junction channels in adult mouse heart assessed by inducible gene deletion. J. Mol. Cell. Cardiol. 36, 101-110.

Elfgang C, Eckert R, Lichtenberg-Frate H, Butterweck A, Traub O, Klein RA, Hulser DF and Willecke K. 1995. Specific permeability and selective formation of gap junction channels in connexin-transfected HeLa cells. J. Cell Biol. 129, 805-817.

Essenfelder GM, Bruzzone R, Lamartine J, Charollais A, Blanchet-Bardon C, Barbe MT, Meda P and Waksman G. 2004. Connexin30 mutations responsible for hidrotic ectodermal dysplasia cause abnormal hemichannel activity. Hum. Mol. Genet. 13, 1703-1714.

Evans WH and Martin PEM. 2002 Gap junctions: structure and function. Mol. Membr. Biol. 19, 121-136.

Evans WH, De Vuyst E and Leybaert L. 2006. The gap junction cellular internet: connexin hemichannels enter the signaling limelight. Biochem. J. 397, 1-14.

Falk MM, Kumar NM and Gilula NB. 1994. Membrane insertion of gap junction connexins: polytopic channel forming membrane proteins. J. Cell. Biol. 127, 343-355.

Falk MM. 2000. Biosynthesis and structural composition of gap junction intercellular membrane channels. Eur. J. Cell Biol. 79, 564-574.

Fishman GI, Moreno AP, Spray DC and Leinwand LA. 1991. Functional analysis of human cardiac gap junction channel mutants. Proc. Natl. Acad. Sci. USA. 88, 3525-3529.

Gemel J, Valiunas V, Brink PR and Beyer EC. 2004. Connexin43 and connexin26 form gap junctions, but not heteromeric channels in co-expressing cells. J. Cell Sci. 117, 2469-2480.

Giepmans BNG and Moolenaar WH. 1998. The gap junction protein connexin43 interacts with the second PDZ domain of the zona occludens-1 protein. Curr. Biol. 8, 931-934.

Giepmans BNG, Verlaan I and Moolenaar WH. 2001. Connexin-43 interactions with ZO-1 and α- and β-tubulin. Cell Commun. Adhes. 8, 219-223.

Giepmans BNG. 2004. Gap junctions and connexin-interacting proteins. Cardiovasc. Res. 62, 233-245.

Gollob MH, Jones DL, Krahn AD, Danis L, Gong X-Q, Shao Q, Liu X, Veinot JP, Tang ASL, Stewart AFR, Tesson F, Klein GJ, Yee R, Skanes AC, Guiraudon GM, Ebihara L and Bai DB. 2006. Somatic mutations in the connexin 40 gene (GJA5) in atrial fibrillation. N. Engl. J. Med. 354, 2677-88.

Gong X-Q, Shao Q, Lounsbury CS, Bai D and Laird DW. 2006. Functional characterization of a GJA1 frameshift mutation causing oculodentodigital dysplasia and palmoplantar keratoderma. J. Biol. Chem. 281, 31801-31811.

Gong X-Q, Shao Q, Langlois S, Bai D and Laird DW. 2007. Differential potency of dominant negative connexin43 mutants in oculodentodigital dysplasia. 282, 19190-19202.

Gonzalez D, Gomez-Hernandez JM and Barrio LC. 2007. Molecular basis of voltage dependence of connexin channels: an integrative appraisal. Prog. Biophys. Mol. Biol. 94, 66-106.

Goodenough DA and Paul DL. 2003. Beyond the gap: functions of impaired connexon channels. Nat. Rev. Mol. Cell. Biol. 4, 285-294.

Gu H, Ek-Vitorin JF, Taffet SM and Delmar M. 2000. Co-expression of connexins 40 and 43 enhances the pH sensitivity of gap junctions. Circ. Res. 86, e98-e103.

Guerrero PA, Schuessler RB, Davis LM, Beyer EC, Johnson CM, Yamada KA and Saffitz JE. 1997. Slow ventricular conduction in heterozygous for a connexin43 null mutation. J. Clin. Invest. 99, 1991-1998.

Gutstein DE, Morley GE, Tamaddon H, Vaidya D, Schneider MD, Chen J, Chien KR, Stuhlmann H and Fishman GI. 2001a. Conduction slowing and sudden arrhythmic death in mice with cardiac-restricted inactivation of connexin43. Circ. Res. 88, 333-339.

Gutstein DE, Morley GE, Vaidya D, Liu F, Chen FL, Stuhlmann and Fishman GI. 2001b. Heterogeneous expression of gap junction channels in the heart leads to conduction defects and ventricular dysfunction. Circ. 104, 1194-1199.

Hagendorff A, Schumacher B, Kirchhoff S, Luderitz B and Willecke K. 1999. Conduction disturbances and increased atrial vulnerability in connexin40-deficient mice analyzed by transesophageal stimulation. Circ. 99, 1509-1515.

Hamid Q, Wharton J, Terenghi G, Hassall CJS, Aimi J, Taylor KM, Nakazato H, Dixon JE, Burnstock G and Polak JM. 1987. Localization of atrial natriuretic peptide mRNA and immunoreactivity in the heart and human atrial appendage. Proc. NAtl. Acad. Sci. USA. 84, 6760-6764.

Haubrich S, Schwarz H-J, Bukauskas F, Lichtenberg-Frate H, Traub O, Weingart R and Willecke K. 1996. Incompatibility of connexin 40 and 43 hemichannels in gap junctions between mammalian cells is determined by intracellular domains. Mol. Biol. Cell. 7, 1995-2006.

Heyman NS, Kurjiaka DT, Ek Vitorin JF and Burt JM. 2009. Regulation of gap junctional charge selectivity in cells co-expressing connexin 40 and connexin 43. Am. J. Physiol. Heart Circ. Physiol. 297, H450-H459.

He DS, Jiang JX, Taffet SM and Burt JM. 1999. Formation of heteromeric gap junction channels by connexins 40 and 43 in vascular smooth muscle cells. Proc. Natl. Acad. Sci. USA. 96, 6495-6500.

Hu X, Ma M and Dahl G. 2006. Conductance of connexin hemichannels segregates with the first transmembrane segment. Biophys. J. 90, 140-150.

Hunter AW and Gourdie RG. 2008. The second PDZ domain of zonula occludens-1 is dispensable for targeting to connexin43 gap junctions. Cell. Commun. Adhes. 15, 55-63.

Jin C, Martyn KD, Kurata WE, Warn-Cramer BJ and Lau AF. 2004. Connexin43 PDZ2 binding domain mutants create functional gap junctions and exhibit altered phosphorylation. Cell Commun. Adhes. 11, 67-87.

Jordan K, Solan JL, Dominguez M, Sia M, Hand A, Lampe PD and Laird DW. 1999. Trafficking, assembly, and function of a connexin43-green fluorescent protein chimera in live mammalian cells. Mol. Biol. Cell. 10, 2033-2050.

Kalcheva N, Qu J, Sandeep N, Garcia L, Zhang J, Wang Z, Lampe PD, Suadicani SO, Spray DC and Fishman GI. 2007. Gap junction remodeling and cardiac arrhythmogenesis in a murine model of oculodentodigital dysplasia. Proc. Natl. Acad. Sci. USA. 104, 20512-20516.

Kang J, Kang N, Lovatt D, Torres A, Zhao Z, Lin J, Nedergaard M. 2008. Connexin 43 hemichannel are permeable to ATP. J. Neurosci. 28, 4702-4711.

Kannel WB, Wolf PA, Benjamin EJ and Levy D. 1998. Prevalence, incidence, prognosis, and predisposing conditions for atrial fibrillation: population-based estimates. Am. J. Cardiol. 82, 2N-9N.

Kirchhoff S, Nelles E, Hagendorff A, Kruger P, Traub O and Willecke K. 1998. Reduced cardiac conduction velocity and predisposition to arrhythmias in connexin40-deficient mice. Curr. Biol. 8, 299-302.

Kronengold J, Trexler EB, Bukauskas FF, Bargiello TA and Verselis VK. 2003. Pore-lining residues identified by single channel SCAM studies in Cx46 hemichannels. Cell Commun. Adhes. 10, 193-199.

Kyle JW, Minogue PJ, Thomas BC, Lopez Domowicz DA, Berthoud VM, Hanck DA and Beyer EC. 2008. An intact connexin N-terminus is required for function but not gap junction formation. J. Cell Sci. 121, 2744-2750.

Laing JG and Beyer EC. 1995. The gap junction protein connexin 43 is degraded via the ubiquitin proteasome pathway. J. Biol. Chem. 270, 26399-26403.

Laird DW, Jordan K, Thomas T, Qin H, Fistouris P and Shao Q. 2001. Comparative analysis and application of fluorescent protein-tagged connexins. Microsc. Res. Tech. 52, 263-273.

Lampe PD, TenBroek EM, Burt JM, Kurata WE, Johnson RG and Lau AF. 2000a. Phosphorylation of connexin43 on serine368 by protein kinase C regulates gap junctional communication. J. Cell Biol. 149, 1503-1512.

Lampe PD and Lau AF. 2000b. Regulation of gap junctions by phosphorylation of connexins. Arch. Biochem. Biophys. 384, 205-215

Lampe PD and Lau AF. 2004. The effects of connexin phosphorylation on gap junction communication. Int. J. Biochem. Cell Biol. 36, 1171-1186.

Lauf U, Giepmans BNG, Lopez P, Braconnot S, Chen S-C and Falk MM. 2002. Dynamic trafficking and delivery of connexons to the plasma membrane and accretion to gap junctions in living cells. Proc. Natl. Acad. Sci. USA. 99, 10446-10451.

Lee JR, DeRosa AM and White TW. 2009. Connexin mutations causing skin disease and deafness increase hemichannel activity and cell death when expressed in *Xenopus* oocytes. J. Invest. Dermatol. 129, 870-878.

Lerman BB, Dong B, Stein KM, Markowitz SM, Linden J and Catanzaro DF. 1998. Right ventricular outflow tract tachycardia due to a somatic cell mutation in G protein subunit$_{\alpha i2}$. J. Clin. Invest. 101, 2862-2868.

Lerner DL, Yamada KA, Schuessler RB and Saffitz JE. 2000. Accelerated onset and increased incidence of ventricular arrhythmia induced by ischemia in Cx43-deficient mice. Circ. 101, 547-552.

Li H, Liu T-F, Lazrak A, Peracchia C, Goldberg GS, Lampe PD and Johnson RG. 1996. Properties and regulation of gap junctional hemichannels in the plasma membraned of cultured cells. J. Cell Biol. 134, 1019-1030.

Lin Liang GS, De Miguel M, Gomez-Hernandez JM, Glass JD, Scherer SS, Mintz M, Barrio LC and Fischbeck KH. 2005. Severe neuropathy with leaky connexin32 hemichannels. Ann. Neurol. 57, 749-754.

Lloyd-Jones DM, Wang TJ, Leip EP, Larson MG, Levy D, Vasan RS, D'Agostino RB, Massaro JM, Beiser A, Wolf PA and Benjamin EJ. 2007. Lifetime risk for development of atrial fibrillation: The Framingham Heart Study. Circ. 110, 1042-1046.

Maass K, Shibayama J, Chase SE, Willecke K and Delmar M. 2007. C-terminal truncation of connexin43 changes number, size, and localization of cardiac gap junction plaques. Circ. Res. 101, 1283-1291.

Manias JL, Plante I, Gong X-Q, Shao Q, Churko J, Bai D and Laird DW. 2008. Fate of connexin43 in cardiac tissue harboring a disease-linked connexin43 mutant. Cardiovasc. Res. 80, 385-395.

Martinez AD, Hayrapetyan V, Moreno AP and Beyer EC. 2003. A carboxyl terminal domain of connexin43 is critical for gap junction plaque formation but not for homo- or hetero- oligomerization. Cell Commun. Adhes. 10, 323-328.

Mese G, Richard G and White TW. 2007. Gap junctions: basic structure and function. J. Invest. Dermatol. 127, 2516-2524.

Minogue PJ, Liu X, Ebihara L, Beyer EC and Berthoud VM. An aberrant sequence in a connexin46 mutant underlies congenital cataracts. 2005. J. Biol. Chem. 280, 40788-40795.

Minogue PJ, Tong J-J, Arora A, Russell-Eggitt I, Hunt DM, Moore AT, Ebihara L, Beyer EC, Berthoud VM. 2009. A mutant connexin50 with enhanced hemichannel function leads to cell death. Invest. Ophthalmol. Vis. Sci. 50, 5837-5845.

Moe GK, Rheinboldt WC and Abildskow JA. 1964. A computer model of atrial fibrillation. Am. Heart J. 67, 200-220.

Morley GE, Taffet SM and Delmar M. 1996. Intramolecular interactions mediate pH regulation of connexin43 channels. Biophys. J. 70, 1294-1302.

Musil LS and Goodenough DA. 1993. Multisubunit assembly of an integral plasma membrane channel protein, gap junction connexin43, occurs after exit from the ER. Cell. 74, 1065-1077.

Nagasawa K, Chiba H, Fujita H, Kojima T, Saito T, Endo T and Sawada N. 2006. Possible involvement of gap junctions in the barrier function of tight junctions of brain and lung endothelial cells. J. Cell. Physiol. 208, 123-132.

Nambara C, Kawasaki Y and Yamasaki H. 2007. Role of the cytoplasmic loop domain of Cx43 in its intracellular localization and function: possible interaction with cadherin. J. Membrane Biol. 217, 63-69.

Naus CC, Hearn S, Zhu D, Nicholson BJ and Shivers RR. 1993. Ultrastructural analysis of gap junctions in C6 glioma cells transfected with connexin43 cDNA. Exp. Cell Res. 206, 72-84.

Orthmann-Murphey JL, Enriquez AD, Abrams CK and Scherer SS. 2007. Loss-of-function GJA12/Connexin47 mutations cause Pelizaeus-Merzbacher-like disease. Mol. Cell. Neurosci. 34, 629-641.

Pal JD, Berthoud VM, Beyer EC, Mackay D, Shiels A and Ebihara L. 1999. Molecular mechanism underlying a Cx50-linked congenital cataract. Am. J. Physiol. Cell. Physiol. 276, 1443-1446.

Paul DL, Ebihara L, Takemoto LJ, Swenson KI and Goodenough DA. 1991. Connexin46, a novel lens gap junction protein, induces voltage-gated currents in nonjunctional plasma membrane of *Xenopus* oocytes. J. Cell. Biol. 115, 1077-1089.

Paznekas WA, Boyadjiev SA, Shapiro RE, Daniels O, Wollnik B, Keegan CE, Innis JW, Dinulos MB, Christian C, Hannibal MC and Jabs EW. 2003. Connexin 43 (GJA1) mutations cause the pleiotropic phenotype of oculodentodigital dysplasia. Am. J. Hum. Genet. 72, 408-418.

Purnick PEM, Benjamin DC, Verselis VK, Bargiello TA and Dowd TL. 2000. Structure of the amino terminus of a gap junction protein. Arch. Biochem. Biophys. 381, 181-190.

Quist AP, Rhee SK, Lin H and Lal R. 2000. Physiological role of gap-junctional hemichannels: extracellular calcium-dependent isosmotic volume regulation. J. Cell Biol. 148, 1063-1074.

Rackauskas M, Kreuzberg MM, Pranevicius M, Willecke K, Verselis VK and Bukauskas FF. 2007. Gating properties of heterotypic gap junction channels formed of connexins 40, 43, and 45. Biophys. J. 92, 1952-1965.

Reaume AG, De Sousa PA, Kulkami S, Langille BL, Zhu D, Davied TC, Juneja SC, Kidder GM and Rossant J. 1995. Cardiac malformation in neonatal mice lacking connexin43. Science. 267, 1831-1834.

Retamal MA, Schalper KA, Shoji KF, Bennett MVL and Saez JC. 2007. Opening of connexin 43 hemichannels is increased by lowering intracellular redox potential. Proc. Natl. Acad. Sci. U. S. A. 104, 8322-8327.

Ri Y, Ballesteros JA, Abrams CK, Oh S, Verselis VK, Weinstein H and Bargiello TA. 1999. The role of a conserved proline residue in mediating conformational changes associated with voltage gating of Cx32 gap junctions. Biophys. J. 76, 2887-2898.

Roberts JR and Gollob MH. 2009. Impact of genetic discoveries on the classification of lone atrial fibrillation. J. Am. Coll. Cardiol. 55, 705-712.

Roos A and Boron WF. 1981. Intracellular pH. Physiol. Rev. 61, 296-434.

Schalper KA, Palacios-Prado N, Orellana JA and Saez JC. 2008. Currently used methods for identification and characterization of hemichannels. Cell Commun. Adhes. 15, 207-218.

Seki A, Coombs W, Taffet SM and Delmar M. 2004a. Loss of electrical communication, but not plaque formation, after mutation in the cytoplasmic loop of connexin43. Heart Rhythm. 1, 227-233.

Seki A, Duffy HS, Coombs W, Spray DC, Taffet SM and Delmar M. 2004b. Modifications in the biophysical properties of connexin43 channels by a peptide of the cytoplasmic loop region. Circ. Res. 95, e22-e28.

Shaw RM, Fay AJ, Puthenveedu MA, Zastrow MV, Jan Y-N and Jan LY. 2007. Microtubule plus-end-tracking proteins target gap junctions directly from the cell interior to adherens junctions. Cell. 128, 547-560.

Shibayama J, Paznekas W, Seki A, Taffet S, Jabs EW, Delmar M and Musa H. 2005. Functional characterization of connexin43 mutations found in patients with oculodentodigital dysplasia. Circ. Res. 96, e83-91.

Shiels A, Mackay D, Ionides A, Berry V, Moore A and Bhattacharya S. 1998. A missense mutation in the human connexin50 gene (GJA8) underlies autosomal dominant "zonular pulverent" cataract, on chromosome 1q. Am. J. Hum. Genet. 62, 526-532.

Simek J, Churko J, Shao Q and Laird DW. 2008. Cx43 has distinct mobility within plasma-membrane domains, indicative of progressive formation of gap junction plaques. J. Cell Sci. 122, 554-562.

Skerrett IM, Merritt M, Zhou L, Zhu H, Cao F, Smith JF and Nicholson BJ. 2001. Applying the Xenopus oocyte expression system to the analysis of gap junction proteins. Methods Mol. Biol. 154, 225-249.

Skerrett IM, Aronowitz J, Cymes G, Kasperek E, Cao FL and Nicholson BJ. 2002. Identification of amino acid residues lining the pore of a gap junction channel. J. Cell Biol. 159, 349-359.

Sohl G and Willecke K. 2004. Gap junctions and the connexin protein family. Cardiovasc. Res. 62, 228-232.

Srinivas M, Kronengold J, Bukauskas FF, Bargiello TA and Verselis VK. 2005. Correlative studies of gating in Cx46 and Cx50 hemichannels and gap junction channels. Biophys. J. 88, 1725-1739.

Stergiopoulos K, Alvarado JL, Mastroianni M, Ek-Vitorin JF, Taffet SM and Delmar M. 1999. Hetero-domain interactions as a mechanism for the regulation of connexin channels. Circ. Res. 84, 1144-1155.

Stong BC, Chang Q, Ahmed S and Lin X. 2006. A novel mechanism for connexin 26 mutation linked deafness: cell death caused by leaky gap junction hemichannels. Laryngoscope. 116, 2205-2210.

Stout CE, Costantin JL, Naus CCG and Charles AC. 2002. Intercellular calcium signaling in astrocytes via ATP release through connexin hemichannels. J. Biol. Chem. 277, 10482-10488.

Suchyna TM, Xu LX, Gao F, Fourtner CR and Nicholson BJ. 1993. Identification of a proline residue as a transduction element involved in voltage gating of gap junctions. Nature. 365, 847-849.

Thomas SA, Schuessler RB, Berul CI, Beardslee MA, Beyer EC, Mendelsohn ME and Saffitz JE. 1998. Disparate effects of deficient expression of connexin43 on atrial and ventricular conduction. Circ. 97, 686-691.

Thomas T, Jordan K and Laird DW. 2001. Role of cytoskeletal elements in the recruitment of Cx43-GFP and Cx26-YFP into gap junctions. Cell Commun. Adhes. 8, 231-236.

Toyofuku T, Yabuki M, Otsu K, Kuzuya T, Hori M and Tada M. 1998. Direct association of the gap junction protein connexin-43 with ZO-1 in cardiac myocytes. J. Biol. Chem. 273, 12725-12731.

Trexler EB, Bennett MVL, Bargiello TA and Verselis VK. 1996. Voltage gating and permeation in a gap junction hemichannel. Proc. Natl. Acad. Sci. USA. 93, 5836-5841.

Trexler EB, Bukauskas FF, Kronengold J, Bargiello TA and Verselis VK. 2000. The first extracellular loop domain is a major determinant of charge selectivity in connexin46 channels. Biophys. J. 79, 3036-3051.

Valiunas V, Weingart R and Brink PR. 2000. Formation of heterotypic gap junction channels by connexin 40 and 43. Circ. Res. 86, e42-e49.

Valiunas V, Gemel J, Brink PR and Beyer EC. 2001. Gap junction channels formed by co-expressed connexin40 and connexin43. Am. J. Physiol. Heart Circ. Physiol. 281, H1675-H1689.

Verheule S, Van Batenburg C, Coenjaerts FEJ, Kirchhoff S, Willecke K and Jongsma HJ. 1999. Cardiac conduction abnormalities in mice lacking the gap junction protein connexin40. J. Cardiovasc. Electrophysiol. 10;1380-1389.

Verselis VK, Ginter CS and Bargiello TA. 1994. Opposite voltage gating polarities of two closely related connexins. Nature. 368, 348-351.

Vozzi C, Dupont E, Coppen SR, Yeh H-I and Severs NJ. 1999. Chamber-related differences in connexin expression in the human heart. J. Mol. Cell Cardiol. 31, 991-1003.

Wang H-L, Wu T, Chang W-T, Li AH, Chen M-S, Wu C-Y and Fang W. 2000. Point mutation associated with X-linked dominant Charcot-Marie-Tooth disease impairs the P2 promoter activity of human connexin32 gene. Brain Res. Mol. Brain Res. 78,146-153.

White TW, Paul DL, Goodenough DA and Bruzzone R. 1995. Functional analysis of selective interactions among rodent connexins. Mol. Biol. Cell. 6, 459-470.

White TW and Bruzzone R. 1996. Multiple connexin proteins in single intercellular channels: connexin compatibility and functional consequences. J. Bioenerg. Biomembr. 28, 339-350.

Wolf PA, Abbott RD and Kannel WB. 1991. Atrial fibrillation as an independent risk factor for stroke: The Framingham Study. Stroke. 22, 983-988.

Ye ZC, Wyeth MS, Baltan-Tekkok S, Ransom BR. 2003. Functional hemichannel in astrocytes: a novel mechanism of glutamate release. J. Neurosci. 23, 3588-3596.

Zhou X-W, Pfahnl A, Werner R, Hudder A, Llanes A, Luebke A and Dahl G. 1997. Identification of a pore lining segment in gap junction hemichannels. Biophys. J. 72, 1946-1953.

Contribution of Collaborators

Our collaborators at the University of Texas Health Science Centre (San Antonio, Texas, USA), Ji Xu (MSc) and Bruce Nicholson (PhD), have performed the experiments shown in figure 10.

We have requested the help of Louis Pelletier at the Department of Pathology of the University of Ottawa for immunohistochemical stainings on atrial tissue of affected and control patients shown in figure S1.

Collaborators at the Cleveland Clinic (Cleveland, Ohio, USA), Robert Wirka (MD), Jonathan Smith (PhD) and Mina Chung (MD), have identified the arginine113serine mutation in Cx40 and have requested our help to perform functional characterization.

Collaborators at the Rosalind Franklin University (Chicago, Illinois, USA), Jun-Jie Tong (MD), Wasif Raja (MD), and Lisa Ebihara (MD, PhD), and at the Texas Tech University Health Science Centre, Mauricio Retamal (MD) and Luis Reuss (MD), have generated the data shown in figures S2 and S3.

Appendix A, Supplementary figures

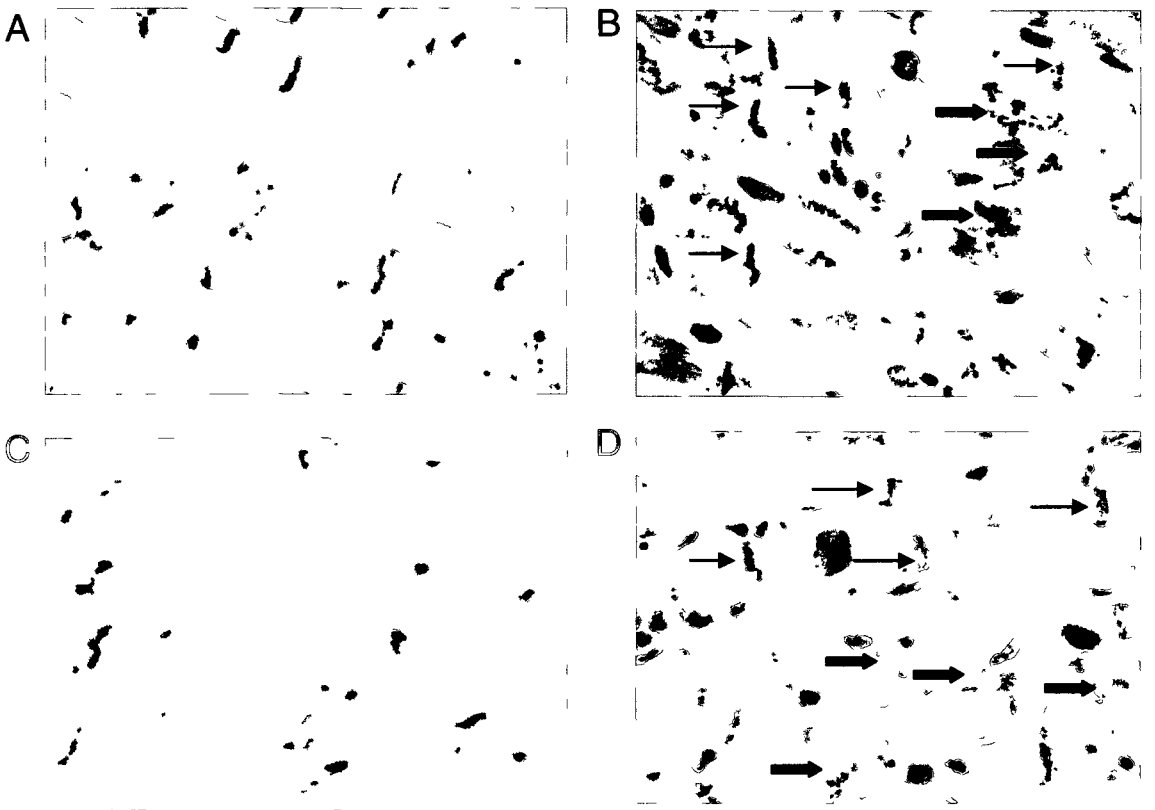

Figure S1. Cellular localization of Cx40 and Cx43 in atrial tissue of control and affected patients. Immunohistochemical stainings of Cx43 (A, B) and Cx40 (C, D) in control patients unaffected by AF (A, C) and affected patient with the Cx43 mutation (Cx43-932delC) (B, D). Thin arrows indicate typical staining of intercalated disks while thick arrows indicate intracellular staining uncharacteristic of connexin localization. These experiments were performed by Louise Pelletier from the Department of Pathology at the University of Ottawa.

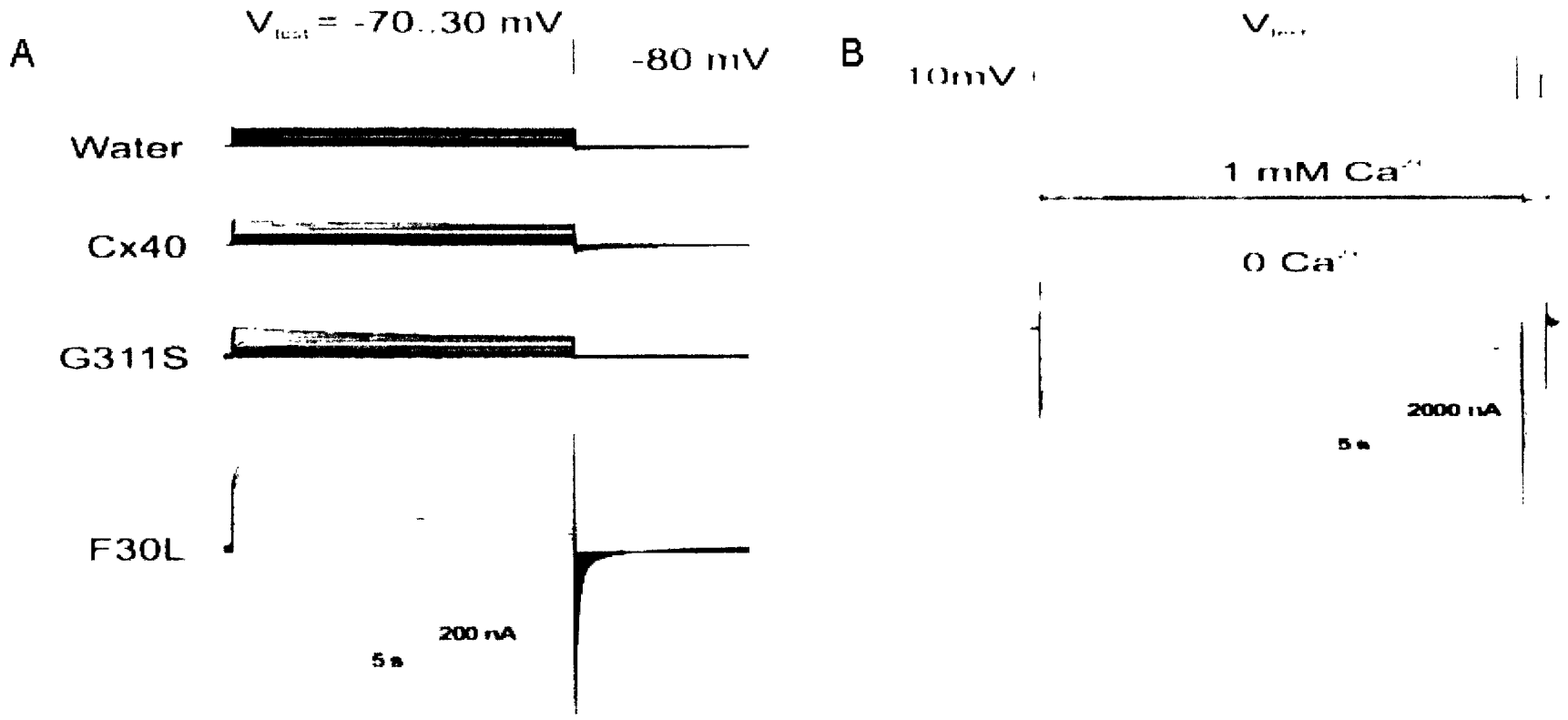

Figure S2. Hemichannel current measurements of wild-type and mutant Cx40 in *Xenopus* oocytes. (A) Representative current traces of oocytes injected with either water as a control, wild-type Cx40, Cx40-G311S or Cx40-F30L RNA. (B) Current measurements of oocytes injected with F30L RNA. The oocytes were either incubated in the presence (1mM) or absence (0mM) of calcium in the bath solution. Currents were measured in response to the voltage protocol applied, shown above the current tracings. These experiments were performed by our collaborators at the Rosalind Franklin University in Chicago.

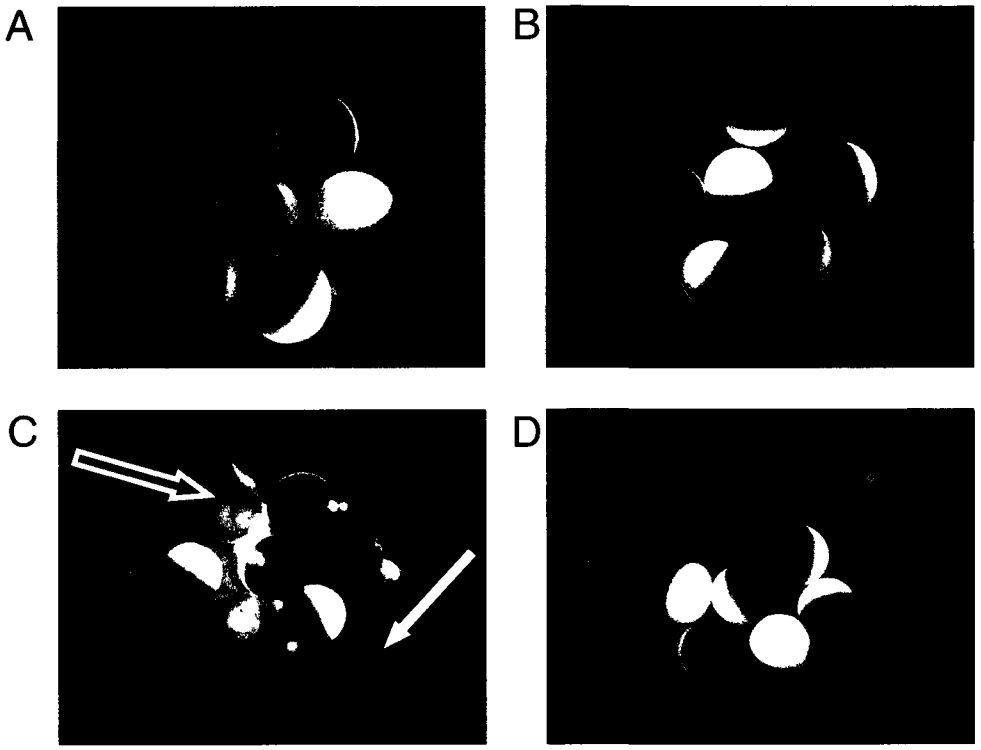

Figure S3. Effects of F30L mutant on cell viability and effect of calcium on hemichannel opening. Oocytes were cultured for 12-18 hours and monitored for cell viability. (A) Control oocytes injected with H_2O. (B) Oocytes injected with Cx40-WT cRNA. (C) F30L expressing oocytes. (D) F30L injected oocytes cultures with media supplemented 2mM Ca+2. These experiments were performed by our collaborators at the Rosalind Franklin University in Chicago.

Appendix B, Publications

Manuscript in press in Circulation.

Paradigm of Genetic Mosaicism and Lone Atrial Fibrillation: Physiological Characterization of a Connexin 43-deletion Mutant Identified from Atrial Tissue

Circulation
JOURNAL OF THE AMERICAN HEART ASSOCIATION

Paradigm of Genetic Mosaicism and Lone Atrial Fibrillation: Physiological Characterization of a Connexin 43 Deletion Mutant Identified From Atrial Tissue

Isabelle L. Thibodeau, Ji Xu, Qiuju Li, Gele Liu, Khanh Lam, John P. Veinot, David H. Birnie, Douglas L. Jones, Andrew D. Krahn, Robert Lemery, Bruce J. Nicholson and Michael H. Gollob

Circulation 2010;122;236-244; originally published online Jul 6, 2010;
DOI: 10.1161/CIRCULATIONAHA.110.961227
Circulation is published by the American Heart Association. 7272 Greenville Avenue, Dallas, TX 72514
 Print ISSN: 0009-7322. Online ISSN: 1524-4539

Paradigm of Genetic Mosaicism and Lone Atrial Fibrillation

Physiological Characterization of a Connexin 43–Deletion Mutant Identified From Atrial Tissue

Isabelle L. Thibodeau, BSc; Ji Xu, MSc; Qiuju Li, MSc; Gele Liu, MD, PhD; Khanh Lam, MD; John P. Veinot, MD; David H. Birnie, MD; Douglas L. Jones, PhD; Andrew D. Krahn, MD; Robert Lemery, MD; Bruce J. Nicholson, PhD; Michael H. Gollob, MD

Background—Atrial fibrillation (AF) is the most common sustained arrhythmia observed in otherwise healthy individuals. Most lone AF cases are nonfamilial, leading to the assumption that a primary genetic origin is unlikely. In this study, we provide data supporting a novel paradigm that atrial tissue–specific genetic defects may be associated with sporadic cases of lone AF.

Methods and Results—We sequenced the entire coding region of the connexin 43 (Cx43) gene (*GJA1*) from atrial tissue and lymphocytes of 10 unrelated subjects with nonfamilial, lone AF who had undergone surgical pulmonary vein isolation. In the atrial tissue of 1 patient, we identified a novel frameshift mutation caused by a single nucleotide deletion (c.932delC) that predicted 36 aberrant amino acids followed by a premature stop codon, leading to truncation of the C-terminal domain of Cx43. The mutation was absent from the lymphocyte DNA of the patient, indicating genetic mosaicism. Protein trafficking studies demonstrated intracellular retention of the mutant protein and a dominant-negative effect on gap junction formation of both wild-type Cx43 and Cx40. Electrophysiological studies revealed no electrical coupling of cells expressing the mutant protein alone and significant reductions in coupling when coexpressed with wild-type connexins.

Conclusions—This study reports atrial tissue genetic mosaicism of a novel loss-of-function Cx43 mutation associated with lone AF. These findings implicate somatic genetic defects of Cx43 as a potential cause of AF and support the paradigm that sporadic, nonfamilial cases of lone AF may arise from genetic mosaicism that creates heterogeneous coupling patterns, predisposing the tissue to reentrant arrhythmias. (***Circulation.* 2010;122:236-244.**)

Key Words: arrhythmia ■ connexins ■ electrophysiology ■ fibrillation ■ gap junctions ■ genetics

Atrial fibrillation (AF) is the most common sustained cardiac arrhythmia, may cause significant morbidity, and is a common cause of stroke.[1] AF confers an increased mortality risk that is independent of coexisting risk factors.[2] Current management strategies for AF are not optimal. Pharmacological therapies target nonspecific ion channels, may be proarrhythmic or lead to intolerable side effects, and often become refractory over time. Catheter ablation therapy has received much attention. However, the reported efficacy of the procedure varies considerably between institutions[3-6]; significant complications may occur[7,8]; and long-term success (>24 months) in large cohorts has not been reported despite the use of this procedure for more than a decade. These limitations provide the impetus to discover genetic determinants of AF, which may identify novel and specific protein targets for the development of more efficacious drugs.

Clinical Perspective on p 244

In recent years, progress in understanding the genetic basis of AF has been derived from the study of familial forms of the disease.[9-15] However, the vast majority of AF in otherwise healthy individuals is sporadic and nonfamilial. Genetic defects identified in rare families are uncommonly identified in sporadic cases,[16,17] suggesting that alternative molecular pathways may be more relevant in the common scenario of lone, nonfamilial AF.

Traditionally, common sporadic diseases such as AF have not been considered to have a genetic basis. Increasingly, sporadic cases of human disease have been identified as being caused by somatic or tissue-specific genetic mutations in culprit genes.[18-21] Such somatic mutations are present in a subpopulation of cells in the diseased tissue, creating a

Received April 21, 2009, accepted May 19, 2010

From the Departments of Medicine (A D K , D L J) and Physiology and Pharmacology (D L J), University of Western Ontario, London, Ontario, Canada, Department of Biochemistry, University of Texas Health Science Center at San Antonio (J X , B J N), and Department of Pathology (J P V), Arrhythmia Research Laboratory (I L T , Q L , G L , M H G), Arrhythmia Service, Division of Cardiology (J P V , D H B , R L , M H G), Department of Surgery (K L), and Department of Cellular and Molecular Medicine (M H G), University of Ottawa Heart Institute, Ottawa, Ontario, Canada

Correspondence to Dr Michael H. Gollob, Arrhythmia Research Laboratory, Arrhythmia Service, and Department of Cellular and Molecular Medicine, University of Ottawa, University of Ottawa Heart Institute, 40 Ruskin St, Room H350, Ottawa, Ontario, Canada K1Y 4W7 E-mail mgollob@ottawaheart ca

***Circulation* is available at http://circ.ahajournals.org** **DOI: 10.1161/CIRCULATIONAHA.110.961227**

mosaic gene expression pattern sufficient to induce a disease phenotype [18,20] Although these observations have been described primarily for tumor-prone syndromes, we previously described cardiac-specific somatic mutations of the connexin 40 (Cx40) gene (*GJA5*) to be associated with early-onset, sporadic AF [22]

In the myocardium, gap junction channels are the principal determinant of action potential propagation and conduction velocity [23] These specialized channels are made up of connexin proteins, which oligomerize into hexameric structures known as connexons or hemichannels Adjacent and connected myocytes each contribute connexons to form functional gap junction channels, which serve to electrically couple myocytes and to optimize conduction of the depolarizing wavefront through the myocardium Regional variability or heterogeneity in conduction velocity is the prerequisite substrate of electrical reentry, a fundamental component for the initiation and perpetuation of AF [24,25] Although structural heart disease leading to fibrotic deposition and altered tissue geometry may promote reentry, an alternative mechanism in otherwise normal structural hearts may involve primary alterations in the functional expression and/or tissue distribution of cardiac gap junctions [26,29] Animal models with complete myocardial absence of connexin isoforms, expression of mutant connexins, and inhomogeneous or mosaic distribution of connexins have all demonstrated increased vulnerability to cardiac reentrant arrhythmias [26–28]

In this article, we report that genetic mosaicism within atrial tissue of the most abundant cardiac connexin, Cx43, is associated with sporadic, nonfamilial AF This study expands the spectrum of genetic defects associated with AF and further supports the concept that sporadic AF may have a genetic basis identified from the diseased tissue

Methods

Study Subjects

Left atrial appendage tissue specimens were obtained during surgical pulmonary vein isolation from 10 unrelated patients with sporadic lone AF and were confirmed to lack mutations in the Cx40 gene (*GJA5*), which have previously been reported to be detected from the atrial tissue of lone AF patients [22] Genetic analysis was then performed on the Cx43 gene (*GJA1*), *KCNQ1*, *KCNA5*, and *SCN5A* All patients recruited for the study were required to have documentation of normal left ventricular function and valve structure by 2 dimensional echocardiography and had age of onset of AF <55 years

All patients also provided blood samples for lymphocyte DNA analysis Affected and control patients in this study were of Western European descent Cardiac tissue and blood samples were collected with written informed consent and were approved for study by the institutional review board of the University of Ottawa Heart Institute

Mutation Detection

Genetic analysis was performed on genomic DNA isolated from both left atrial appendage tissue and lymphocytes The entire coding sequence and splice junctions of *GJA1*, *KCNQ1*, *KCNA5*, and *SCN5A* were directly sequenced Mutation confirmation was performed by resequencing of an independently derived polymerase chain reaction (PCR) product To determine the proportion of mutant alleles contained within the atrial tissue specimen, PCR products were subcloned into the pGEM T vector (Promega, Madison, Wis), and allele sequence was confirmed by direct sequencing of sub cloned alleles All sequencing was performed on an ABI 3100 DNA sequencer Primer sequences and PCR protocols are available on request For amplification and sequencing of the *GJA1* gene, PCR primers with mismatches to the Cx43 pseudogene (*GJA1P1*) sequence were used to specifically amplify *GJA1* and to avoid amplification of *GJA1P1*, as described previously by Paznekas et al [30]

Protein Trafficking Studies

Wild type (wt) Cx43 was cloned into the pcDNA3 1 vector, and mutant Cx43 was engineered by site directed mutagenesis of a wt-Cx43 clone using the QuickChange mutagenesis kit (Stratagene, La Jolla, Calif) Wt and mutant connexin sequences were subcloned into pEYFP N1 and/or pECFP N1 vectors All connexin clones were sequenced to confirm the accuracy of the predicted nucleotide sequence Protein trafficking studies of wt and mutant connexins in HeLa cells were achieved by transfection of untagged or C terminal fluorescently tagged connexins HeLa cells were grown at 37°C in Dulbecco modified Eagle medium supplemented with 10% FBS and plated on coverslips in 24-well plates to 70% to 80% confluence Cells were transfected in Opti MEM medium containing Lipofectamine 2000 and a total of 1 μg mutant and/or wt connexins For cellular localization of wt and mutant connexin proteins, cotransfections were performed with either a tagged endoplasmic reticulum protein marker (calreticulin) or Golgi protein marker (1,4 galactosyltransferase) (generous gifts of Dr Regis Grailhe, Institut Pasteur, and Dr Heidi McBride, University of Ottawa, respectively) To simulate the effect of heterozygosity and to test the effect of mutant Cx43 protein on trafficking of wt Cx43 or wt Cx40, we cotransfected a 1 1 ratio of wt to mutant constructs Live cells were visualized with confocal microscopy 24 to 48 hours after transfection For immunodetection of untagged constructs, cells were rinsed with PBS, followed by fixation and permeabilization in ice cold methanol and acetone at −20°C Cells were washed with PBS and then blocked with PBS/0 5% BSA for 45 minutes The monoclonal mouse anti Cx43 antibody (Chemicon International, Temecula, Calif), recognizing amino acids 131 to 142 of the intracellular loop, was diluted to 1 50 in blocking solution and incubated for 45 minutes at room temperature Cells were rinsed with blocking solution, followed by incubation for 45 minutes with the DyLight488 conjugated goat anti-mouse IgG secondary antibody (Jackson ImmunoResearch Laboratories, West Grove, Pa) diluted to 1 1000 in blocking solution Immunolabeled cells were visualized with confo cal microscopy and were assigned the color red All transfections were repeated in duplicate A transfection is considered successful only if a minimum of 10 cell pairs can be visualized per transfection For all trafficking studies, >20 cell pairs were visualized

Immunohistochemistry

Immunohistochemistry was performed on 7-μm-thick sections of formalin-fixed and paraffin-embedded left atrial appendage tissue Tissue sections were deparaffinized, and antigen retrieval was performed by microwave in a citrate buffer (pH 5 6) Specimens were blocked in normal horse serum and incubated with an anti Cx43 antibody (Chemicon) specific to amino acid residues 131 to 142 within the cytoplasmic loop common to both wt and mutant Cx43 Similarly, immunostaining was performed for Cx40 with an anti Cx40 antibody (Santa Cruz Biotechnology, Inc, Santa Cruz, Calif) recognizing specific residues within the C terminus Primary antibody was detected with the DAB (diaminobenzidine) chromogen system (DAKO, Carpinteria, Calif)

Electrophysiological Studies

Electrophysiological recordings were carried out first in N2A cells, a connexin deficient cell line N2A cells were grown at 37°C in 35-mm culture dishes to 50% to 70% confluence in Dulbecco modified Eagle medium containing 10% FBS, 100 U/mL penicillin, and 100 μg/mL streptomycin Cells were transfected in Opti-MEM medium containing Lipofectamine 2000 and 2 μg fluorescently tagged mutant and/or wt connexins Patch-clamp analysis was performed 24 to 48 hours after transfection To simulate the effect of heterozygosity and to test the effect of mutant Cx43 protein on

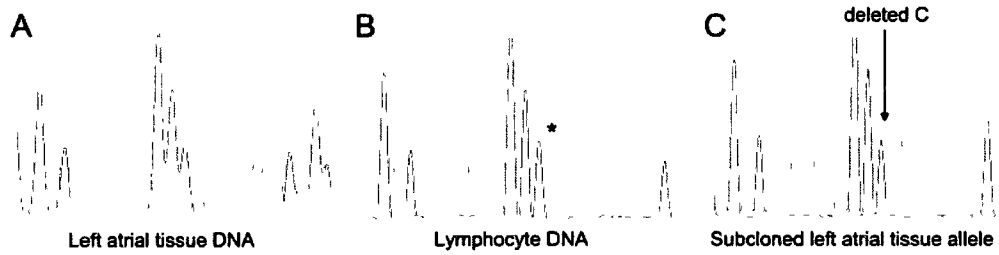

Figure 1. Detection of c.932delC-Cx43 mutation. A, The sequencing electropherogram from left atrial tissue of the affected patient. The sudden change to overlapping nucleotides is characteristic of a frameshift mutation. In contrast, sequencing of genomic DNA isolated from lymphocytes of the patient showed only normal Cx43 sequence with no evidence of frameshift (B). Subcloning and sequencing of left atrial PCR products (C) identified the identical cytosine nucleotide deletion allele (c.932delC) in 9 of 27 sequenced clones (asterisk in B indicates the location of the deleted nucleotide).

wt-Cx43 or wt-Cx40, we cotransfected a 1:1 ratio of wt to mutant constructs.

Dual, whole-cell, voltage-clamp recordings were carried out at room temperature on N2A cells perfused with a solution containing (in mmol/L) NaCl 140, KCl 5, CsCl 2, $CaCl_2$ 2, $MgCl_2$ 1, Hepes 5, D-glucose 5, pyruvate 2, and $BaCl_2$ 1 (pH 7.4). The recording pipette had a resistance of 3 to 5 MΩ when filled with an internal solution containing (in mmol/L) CsCl 130, EGTA 10, $CaCl_2$ 0.5, MgATP 3, Na_2ATP 2, and Hepes 10 (pH=7.2) with CsOH. The current signal was digitized at a sampling rate of 1 to 2 kHz with a Digidata 1322a (Axon Instruments Inc, La Jolla, Calif) and analyzed with pClamp9 software. Each cell of a pair was initially held at a common holding potential of 0 mV. To evaluate junctional coupling, 300-ms hyperpolarizing pulses to −30 mV were applied to 1 cell, from the holding potential of 0 mV, to establish a transjunctional voltage gradient (V_j), while the junctional current was measured in the second cell. Macroscopic junctional conductance (g_j) was calculated as follows: $g_j=I_j/V_j$, where I_j is the measured junctional current and V_j is the transjunctional voltage. In all cases, cells were studied after multiple independent transfections. To facilitate functional testing, we selected cell pairs with visible plaques at the cell-cell junction.

Electrophysiological recordings were repeated in *Xenopus* oocyte cells injected with specific cRNA quantities of untagged wt and mutant constructs, avoiding the potential issues of variable cellular uptake of clones that may occur during cotransfection of mammalian cells. Wt-Cx40, wt-Cx43, and mutant Cx43 were first subcloned into pGEM-7zf vector. cRNA was prepared by use of the mMessage mMachine kit from Ambion Inc (Austin, Tex) with Cx40 under T3 promoter and Cx43 under SP6 promoter. Oocytes were treated as previously described[31] and injected with 4 ng antisense phosphorothioated oligonucleotide directed against nucleotides 327 to 353 of endogenous *Xenopus* Cx38 with sequence G*C*C* ACC AGA ATC CTT GAT TCA TTC* T*C*C (asterisks represent phosphorothioate bond). After 3 days, oocytes were injected again with connexin RNA mixed with 4 ng antisense oligonucleotide. After injection, oocytes were incubated at 17°C for 24 hours, stripped off their vitelline membrane, and paired overnight in agar wells. Oocytes were continuously bathed in half-strength L15 media (Sigma, St Louis, Mo). Junctional currents were assessed by dual oocyte voltage-clamp technique with 2 Geneclamp500 amplifiers (Axon Instruments). Oocytes were clamped at ≈−30 mV, and transjunctional conductances were measured by a 10-mV voltage pulse. In addition, a series of 10-second voltage pulses were used to generate a gating profile of the expressed channels over a transjunctional voltage (Vj) range of −100 to 100 mV to ensure that the properties were consistent with the connexin expressed. Data were acquired and analyzed with pClamp8 software (Axon Instruments).

All data are expressed as mean±SEM. An unpaired Student *t* test was used to test statistical significance. Differences were deemed significant at $P<0.05$.

Results

Mutation Detection and Clinical Phenotype

After comprehensive testing in all patients, a frameshift mutation within the coding region of the Cx43 gene was detected in a single patient by direct DNA sequencing of left atrial tissue (Figure 1). Sequencing of lymphocyte DNA from this patient revealed a normal Cx43 sequence, indicating genetic mosaicism. Direct sequencing of subcloned left atrial tissue PCR products identified the specific genetic defect to represent a single base deletion of nucleotide 932 (c.932delC). To estimate the proportion of mutant alleles present within atrial tissue, direct sequencing of multiple subcloned alleles revealed a mutant allele frequency of 33% (9 of 27 clones). The Cx43 c.932delC mutation occurs within the codon for amino acid residue 311 of the putative 382–amino acid Cx43 protein. The mutation predicts 36 aberrant amino acids after amino acid residue 310 (tryptophan), followed by a premature stop codon, resulting in a truncated Cx43 protein. Direct sequencing of 100 alleles from heart tissue in individuals unaffected by AF and 200 alleles from lymphocyte DNA of healthy control subjects showed no evidence of the mutation.

The affected patient had documented AF at 48 years of age after years of episodic palpitations. Recurrent episodes were initially well controlled with propafenone and eventually amiodarone. The patient had a normal QRS duration and no observed ventricular arrhythmias or pronounced ectopy during repeated Holter recordings. At 58 years of age, the patient was refractory to medical therapy and had persistent AF. The patient had no history of hypertension, diabetes mellitus, valvular disease, thyroid dysfunction, or syndromic features and no family history of AF. Before surgical intervention, 2-dimensional echocardiography documented normal left ventricular function and a left atrial size at the upper limits of normal (4.0 cm). Coronary angiography demonstrated normal epicardial arteries. Surgical intervention consisted of isolation of the pulmonary veins and left atrial posterior wall through a combination of incision and cryoablation. A line of conduction block from the isolated segment to the mitral annulus was also performed. At the 2-year follow-up, the patient was in normal sinus rhythm with no symptomatic recurrence of palpitation or documented AF.

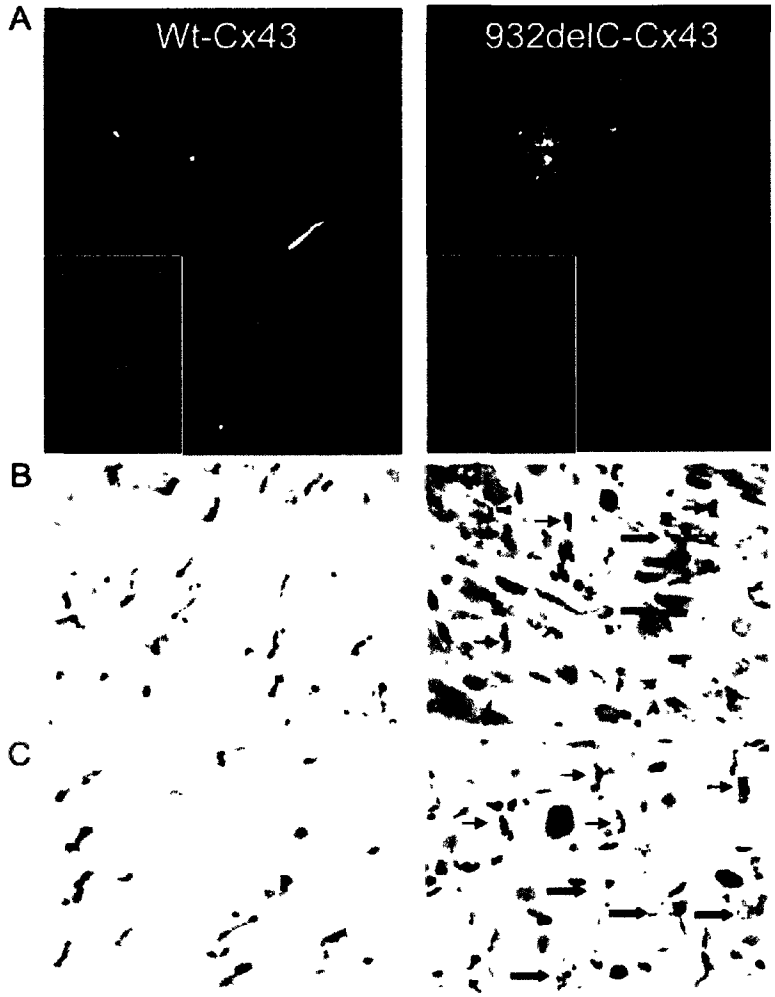

Figure 2. Cellular localization of c.932delC-Cx43 in HeLa cells and atrial tissue. A, HeLa cells were transfected with YFP-tagged wt-Cx43 (left) or c.932delC-Cx43 (right). Cells expressing wt-Cx43 readily form visible gap junction plaques at the cell-to-cell interface, whereas mutant Cx43-expressing cells showed significant intracellular retention of the tagged protein. Panel A inset represents immunostaining of untagged connexin constructs. B, left, Normal gap junction formation at intercalated disks of adjacent cardiac myocytes in atrial tissue from a control patient with no history of atrial fibrillation. In contrast, atrial tissue from the affected patient harboring the c.932delC-Cx43 mutation showed a mosaic pattern of staining, with normal-appearing intercalated disks (thin arrows) and significant intracellular staining of Cx43 in adjacent cells (thick arrows) (right). C, A similar mosaic pattern of staining is seen for Cx40 in the atrial tissue.

Protein Trafficking and Immunohistochemistry of Atrial Tissue

Mutant c.932delC-Cx43 was expressed in HeLa cells to assess the ability of the aberrant protein to form visible gap junction plaques. In contrast to cells expressing wt-Cx43, mutant Cx43 showed predominantly intracellular retention and only rarely showed sparse visible plaques at cell-to-cell junctions (Figure 2A). To assess whether the abnormal trafficking observed in this cell was reflected in vivo, left atrial appendage tissue of the affected patient was stained with an anti-Cx43 antibody specific to residues within the cytoplasmic loop. As predicted by the protein trafficking studies in HeLa cells, a mosaic pattern of intracellular retention of Cx43 protein and abnormal gap junction formation was observed (Figure 2B). Similarly, although to a lesser extent, intracellular retention of Cx40 was also observed in the atrial tissue, suggesting an effect of the mutant Cx43 on wt-Cx40 trafficking (Figure 2C).

To determine the subcellular localization of the mutant protein, c.932delC-Cx43 was cotransfected with either tagged endoplasmic reticulum or Golgi markers. These results indicated that the aberrant, truncated Cx43 mutant was retained primarily within the Golgi apparatus (Figure 3A and 3B). To determine the effect of mutant Cx43 in the heterozygous state, cotransfection of mutant and wt-Cx43 was performed in HeLa cells. A similar pattern of intracellular retention was observed, confirming a dominant-negative effect of the mutant protein (Figure 4A). In addition, to test the hypothesis that Cx43 and Cx40 isoforms may interact during the oligomerization process in the formation of hexameric connexons, mutant Cx43 and wt-Cx43 were cotransfected with wt-Cx40. Cotransfection of the wt isoforms resulted in colocalization at cell-to-cell junctions (Figure 4B), whereas transfection of mutant Cx43 abolished appropriate trafficking of wt-Cx40, indicating an interaction of these connexin isoforms during the oligomerization and trafficking process (Figure 4C).

Electrophysiological Function

Electrical coupling was recorded from paired N2A cells, a connexin-deficient cell line. In all cases, only cell pairs with visible gap junction plaques at the cell-to-cell interface were used for recordings. Cells expressing only mutant c.932delC-Cx43 rarely showed scant plaques and demonstrated a >5-fold reduction in cell-to-cell gap junction conductance compared with cells expressing wt-Cx43 ($P<0.01$; Figure 5B). Consistent with the dominant-negative effect of the mutant protein on wt-Cx43 observed in the protein trafficking stud-

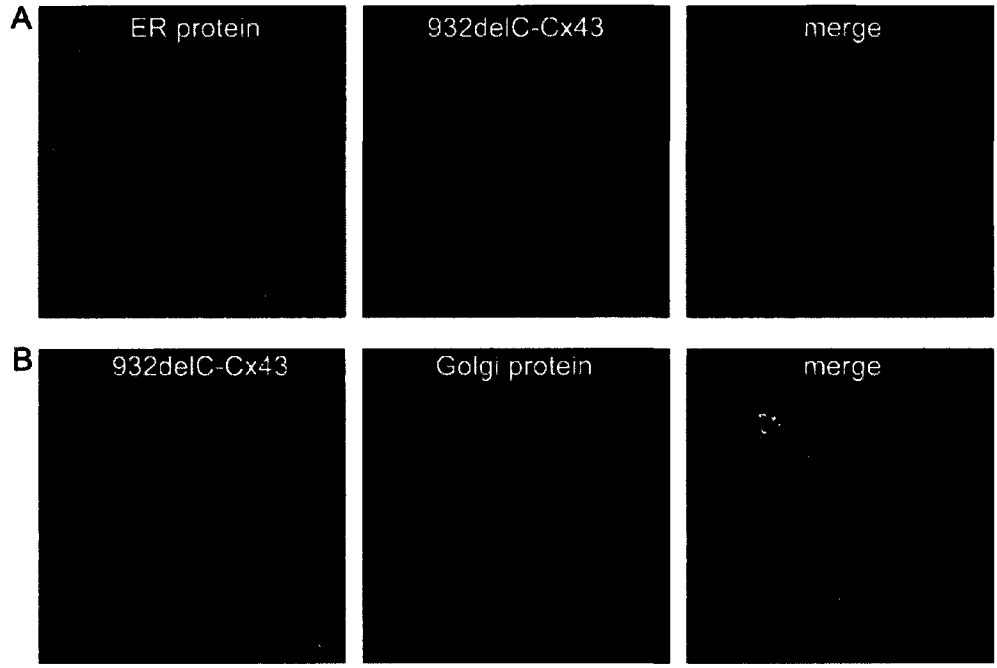

Figure 3. Subcellular localization of c 932delC Cx43 Fluorescently tagged mutant Cx43 and protein markers of the endoplasmic reticulum (ER) or Golgi apparatus were cotransfected in HeLa cells A, Minimal overlap of mutant Cx43 with the ER marker B Mutant Cx43 is predominantly retained within the Golgi network

ies, coexpressing cells demonstrating visible plaques also had a significant reduction in electrical coupling ($P=0.04$) A transdominant-negative effect of mutant Cx43 on wt-Cx40 gap junction conductance was also demonstrated on paired cells with visible gap junction plaques ($P=0.04$), supporting an interaction of Cx43 with Cx40 at the cell-to-cell interface

Electrophysiological studies in *Xenopus* oocytes confirmed a complete loss of function for the mutant protein ($P=0.00003$) and the dominant-negative effect of the mutant Cx43 on wt-Cx43 electrical coupling, to a much greater degree than had been seen in N2A cells ($P=0.00004$, Figure 5C) The transdominant effect of mutant Cx43 over wt-Cx40 that had been observed in N2A cells was not evident at all in the *Xenopus* oocyte cell model However, when wt-Cx43 was coinjected with wt-Cx40 and mutant Cx43 in ratios mimicking what would be seen intracellularly in vivo, a transdominant effect was present ($P=0.007$), suggesting that the heteromeric assembly of the wt connexin isoforms was necessary for the mutant protein to exert an inhibitory effect

Discussion

The cause of AF in otherwise healthy young individuals without a family history of disease is traditionally classified as lone or idiopathic However, as has been learned from other apparent sporadic diseases, the contribution of genetic factors may be significant [18–21,32,34] Genetic predisposition to disease, in the absence of a familial pattern, may be the result of multiple genetic variations throughout the genome, each contributing to the risk of the disease phenotype [32] Alternatively, environmental influences in the setting of a vulnerable genetic background may be required to trigger a disease process [33] Least recognized is the phenomenon of somatic or tissue-specific genetic mutations, whereby the genetic defect may be detected only by DNA analysis of the diseased tissue [18–22] In this study, we report the presence of an atrial tissue–specific mutation of the *GJA1* gene, encoding Cx43, in an otherwise healthy, young female with AF The mutation was absent from the patient's lymphocyte DNA, indicating genetic mosaicism Subcloning analysis of the mutant allele estimated an allele frequency of 33% within the left atrial tissue These findings implicate atrium-specific genetic defects of Cx43 as a potential cause of AF and support the paradigm that sporadic, nonfamilial cases of lone AF may have a genetic basis identified after genetic testing of the affected tissue

Cx43, the most abundant cardiac connexin, is highly expressed in both atrial and ventricular myocardium, in addition to a variety of other tissues during development [23] Germline mutations of Cx43 have been associated with oculodentodigital dysplasia, a rare inherited autosomal-dominant disorder characterized by developmental abnormalities of the face, eyes, limbs, and dentition [30] Cardiac abnormalities, including sick sinus syndrome, ventricular tachycardia, and sudden cardiac death, have been reported in 2 families with oculodentodigital dysplasia,[30] although associated cardiac phenotypes are not commonly reported in this disease The apparent uncommon reporting of cardiac arrhythmias in oculodentodigital dysplasia suggests that the majority of Cx43 mutations do not have a significant effect on the electrical properties of atrial and ventricular myocardium However, the homogeneous distribution throughout myocardium of a germline mutation may not create regional heterogeneity in conduction velocity to the extent necessary to promote electrical reentry In contrast, a mosaic distribution or unequal pattern of connexin isoform or mutant protein expression would be expected to result in regional variations

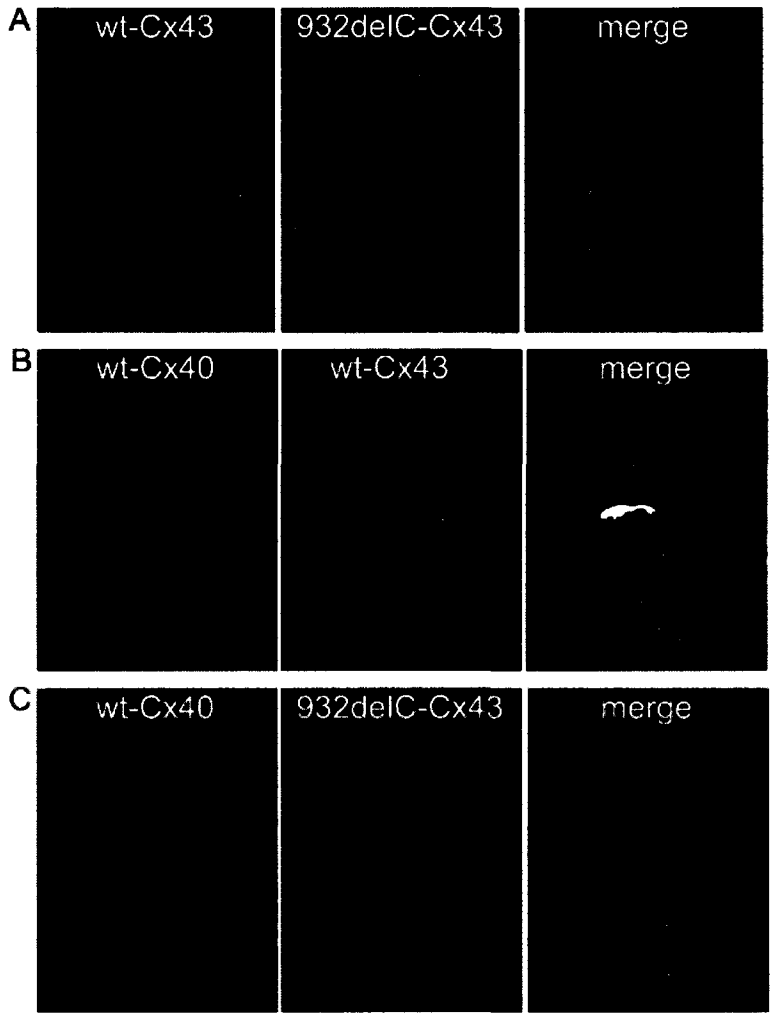

Figure 4. Dominant-negative effect of c 932delC-Cx43 on wt-Cx43 and wt-Cx40 Coexpression of mutant Cx43 impairs gap junction formation of wt-Cx43 (A) B, Normal gap junction formation and colocalization of fluorescently tagged wt-Cx40 and wt-Cx43 at the cell-to-cell interface Mutant Cx43 significantly impairs trafficking of wt-Cx40 suggesting an interaction during oligomerization within the Golgi network (C)

of conduction velocity, creating a localized asymmetry in the depolarizing wave front and enhancing the substrate for electrical reentry This precise concept has been elegantly demonstrated by Gutstein and colleagues,[27] who developed chimeric mice with heterogenous, patchy myocardial Cx43 expression throughout ventricular myocardium These mice demonstrated discrete areas of conduction delay and spontaneously occurring reentrant cardiac arrhythmias compared with normal electrical activation and absence of arrhythmias in wt-Cx43 mice with homogeneous protein expression [27] These data support the concept that tissue mosaicism of connexin isoforms may be responsible for reentrant arrhythmias in humans The substrate of reentry would be expected to be further exacerbated by a mosaic expression pattern of a loss-of-function connexin protein

The identified atrial tissue Cx43 mutation in our patient is predicted to result in a significant change in the primary structure of the protein The frameshift mutation arises from a single cytosine nucleotide deletion (c 932delC), leading to an altered codon reading frame beginning at amino acid residue 311 of the protein The altered codon sequence predicts 36 aberrant amino acids, followed by a premature stop codon, effectively deleting the last 72 amino acids of the putative Cx43 protein Although we could not confirm the absence of the mutation from ventricular myocardium, our patient only had clinically detected AF and showed a normal QRS duration and no ventricular arrhythmias during long-term follow-up

The functional relevance of the identified mutation was confirmed by protein trafficking studies, immunostaining of atrial tissue from the affected patient, and electrophysiological recordings of gap junction–mediated cell-to-cell coupling Expression of mutant Cx43 in HeLa cells demonstrated significant intracellular retention of the protein Immunostaining of atrial tissue from the affected patient confirmed a mosaic pattern of intracellular retention among myocytes, consistent with the presence of the mutation in a subpopulation of cells and the <50% allele frequency determined by PCR subcloning Cotransfection of the mutant protein with endoplasmic reticulum and Golgi protein markers indicated that intracellular accumulation of the mutant protein occurred within the Golgi apparatus Hexameric oligomerization of Cx43 into hemichannels is known to occur within the Golgi network [35] These observations suggest that the mutant protein interferes with the normal oligomerization process of Cx43, leading to retention of mutant protein within the Golgi Interestingly, previous studies on a Cx43 C-terminal truncated mutant showed normal trafficking and localization to

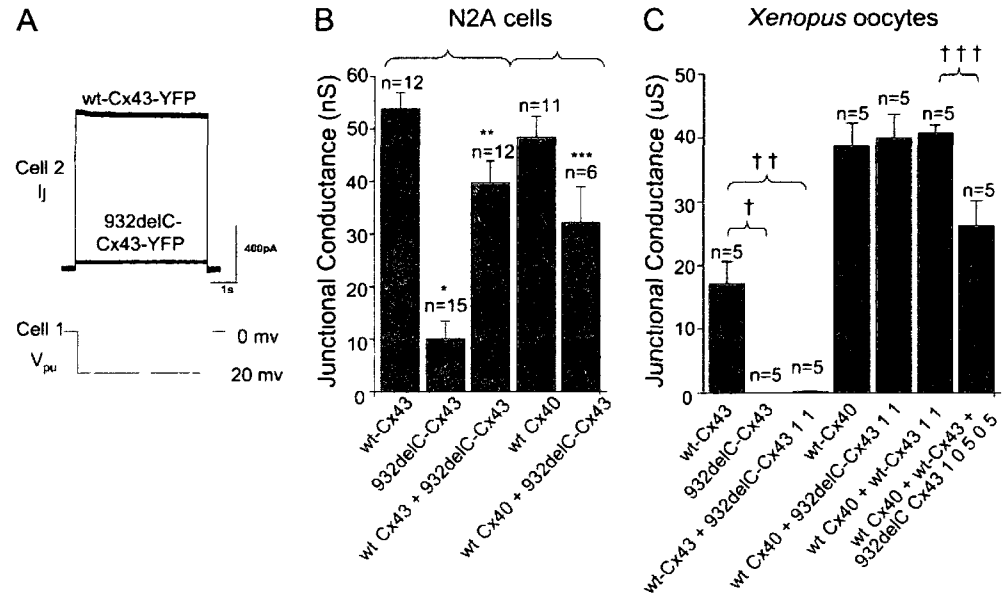

Figure 5. Dominant-negative effect of c 932delC-Cx43 on gap junction conductance Paired N2A cells expressing YFP-tagged mutant Cx43 exhibited severely reduced gap junction conductance compared with cell pairs expressing wt-Cx43-YFP (A) B, Junctional conductances in pairs of N2A cells transfected with wt-Cx43, wt-Cx40, or mutant Cx43 or cotransfected with equal ratios of wt and mutant cDNA Mutant Cx43 significantly impaired the gap junction conductance of both wt-Cx43 and wt-Cx40 (*P=0 01, **P=0 02 vs wt-Cx43, ***P=0 03 vs wt-Cx40) C, Comparison of junctional conductances of *Xenopus* oocyte pairs expressing various combinations of untagged Cx43, Cx40, and mutant Cx43 RNAs injected in the ratios indicated Mutant Cx43 failed to form functional channels but showed a strong dominant-negative effect on wtCx43 Although no dominant-negative effect on wtCx40 was evident, a suppressive effect is seen when wt-Cx43 is coexpressed (†P=0 00003, ††=0 00004, †††P=0 007)

intercalated disks [36] However, the truncated mutant protein reported by Maass et al[36] lacked the presence of aberrant amino acids at the C terminus, in contrast to the mutant detected in this study Similar to the significant trafficking defects observed for c 932delC-Cx43 in our study, previously reported connexin truncation mutations with aberrant C-terminal residues have demonstrated significant intracellular retention and impairment of gap junction formation,[37,38] suggesting that the existence of aberrant C-terminal amino acids impairs the assembly to hemichannels and promotes intracellular retention As predicted by the abnormal trafficking studies, cells expressing c 932delC mutant Cx43 showed a marked reduction in the ability of cell pairs to electrically couple during dual whole-cell patch-clamp analyses

To determine the effect of c 932delC-Cx43 in the heterozygous state, cells cotransfected with equal ratios of mutant and wt connexins were evaluated Mutant Cx43 exerted a dominant-negative effect on wt-Cx43, demonstrating intracellular retention of wt and mutant Cx43 in a pattern similar to that observed for mutant Cx43 alone Similarly, electrical coupling of cell pairs in the heterozygous state was significantly impaired Because Cx40 is also highly expressed in the atria and is believed to form heteromeric channels with Cx43, we examined the effect of c 932delC-Cx43 on the trafficking and electrical coupling properties of wt-Cx40 In the N2A mammalian cell model, cotransfection of wt-Cx43 and wt-Cx40 resulted in very evident gap junction plaques at cell-to-cell interfaces, and robust electrical coupling of cell pairs was recorded However, mutant Cx43 cotransfection with wt-Cx40 resulted in the intracellular retention of Cx40 and a significant reduction in the electrical coupling of cell pairs

In the *Xenopus* oocyte cell system, an even more robust dominant-negative effect of mutant Cx43 on wt-Cx43 was evident However, the transdominant effect of mutant Cx43 on wt-Cx40 seen in N2A cells was not evident in oocytes unless wt-Cx43 was also present This apparent discrepancy between expression systems may be due to the difference in incubating temperatures of the cells during the oligomerization process, mammalian cells are incubated at a physiological temperature (37°C), as opposed to the 17°C incubation temperature for oocytes This lower temperature may still allow oligomerization of wt and mutant Cx43, and also the two wt connexins, but may not support oligomerization of mutant Cx43 with Cx40 The addition of wt-Cx43 to the mix of wt-Cx40 and mutant Cx43 in the oocyte system, however, did result in significantly reduced gap junction electrical coupling, suggesting that the mutant Cx43 can affect wt-Cx40 that is in heteromeric oligomers with wt-Cx43 This situation is likely to be close to what would be encountered in situ in the atrium These results also confirm the oligomerization of Cx43 and Cx40 isoforms, probably within the Golgi apparatus, and support the concept that these heteromeric hemichannels contribute to functional gap junctions in atrial tissue [39,40] However, it remains unknown whether heteromeric and homomeric forms contribute equally because it has been suggested from atrial recordings under conditions in which Cx43 and Cx40 levels have been modulated that heteromeric forms may contribute less to functional coupling than might be predicted from their expected abundance [41,42]

As our population ages, it is predicted that the prevalence of AF in the United States alone will exceed 5 000 000 by the year 2050 [43] Consequently, the socioeconomic burden asso-

ciated with the management of this disease will continue to rise.[44] Despite the growing disease prevalence, progress in the development of efficacious drug therapy has been minimal over the previous decade. Genetics research aims to identify genes predisposing to or causative for disease in the hope of identifying novel molecular targets as potential substrates for drug treatment. The observation that loss-of-function mutations of cardiac connexins are associated with AF supports the targeting of gap junction channels for pharmacological intervention. A recently developed, orally available gap junction modifier has been reported to increase conduction velocity and to significantly reduce AF inducibility in a canine model of AF.[45] In addition, this novel agent had no effect on measures of atrial tissue refractoriness, heart rate, blood pressure, or ECGs. These data hold promise that enhancers of gap junction conductance may be therapeutic in preventing reentry arrhythmias.

Conclusions

We report the presence of genetic mosaicism of a Cx43 mutant protein within the atrial tissue of a patient with lone AF The mutant protein results in a loss-of-gap junction function of both wt-Cx43 and wt-Cx40 channels. The observed findings support the notion that sporadic, lone AF may have a genetic basis and provide the impetus for therapeutic approaches for modification of cardiac gap junction function as a potential therapy for management of this common arrhythmia.

Acknowledgment

We thank our patients for their dedicated support.

Sources of Funding

This work was supported in part by grants from the Heart and Stroke Foundations of Ontario (Dr Gollob) and the Canadian Institutes for Health Research (Dr Gollob) Dr Gollob is supported by the Early Researcher Award program from the Government of Ontario and by the Heart and Stroke Foundation of Ontario Clinician-Scientist Award

Disclosures

None

References

1 Wolf PA, Abott RD, Kannel WB Atrial fibrillation as an independent risk factor for stroke the Framingham study *Stroke* 1991,22 983–988
2 Benjamin EJ, Wolf PA, D'Agostino RB, Silbershatz H, Kannel W, Levy D Impact of atrial fibrillation on the risk of death the Framingham Heart Study *Circulation* 1998,98 946–952
3 Pappone C, Oreto G, Rosanio S, Vicedomini G, Tocchi M, Gugliotta F, Salvati A, Dicandia C, Calabrò MP, Mazzone P, Ficarra E, Di Gioia C, Gulletta S, Nardi S, Santinelli V, Benussi S, Alfieri O Atrial electroanatomic remodeling after circumferential radiofrequency pulmonary vein ablation efficacy of an anatomic approach in a large cohort of patients with atrial fibrillation *Circulation* 2001,104 2539–2544
4 Marrouche NF, Martin DO, Wazni O, Gillinov AM, Klein A, Bhargava M, Saad E, Bash D, Yamada H, Jaber W, Schweikert R, Tchou P, Abdul Karim A, Saliba W, Natale A Phased-array intracardiac echocardiography monitoring during pulmonary vein isolation in patients with atrial fibrillation impact on outcome and complications *Circulation* 2003,107 2710–2716
5 Vasamreddy CR, Dalal D, Eldadah Z, Dickfeld T, Jayam VK, Henrickson C, Meininger G, Dong J, Lickfett L, Berger R, Calkins H Safety and efficacy of circumferential pulmonary vein catheter ablation of atrial fibrillation *Heart Rhythm* 2005,2 42–48
6 Cheema A, Dong J, Dalal D, Vasamreddy CR, Marine JE, Henrikson CA, Spragg D, Cheng A, Nazarian S, Sinha S, Halperin H, Berger R, Calkins H Long-term safety and efficacy of circumferential ablation with pulmonary vein isolation *J Cardiovasc Electrophysiol* 2006,17 1080–1085
7 Sonmez B, Demirsoy E, Yagan N, Unal M, Arbatli H, Sener D, Baran T, Ilkova F A fatal complication due to radiofrequency ablation for atrial fibrillation atrio-esophageal fistula *Ann Thorac Surg* 2003,76 281–283
8 Spragg DD, Dalal D, Cheema A, Scherr D, Chilukuri K, Cheng A, Henrikson CA, Marine JE, Berger RD, Dong J, Calkins H Complication of catheter ablation for atrial fibrillation incidence and predictors *J Cardiovasc Electrophysiol* 2008,19 627–631
9 Chen Y-H, Xu W-J, Bendahhou S, Wang X-L, Wang Y, Xu W-Y, Jin H-W, Sun H, Su X-Y, Zhuang Q-N, Yang Y-Q, Li Y-B, Liu L, Xu H-J, Li X-F, Ma N, Mou C-P, Chen Z, Barhanin J, Huang W KCNQ1 gain-of-function mutation in familial atrial fibrillation *Science* 2003, 299 251–254
10 Yang Y, Xia M, Jin Q, Bendahhaou S, Shi J, Chen Y, Liang B, Lin J, Liu B, Zhou Q, Zhang D, Wang R, Ma N, Su X, Niu K, Pei Y, Xu W, Chen Z, Wan H, Cui J, Barhanin J, Chen Y Identification of a KCNE2 gain-of-function mutation in patients with familial atrial fibrillation *Am J Hum Genet* 2004,75 899–905
11 Xia M, Jin Q, Bendahhaou S, He Y, Larroque M M, Chen Y, Zhou Q, Yang Y, Liu Y, Liu B, Zhu Q, Zhou Y, Lin J, Liang B, Li L, Dong X, Pan Z, Wang R, Wan H, Qiu W, Xu W, Eurlings P, Barhanin J, Chen Y A Kir2 1 gain-of-function mutation underlies familial atrial fibrillation *Biochem Biophys Res Commun* 2005,332 1012–1019
12 Olson T, Alekseev A, Liu X, Park S, Zingman L, Bienengraeber M, Sattiraju S, Ballew J, Jahangir A, Terzic A Kv1 5 channelopathy due to KCNA5 loss-of-function mutation causes human atrial fibrillation *Hum Mol Genet* 2006,15 2185–2191
13 Darbar D, Kannankeril PJ, Donahue BS, Kucera G, Stubblefield T, Haines JL, George AL, Roden DM Cardiac sodium channel (SCN5A) variants associated with atrial fibrillation *Circulation* 2008,117 1927–1935
14 Hodgson-Zingman DM, Karst ML, Zingman LV, Heublein DM, Darbar D, Herron KJ, Ballew JD, de Andrade M, Burnett JC Jr, Olson TM Atrial natriuretic peptide frameshift mutation in familial atrial fibrillation *N Engl J Med* 2008,359 158–165
15 Li Q, Huang H, Liu G, Lam K, Rutberg J, Green MS, Birnie DH, Lemery R, Chahine M Gollob MH Gain-of-function mutation of Nav1 5 in atrial fibrillation enhances cellular excitability and lowers the threshold for action potential firing *Biochem Biophys Res Commun* 2009,380 132–137
16 Ellinor PT, Petrov-Kondratov VI, Zakharova E, Nan EG, MacRae RA Potassium channel mutations rarely cause atrial fibrillation *BMC Med Genet* 2006,7 70
17 Chen LY, Ballew JD, Herron KJ, Rodeheffer RJ, Olson TM A common polymorphism in SCN5A is associated with lone atrial fibrillation *Clin Pharmacol Ther* 2007,81 35–41
18 Colman SD, Rasmussen SA, Ho VT, Abernathy CR, Wallace MR Somatic mosaicism in a patient with neurofibromatosis type 1 *Am J Hum Genet* 1996,58 484–490
19 Evans DG, Wallace AJ, Wu CL, Trueman L, Ramsden RT, Strachan T Somatic mosaicism a common cause of classic disease in tumor-prone syndromes? Lessons from type 2 neurofibromatosis *Am J Hum Genet* 1998,63 727–736
20 Erickson RP Somatic gene mutation and human disease other than cancer *Mutat Res* 2003,543 125–136
21 Puck JM, Straus SE Somatic mutations not just for cancer anymore *N Engl J Med* 2004,351 1388–1390
22 Gollob MH, Jones DL, Krahn AD, Danis L, Gong X-Q, Shao Q, Liu X, Veinot JP, Tang ASL, Stewart AFR, Tesson F, Klein GJ, Yee R, Skanes AC, Guiraudon GM, Ebihara L, Bai D Somatic mutations in the connexin 40 gene (GJA5) in atrial fibrillation *N Engl J Med* 2006 354 2677–2688
23 Kanno S, Saffitz JE The role of myocardial gap junctions in electrical conduction and arrhythmogenesis *Cardiovasc Pathol* 2001,10 169–177
24 Konings KT, Kirchhof CJ, Smeets JR, Wellens HJ, Penn OC, Allessie MA High-density mapping of electrically induced atrial fibrillation in humans *Circulation* 1994,89 1665–1680
25 Spach MS, Josephson ME Initiating reentry the role of nonuniform anisotropy in small circuits *J Cardiovasc Electrophysiol* 1994,5 182–209
26 Hagendorff A, Schumacher B, Kirchhoff S, Luderitz B, Willecke K Conduction disturbances and increased atrial vulnerability in connexin40-

deficient mice analyzed by transesophageal stimulation *Circulation* 1999,99 1508–1515
27 Gutstein DE, Morely GE, Vaidya D, Liu F, Chen FL, Stuhlmann H, Fishman GI Heterogeneous expression of gap junction channels in the heart leads to conduction defects and ventricular dysfunction *Circulation* 2001,104 1194–1199
28 Kalcheva N, Qu J, Sandeep N, Garcia L, Zhang J, Wang Z, Lampe PD, Suadicani SO, Spray DC, Fishman GI Gap junction remodeling and cardiac arrhythmogenesis in a murine model of oculodentodigital dysplasia *Proc Natl Acad Sci U S A* 2007,104 20512–20516
29 Dupont E, Ko Y, Rothery S, Coppen SR, Baghai M, Haw M, Severs NJ The gap-junctional protein connexin40 is elevated in patients susceptible to postoperative atrial fibrillation *Circulation* 2001,103 842–849
30 Paznekas WA, Boyadjiev SA, Shapiro RE, Daniels O, Wollnik B, Keegan CE, Innis JW, Dinulos MB, Christian C, Hannibal MC, Jabs EW Connexin 43 (GJA1) mutations cause the pleiotropic phenotype of oculodentodigital dysplasia *Am J Hum Genet* 2003,72 408–418
31 Skerrett IM, Merritt M, Zhou L, Zhu H, Cao F, Smith JF, Nicholson BJ Applying the *Xenopus* oocyte expression system to the analysis of gap junction proteins *Methods Mol Biol* 2001,154 225–249
32 Zheng SL, Sun J, Wiklund F, Smith S, Stattin P, Li G, Adami HO, Hsu FC, Zhu Y, Balter K, Kader AK, Turner AR, Liu W, Bleecker ER, Meyers DA, Duggan D, Carpten JD, Chang BL, Isaacs WB, Xu J, Gronberg H Cumulative association of 5 genetic variants with prostate cancer *N Engl J Med* 2008,358 910–919
33 Qi L, Cornelis MC, Zhang C, van Dam RM, Hu FB Genetic predisposition Western dietary pattern, and the risk of type 2 diabetes in men *Am J Clin Nutr* 2009,89 1453–1458
34 McPherson R, Pertsemlidis A, Kavaslar N, Stewart A, Roberts R, Cox DR, Hinds DA, Pennacchio LA, Tybjaerg-Hansen A, Folsom AR, Boerwinkle E, Hobbs HH, Cohen JC A common allele on chromosome 9 associated with coronary heart disease *Science* 2007,316 1488–1491
35 Koval M Pathways and control of connexin oligomerization *Trends in Cell Biol* 2006,16 159–166
36 Maass K, Shibayama J, Chase SE, Willecke K, Delmar M C-terminal truncation of Connexin43 changes number, size, and location of cardiac gap junction plaques *Circ Res* 2007,101 1283–1291
37 Minogue PJ, Liu X, Ebihara L, Beyer EC, Berthoud VM An aberrant sequence in a connexin46 mutant underlies congenital cataracts *J Biol Chem* 2005,280 40788–40795
38 Gong XQ, Shao Q, Lounsbury CS, Bai D, Laird DW Functional characterization of a GJA1 frameshift mutation causing oculodentodigital dysplasia and palmoplantar keratoderma *J Biol Chem* 2006,281 31801–31811
39 He DS, Jiang JX, Taffet SM, Burt JM Formation of heteromeric gap junction channels by connexins 40 and 43 in vascular smooth muscle cells *Proc Natl Acad Sci U S A* 1999,96 6495–6500
40 Cottrell GT, Wu Y, Burt JM Functional characteristics of heteromeric Cx40-Cx43 gap junction channel formation *Cell Commun Adhes* 2001, 8 193–197
41 Lin X, Gemel J, Glass A, Zemlin CW, Beyer EC, Veenstra RD Connexin40 and connexin43 determine gating properties of atrial gap junction channels *J Mol Cell Cardiol* 2010,48 238–245
42 Beauchamp P, Yamada KA, Baertschi AJ, Green K, Kanter EM, Saffitz JE, Kleber AG Relative contributions of connexins 40 and 43 to atrial impulse propagation in synthetic strands of neonatal and fetal murine cardiomyocytes *Circ Res* 2006,99 1216–1224
43 Go AS, Hylek EM, Phillips KA, Change Y, Henault LE, Selby JV, Singer DE Prevalence of diagnosed atrial fibrillation in adults national implications for rhythm management and stroke prevention the Anticoagulation and Risk Factors in Atrial Fibrillation (ATRIA) Study *JAMA* 2001,285 2370–2375
44 Wattigney WA, Mensah GA, Croft JB Increasing trends in hospitalization for atrial fibrillation in the United States, 1985 through 1999 implications for primary prevention *Circulation* 2003,108 711–716
45 Rossman EI, Liu K, Morgan GA, Swillo RE, Krueger JA, Butera J, Gruver M, Kantrowitz J, Feldman HS, Petersen JS, Haugan K, Gardell SJ, Hennan JK The gap junction modifier, GAP-134, improves conduction and reduces atrial fibrillation/flutter in the canine sterile pericarditis model *J Pharmacol Exp Ther* 2009,329 1127–1133

CLINICAL PERSPECTIVE

Atrial fibrillation is the most common sustained cardiac arrhythmia and is a common cause of stroke. Epidemiological studies project an exponential rise in the prevalence of atrial fibrillation in Western societies, coincident with the increasing age of the population. Management strategies for atrial fibrillation are not highly efficacious. Pharmacological therapies may lead to intolerable side effects and often become refractory over time. Success rates from catheter ablation procedures vary considerably between institutions and may lead to major complications, and long-term success (>24 months) in large cohorts has not been reported despite the use of this procedure for more than a decade. Thus, a further understanding of the molecular mechanisms promoting vulnerability to fibrillation of the atria is critical in facilitating the development of more efficacious therapies. In this study, we provide data implicating a loss-of-function mutation in the gene encoding the gap junction protein connexin 43 as a mechanism leading to augmentation of heterogeneous myocardial electrical coupling, predisposing atrial myocardium to reentrant arrhythmias. Specific drug development enhancing gap junction function may attenuate arrhythmia vulnerability.